

DESIGN OF A RADIO FREQUENCY IDENTIFICATION (RFID) ANTENNA

A THESIS SUBMITTED TO  
THE GRADUATE SCHOOL OF NATURAL AND APPLIED SCIENCES  
OF  
MIDDLE EAST TECHNICAL UNIVERSITY

BY

SEFA KALAYCI

IN PARTIAL FULFILLMENT OF THE REQUIREMENTS  
FOR  
THE DEGREE OF MASTER OF SCIENCE  
IN  
ELECTRICAL AND ELECTRONICS ENGINEERING

MAY 2009

Approval of the thesis:

**DESIGN OF A RADIO FREQUENCY IDENTIFICATION (RFID)  
ANTENNA**

submitted by **SEFA KALAYCI** in partial fulfillment of the requirements for the degree of **Master of Science in Electrical and Electronics Engineering Department, Middle East Technical University** by,

Prof. Dr. Canan Özgen \_\_\_\_\_  
Dean, Graduate School of **Natural and Applied Sciences**

Prof. Dr. İsmet Erkmn \_\_\_\_\_  
Head of Department, **Electrical and Electronics Engineering**

Prof. Dr. M. Tuncay Birand \_\_\_\_\_  
Supervisor, **Electrical and Electronics Engineering Dept., METU**

**Examining Committee Members:**

Prof. Dr. Altuncan Hızal \_\_\_\_\_  
Electrical and Electronics Engineering Dept., METU

Prof. Dr. M. Tuncay Birand \_\_\_\_\_  
Electrical and Electronics Engineering Dept., METU

Prof. Dr. Murat Aşkar \_\_\_\_\_  
Electrical and Electronics Engineering Dept., METU

Prof. Dr. Gülbin Dural \_\_\_\_\_  
Electrical and Electronics Engineering Dept., METU

Berkan Ertan \_\_\_\_\_  
HC SESMM, ASELSAN A.Ş.

**Date:** **12.05.2009**

**I hereby declare that all information in this document has been obtained and presented in accordance with academic rules and ethical conduct. I also declare that, as required by these rules and conduct, I have fully cited and referenced all material and results that are not original to this work.**

Name, Last Name: Sefa Kalaycı

Signature :

## ABSTRACT

### DESIGN OF A RADIO FREQUENCY IDENTIFICATION (RFID) ANTENNA:

Kalaycı, Sefa

M.S., Department of Electrical and Electronics Engineering

Supervisor: Prof. Dr. M. Tuncay Birand

May 2009, 126 pages

Fundamental features of Radio Frequency Identification (RFID) systems used in different application areas will be reviewed. Techniques used in realizing RFID antenna systems will be studied and the procedure to realize a specific RFID antenna type possessing desired characteristics will be described. Electrical properties such as radiation pattern, impedance will be predicted using analytical and/or computer simulation techniques. Experimental investigations will be carried out to complement the theoretical work.

Key words: Radio Frequency Identification (RFID), Transponder, Antenna Design, UHF Tags, 2-Wire Folded Dipole, 3-Wire Folded Dipole, Impedance Matching Techniques, T-Match, Proximity-Coupled Loop, Nested-Slot Antenna Structures, Meandered Line Antennas.

ÖZ

RADYO FREKANSI KİMLİK TANIMLAMA (RFID)  
ANTEN TASARIMI

Kalaycı, Sefa

Yüksek Lisans, Elektrik-Elektronik Mühendisliği Bölümü

Tez Yöneticisi: Prof. Dr. M. Tuncay Birand

Mayıs 2009, 126 sayfa

Çeşitli uygulama alanlarında kullanılan Radyo Frekans Kimlik Tanımlama (Radio Frequency Identification: RFID) sistemlerinin temel özellikleri incelenecektir. RFID anten sistemlerinin gerçekleştirilmesinde kullanılan teknikler incelenerek arzu edilen karakteristiklere sahip bir anten tipinin tasarımına ait süreç tanımlanacaktır. Antene ait ışınım diyagramı, empedans gibi elektriksel parametreler analitik ve/veya bilgisayar simülasyon teknikleri kullanılarak kestirilecektir. Teorik çalışmaları tamamlayacak deneysel çalışmalar yürütülecektir.

Anahtar Kelimeler: RFID Etiketi Anten Tasarımı, UHF Etiketler, 2-Telli Katlanmış Dipol Anten, 3-Telli Katlanmış Dipol Anten, Empedans Uyumluluk Teknikleri, T-Uyumluluk, Yakın Mesafe Endüktif Halka Beslemeli Anten Sistemleri, Bükülmüş Çizgi Antenler.

*To Mom, Dad, Sisters, Nieces and Nephews*

## ACKNOWLEDGEMENTS

I would like to express my gratitude and deep appreciation to my supervisor Prof. Dr. M. Tuncay Birand for his guidance and positive suggestions.

I would like to thank Berkan Ertan and Ziya Doğru from Aselsan A.Ş. and İbrahim Uğurlu and Nevzat Ecevit from UDEA Electronics, for such a friendly work environment they had provided. I have learned much from their suggestions and experiences.

I would also like to express my thanks for their great friendship and assistance to Bülent Başaran, Uğur Keskin, Mükremin Çetinkaya and Ferhunde Yıldırım.

Finally, I would like to thank my Mom, Dad, Sisters for their love, support and patience over the years. This thesis is dedicated to them.

# TABLE OF CONTENTS

ABSTRACT .....	iv
ÖZ .....	vi
ACKNOWLEDGEMENTS.....	ix
TABLE OF CONTENTS .....	x
LIST OF TABLES .....	xiii
LIST OF FIGURES .....	xiv
LIST OF ABBREVIATIONS.....	xvi
INTRODUCTION.....	1
1.1 Scope and Outline of the Thesis.....	3
RFID TECHNOLOGY .....	5
2.1 RFID Fundamentals .....	5
2.1.1 RFID System Layers .....	5
2.1.2 RFID Information Flow: .....	7
2.1.3 Other Auto-ID Technologies: .....	8
2.1.4 RFID Technology Applications:.....	9
2.2 History of RFID.....	10
2.3 RFID Transponders and Interrogators .....	13
2.3.1 Transponder (Tag).....	13
2.3.1.1 RFID Tag Components.....	14
2.3.1.2 Classification of RFID Tags .....	16
2.3.1.2.1 Power Source.....	16
2.3.1.2.2 RFID Tag Characteristics.....	19
2.3.1.2.3 RFID Tag Functionality.....	22
2.3.1.2.4 RFID Tag-Reader Protocols.....	23

2.3.2 Interrogator (Reader).....	24
2.3.2.1 The HF Interface .....	25
2.3.2.2 The Control Group .....	26
2.4 RF in RFID and Coupling Mechanisms.....	28
2.4.1 RF in RFID .....	28
2.4.2 Coupling Mechanisms.....	36
2.4.2.1 Near-Field Coupling .....	37
2.4.2.1.1 Inductive Coupling.....	39
2.4.2.2 Far-Field Coupling .....	40
2.4.2.2.1 Modulated Backscatter Coupling.....	40
2.4.2.2.2 Beacon (Transmitter) Type.....	42
2.4.2.2.3 Transponder Type.....	42
2.5 Chapter Summary.....	43
RFID TAG ANTENNA DESIGN .....	44
PROCEDURES AND PROBLEMS .....	44
3.1 Performance Criteria.....	44
3.1.1 Tag Characteristics.....	46
3.1.2 Propagation Environment Limitations .....	47
3.2 Design Requirements.....	48
3.3 Design Process.....	49
3.4 Prototyping and Validation .....	51
3.5 Chapter Summary.....	53
FOLDED DIPOLE ANTENNA DESIGNS.....	54
4.1 Design Approach .....	55
4.2 Antenna Designs.....	56
4.3 Simulation Results and Discussion.....	58
4.3.1 The Influence on Resonant Frequency.....	63
4.3.2 The Influence on Input Impedance .....	69
4.4 Chapter Summary.....	73
OTHER IMPEDANCE MATCHING TECHNIQUES .....	75

5.1 T-Match Antenna Design.....	76
5.1.1 Design Approach .....	77
5.1.2 Antenna Design.....	78
5.1.3 Simulation Results and Discussions .....	78
5.2 Inductively Coupled Loop Antenna Design.....	82
5.2.1 Design Approach .....	83
5.2.2 Antenna Design.....	84
5.2.3 Simulation Results and Discussions .....	84
5.3 Nested Slot Antenna Design .....	87
5.3.1 Design Approach .....	89
5.3.2 Antenna Design.....	89
5.2.3 Simulation Results and Discussions .....	90
5.4 Chapter Summary .....	93
MEANDERED LINE DIPOLE .....	94
ANTENNA DESIGNS.....	94
6.1 Design Approach .....	95
6.2 Antenna Designs.....	96
6.3 Simulation Results and Discussions .....	103
6.4 Chapter Summary .....	118
CONCLUSIONS.....	119
REFERENCES .....	121

# LIST OF TABLES

## TABLES

Table 2.1 Some of the differences between RFID and barcode [1].....	9
Table 2.2 The milestones in RFID technology [2]. .....	11
Table 2.3 Active vs. Passive Tag.....	18
Table 2.4 Active vs. passive tag tradeoffs.....	18
Table 2.5 List of the RFID frequencies and related applications [1].....	21
Table 2.6 List of the various classifications and their related functionality [5] ....	22
Table 4.1 Simulated antenna parameters and calculated theoretical.....	63
Table 5.1 Simulated antenna parameters and calculated theoretical.....	81
Table 5.2 Simulated antenna parameters and calculated theoretical.....	87
Table 5.3 Simulated antenna parameters and calculated theoretical. ....	93
Table 6.1 Simulated and measured antenna parameters.....	118

# LIST OF FIGURES

## FIGURES

Figure 2.1 An overview of the RFID system physical layer [1].....	6
Figure 2.2 RFID Tag picture showing the components. ....	13
Figure 2.3 Basic RFID IC block diagram [8]. ....	15
Figure 2.4 General RFID reader block diagram. ....	24
Figure 2.5 RFID reader sub-block diagram.....	25
Figure 2.6 Geometrical representation of the sinusoidal current filament.....	29
Figure 2.7 Field regions of an antenna.....	30
Figure 2.8 Elevation plane amplitude patterns for a thin dipole.....	33
Figure 2.9 Three and Two-dimensional amplitude patterns.....	34
Figure 2.10 Current distributions along the length of a linear wire antenna [7]. .	35
Figure 2.11 Near-field (LF and HF) and far-field (UHF) coupling mechanisms. 38	
Figure 2.12 Generation of the modulated backscatter by the modulation .....	41
Figure 3.1 Antenna impedance, chip impedance, and range as a function.....	45
Figure 3.2 RFID tag antenna design process [10].....	50
Figure 3.3 RFID tag range measurement using anechoic chamber [10].....	52
Figure 4.1 The three different folded dipole RFID antenna designs.....	57
Figure 4.2 Simulation results showing the return losses of the antennas.....	59
Figure 4.3 Simulated antenna input impedances with respect to frequency. ....	60
Figure 4.4 Simulated 2-D radiation patterns.....	61
Figure 4.5 Influence on resonant frequency L1 as a parameter.....	64
Figure 4.6 Influence on resonant frequency L2 as a parameter.....	65
Figure 4.7 Influence on resonant frequency L3 as a parameter.....	66
Figure 4.8 Influence on resonant frequency L4 as a parameter.....	67
Figure 4.9 Influence on resonant frequency substrate thickness as a parameter..	68
Figure 4.10 Influence on resonant frequency line width (w) as a parameter. ....	68
Figure 4.11 Influence on input impedance L1 as a parameter.....	69
Figure 4.12 Influence on input impedance L2 as a parameter.....	70
Figure 4.13 Influence on input impedance L3 as a parameter.....	71
Figure 4.14 Influence on input impedance L4 as a parameter.....	71
Figure 4.15 Influence on input impedance substrate thickness as a parameter...	72
Figure 4.16 Influence on input impedance line width (w) as a parameter .....	73
Figure 5.1 The T-match configuration for planar dipoles.....	77
Figure 5.2 The T-match RFID antenna design layout.....	78
Figure 5.3 Simulation result showing the return loss of the antenna.....	79

Figure 5.4 Simulated antenna input impedance with respect to frequency.....	79
Figure 5.5 Simulated 2-D radiation pattern for the T-match 915 MHz UHF .....	80
Figure 5.6 The layout of the inductively coupled feed and its equivalent circ.....	83
Figure 5.7 The inductively coupled loop RFID antenna design layout. ....	84
Figure 5.8 Simulation result showing the return loss of the antenna.....	85
Figure 5.9 Simulated antenna input impedance with respect to frequency.....	85
Figure 5.10 Simulated 2-D radiation pattern for the inductively coupled loop....	86
Figure 5.11 The geometry of the nested-slot suspended-patch .....	88
Figure 5.12 The nested-slot RFID antenna design layout.....	90
Figure 5.13 Simulation result showing the return loss of the antenna.....	90
Figure 5.14 Simulated antenna input impedance with respect to frequency.....	91
Figure 5.15 Simulated 2-D radiation pattern for the nested-slot 915 MHz.....	92
Figure 6.1 The geometry of a meandered-line antenna.....	95
Figure 6.2 The meander-line RFID antenna with loading bar design#1 layout. ..	96
Figure 6.3 The implemented meander-line RFID antenna with loading bar.....	97
Figure 6.4 The meander-line RFID antenna with loading bar design#2 layout. ..	98
Figure 6.5 The implemented meander-line RFID antenna with loading bar.....	98
Figure 6.6 The meander-line RFID antenna with unequal turn design#3.....	99
Figure 6.7 The implemented meander-line RFID antenna having unequal.....	100
Figure 6.8 The meander-line RFID antenna with unequal turn design#4.....	100
Figure 6.9 The implemented meander-line RFID antenna having unequal.....	101
Figure 6.10 The meander-line RFID antenna having multiple unequal turns.....	101
Figure 6.11 The implemented meander-line RFID antenna having multiple.....	102
Figure 6.12 The meander-line RFID antenna having multiple unequal turns.....	102
Figure 6.13 The implemented meander-line RFID antenna having multiple.....	103
Figure 6.14 Results showing the return loss of the meander-line antenna .....	103
Figure 6.15 Results showing the return loss of the meander-line antenna .....	104
Figure 6.16 Results showing the return loss of the meander-line antenna .....	104
Figure 6.17 Results showing the return loss of the meander-line antenna .....	105
Figure 6.18 Results showing the return loss of the meander-line antenna .....	105
Figure 6.19 Results showing the return loss of the meander-line antenna .....	106
Figure 6.20 Simulated meander-line antenna design#1 input impedance.....	107
Figure 6.21 Simulated meander-line antenna designs input impedance.....	108
Figure 6.22 Simulated meander-line antenna designs input impedance .....	109
Figure 6.23 Test environment for measuring radiation patterns of the.....	110
Figure 6.24 Simulated and measured 2-D radiation pattern.....	111
Figure 6.25 Simulated and measured 2-D radiation pattern.....	112
Figure 6.26 Simulated and measured 2-D radiation pattern.....	113
Figure 6.27 Simulated and measured 2-D radiation pattern.....	114
Figure 6.28 Simulated and measured 2-D radiation pattern.....	115
Figure 6.29 Simulated and measured 2-D radiation pattern.....	116

## LIST OF ABBREVIATIONS

CRC	Cyclic Redundancy Code
CW	Continuous Wave
EAN	European Article Number
EAS	Electronic Article Surveillance
EEPROM	Electrically Erasable Programmable Read Only Memory
EIRP	Effective Isolated Radiated Power
EPC	Electronic Product Code
FEM	Finite Elements Method
GPS	Global Positioning System
HF	High Frequency
HFSS	High Frequency Structure Simulator
IC	Integrated Circuit
IFF	Identify Friend or Foe
ISM	Industrial-Scientific-Medical
ISO	International Standards Organization
LCP	Liquid Crystal Polymer
LF	Low Frequency
MoM	Method of Moments
PET	Poly Ethylene Terephthalate
RF	Radio Frequency
RFID	Radio Frequency Identification
ROM	Read Only Memory
RTLS	Real-time Locating Systems
VLF	Very Low Frequency
UHF	Ultra High Frequency

# CHAPTER 1

## INTRODUCTION

Radio Frequency IDentification (RFID) transponders have been extensively used in many services in the industry such as access control, parcel and document tracking, distribution logistics, automotive systems, and livestock or pet tracking. In these applications, a wireless communication link is established between a remote transponder (composed of antenna and integrated circuit (IC)) and an interrogator (reader). In passive tags, the energy necessary to turn on the microchip comes from the reader system itself. A backscattering modulation is accomplished when the chip acts as a switch.

RFID transponders operate in several frequency bands. The specific frequency is controlled by the radio regulatory organization in each country. The general frequencies for RFID are 125-134 kHz (LF), 13.56 MHz (HF), 400-960 MHz (UHF), and 2.45 or 5.8 GHz (Microwave). Although there are other frequencies used, these are the main ones. In the UHF band, there are two areas of interest, one around 400 MHz (e.g.433 MHz) and another around 860 – 960 MHz. Each of the frequency bands has advantages and disadvantages for operation. There exists no single frequency for every application.

The low frequency (125-134 kHz and 13.56 MHz) transponders operate much better near water or humans than do the higher frequency transponders. On the other hand, for passive transponders, the lower frequencies generally have less

range, and they have a slower data transfer rate. High frequency transponders are used when more information needs to be transferred for longer distances.

The higher frequency ranges (i.e. 868 MHz) have more regulatory controls and differentiates from country to country. 860-960 MHz RFID frequency range has also become more and more popular in the previous years since the distortion of the propagating electromagnetic waves due to reflection, refraction, diffraction and power absorption by nearby objects and materials is worse at frequencies higher than UHF (i.e. 2.45 and 5.8 GHz). Environmental conditions that have negative effects in the overall performance of the RFID tags are less for the UHF (i.e 868 MHz) than they are for even higher frequencies (i.e. 2.45 and 5.8 GHz). This is the most important reason why UHF tags are very popular for higher frequency applications.

Along with the power sensitivity of the chip, the transponder's antenna plays a most important role in the overall RFID system performance factors, such as the overall size, the reading range, and the compatibility with tagged objects. The design goal is to achieve the inductance input impedance matching, and to miniaturize the antenna size.

In this thesis, RFID tag antenna design procedures and problems, most used antenna complex conjugate matching (folded dipoles, T-match, proximity-coupled loop and nested-slot), and size reduction techniques (meandered-line structures) for operational bandwidth and gain/radiation pattern/radiation efficiency are introduced for UHF RFID tags. For each design solution, the roles of the main geometrical and material parameters over the complex impedance tuning are investigated.

## 1.1 Scope and Outline of the Thesis

The main theme of this thesis is to investigate RFID tag antenna design procedures and problems, most used antenna complex conjugate matching and size reduction techniques for operational bandwidth and gain/radiation pattern/radiation efficiency for UHF RFID tags. For each design solution, the roles of the main geometrical and material parameters over the complex impedance tuning are investigated.

This thesis can be divided into five main chapters; background, RFID tag antenna design procedures and problems, folded dipole antenna designs, most used antenna complex impedance matching techniques and size reduction techniques.

Chapter 2 is a literature survey providing background information about RFID fundamentals that is necessary for better understanding of the following chapters. This chapter also discusses the reader-tag relationship from a system point of view. In addition, different modulation techniques used in an RFID system are discussed in the first part.

Chapter 3 focuses on the design procedures and problems to be considered designing an RFID tag antenna. Various antenna design requirements are discussed in this chapter.

In chapter 4, several passive RFID tag designs are discussed in detail in terms of RF design for the 915 MHz frequencies because of this increased interest in the industry. For this purpose, two 2-wire folded dipole and one 3-wire folded dipole antenna designs are presented.

In chapter 5, most used RFID tag antenna complex conjugate matching (T-match, proximity-coupled loop and nested-slot) techniques for operational bandwidth and gain/radiation pattern/radiation efficiency are introduced for UHF RFID tags.

For each design solution, the roles of the main geometrical and material parameters over the complex impedance tuning are investigated.

Finally, designs and implementations of two meander-line RFID tag antennas with loading bar and four meander-line RFID tag antennas having unequal turns, which are examples of size reduction techniques, are presented in chapter 6 followed by the conclusions in chapter 7.

## **CHAPTER 2**

### **RFID TECHNOLOGY**

Chapter 2 will provide brief background material about RFID technology which is necessary for better understanding of the following chapters. The first section of the chapter will provide an overview on RFID fundamentals. The second section will present the history of the RFID technology. The third section will give general and technical definitions of transponders and interrogators with their sub-parts. Finally, in the fourth section coupling mechanisms in the RFID system will be discussed.

#### **2.1 RFID Fundamentals**

RFID technology is just one of several technologies known as auto-identification (Auto-ID) technology which uses radio frequency waves to transfer data between a reader (transceiver) and a moveable or stationary objects (transponder or tag) to identify, categorize, and track the objects as they move through a controlled environment [1].

##### **2.1.1 RFID System Layers**

The RFID system consists of two different layers which are physical and information technology (IT).

Physical layer consists of the followings:

- One or more radio-frequency (RF) tags
- One or more interrogators (readers)

- One or more reader antennas
- Deployment environment

Information technology (IT) consists of the followings:

- Hardware such as computers
- Networks
- Software (device drivers, filters, middleware, and user applications)

The Figure 2.1 shown below provides an overview of the RFID system physical layer.

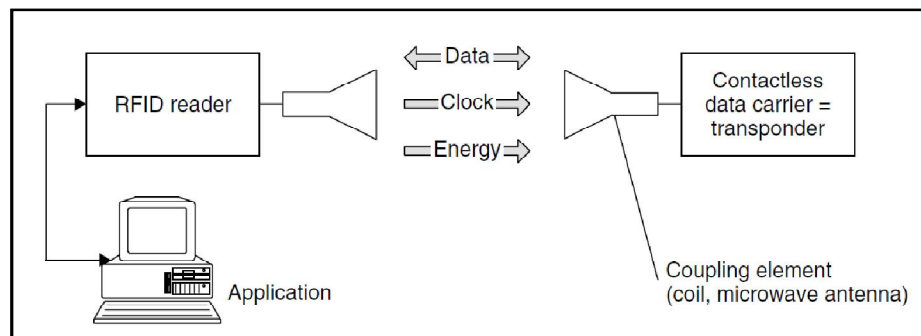


**Figure 2.1 An overview of the RFID system physical layer [1].**

The components of the RFID system physical layer in Figure 2.1 can be explained in the following terminology.

**Tag:** There are several methods of identifying objects using RFID, but the most common is to store a serial number that identifies a product and other information (as required) on a microchip that is attached to an antenna which is literally defined as RFID tag. RFID tags can be either active or passive depending on their power supply to the microchip is internally or externally (from the reader). RFID tags can be read-only or read/write [1].

**Antenna:** Receives and transmits the electromagnetic waves and converts the electrical signal to electromagnetic waves and vice versa. There are two types of antennas in an RFID system. One is resident in the tag while the other is connected to the reader. When one refers to an antenna, it is meant to be the one connected to the reader.

**Reader:** The reader (interrogator) reads data from and writes data to the tag by means of antenna. When reading, it converts analog signal returned from the antenna into digital format and when writing, it converts digital data received from the host computer into analog signal. Reader receives commands from application software and also provides energy to the passive tags [1].

**Deployment environment:** A space within which the RFID system is installed. It includes ambient RF signals present there and the RF reflective and absorbing objects in the close proximity.

**Host Computer:** It manages the readers, store and evaluate obtained data.

**Network:** It helps to transport data and commands.

### **2.1.2 RFID Information Flow:**

RFID information flow from simple tag to the host application can be summarized as follows [1]:

- First, host manages reader(s) and issues commands.
- Reader and tag communicate using a radio-frequency (RF) signal.
  - Carrier signal is generated by the reader (on request from the host application).
  - Carrier signal is sent out from the reader antenna(s).
  - Carrier signal hit tag(s).
  - Tag receives and modifies carrier signal and reflects back the modulated signal.

- Reader antenna(s) receive the modulated signal and sent them to the reader.
- Reader decodes the signal into digital data.
- Digital data is returned to the host application. Data may be filtered and aggregated before being sent to the host application.

### **2.1.3 Other Auto-ID Technologies:**

Other Auto-ID technologies include [1]:

- Barcode (uniform product codes)
- Optical character recognition (OCR)
- Magnetic ink character recognition (MICR)
- Magnetic strip
- Biometrics (such as retinal scans, fingerprints, etc)
- Voice recognition

RFID and barcode are two different technologies and have different applications, which many times overlap. RFID technology has brought many advantages over the existing barcode technology. The big difference between the two is barcode is a line-of-sight technology. Since RFID tags don't need to be line-of-sight like optical barcode technology, its popularity and demand has increased. In addition, barcode can only recognize a single item at a time, whereas RFID can read multiple items. Furthermore, RFID tags can be embedded in an item rather than the physical exposure requirement of barcodes and can be detected using RF signal. RF signal generation also enhances the read range for RFID tags. Barcodes only contain information about the manufacturer or originator of an item and basic information about the object itself; however, RFID is particularly useful for applications in which the item must be identified uniquely. RFIDs also can hold additional functionality which means more bits of information [1].

The Table 2.1 below lists some of the differences between RFID and barcode.

**Table 2.1 Some of the differences between RFID and barcode [1].**

<b>RFID</b>	<b>Barcode</b>
No line of sight required.	Line of sight required.
Uniquely identifies items, cases, pallets.	Identifies only item category.
Simultaneous identification.	Scans only single item at a time.
Read/Write capability.	No write capability.
Can be used in harsher environments.	Smudges make it difficult to read.
More data storage capacity.	Limited data storage capacity.
Low sensitive to the orientation.	Require proper orientation.
More expensive (\$0.15+).	Cheaper to produce (\$0.001).
Require a separate process to create tags and attach them.	Can be easily printed on boxes during manufacturing.

#### **2.1.4 RFID Technology Applications:**

There exists widespread usage of this technology in manufacturing (automotive systems), supply chain (shipping and receiving, warehousing, inventory management), pharmaceutical (product authentication), healthcare (patent and equipment tracking), library and video store, security, cashless payments, hospitality, amusement park and event management, recall and return management, document management, transportation management (rail cars and truck tracking, toll collection, vehicle theft detection and speed tracking), livestock/pet tracking [1].

## **2.2 History of RFID**

The foundation of RFID technology can be traced back to World War II. The Germans, Japanese, Americans and British were all using radar- which had been discovered in 1935 by Scottish physicist Sir Robert Alexander Watson-Watt- to warn of approaching planes while they were far away; however, it was impossible to distinguish enemy planes from country's own ones.

The Germans discovered that by just rolling planes while returning to base changes the radio signal reflected back which would alert the radar crew on the ground. The Germans identify their planes by this simple method. The British developed the first active identify friend or foe (IFF) system by just putting a transmitter on each British plane which received signals from the aircrafts. This identified the planes as friendly [2].

An early exploration of the RFID technology came in October 1948 by Harry Stockman [3]. He stated back at that time that “considerable research and development work has to be done before the remaining basic problems in reflected-power communication are solved, and before the field of useful applications is explored”. His vision flourished until other developments in the transistor, the integrated circuit, the microprocessor, and the communication networks took place. RFID had to wait for a while to be realized [4].

Following the WW II from 1950s to 1960s, the progress in radar and RF communications systems continued (Table 2.2).

The first application field trials initiated in 1960s and the first commercial product came. Investigating solutions for anti-theft by companies revolutionized the whole RFID industry. They explored the anti-theft systems that used RF waves to watch if an item is paid or not. This was the beginning of the 1-bit

Electronic Article Surveillance (EAS) transponders by Checkpoint, Sensormatic, and Knogo. This is by far the most commonly used RFID application.

**Table 2.2 The milestones in RFID technology [2].**

<b>Decade</b>	<b>Event</b>
<b>1940 - 1950</b>	Radar defined and used, major World War II development effort. RFID invented in 1948
<b>1950 - 1960</b>	Early exploration of RFID technology, laboratory experiments.
<b>1960 - 1970</b>	Development of the theory of RFID. Start of applications field trials.
<b>1970 - 1980</b>	Explosion of RFID development. Tests of RFID accelerate. Very early adopter implementations of RFID.
<b>1980 - 1990</b>	Commercial applications of RFID enter mainstream.
<b>1990 - 2000</b>	Emergence of standards. RFID widely deployed. RFID becomes a part of everyday life.

The electronic identification of items caught the attention of large companies as well. In 1970s large companies like RCA, Raytheon (RayTag 1973), and Fairchild (Electronic identification system 1975, electronic license plate for motor vehicles 1977) constructed their own RFID units. Thomas Meyers and Ashley Leigh of Fairchild also built up a passive encoding microwave transponder in 1978 [4].

By 1980s there were conventional applications all around the world. The RFID was spreading quickly without any boundaries. In the United States, RFID technology found itself in transportation (highway tolls) and personnel access (smart ID cards). In Europe, short-range animal tracking, industrial and business

systems RFID applications caught the attention of the industry. In 1987, world's first commercial application for collecting tolls in Norway, and after in the United States by the Dallas North Turnpike (1989) were established using RFID technology.

In 1990s, IBM engineers initiated and patented a UHF RFID system. IBM carried out early research with Wal-Mart, but this was never commercialized. UHF (860-960 MHz) offered longer read range and faster data transfer in contrast to the 125 kHz and 13.56 MHz applications. With these achievements, it led the way to the world's first open highway electronic tolling system in Oklahoma in 1991. This was followed by the world's first combined toll collection and traffic management system in Houston by the Harris County Toll Road Authority (1992). In addition to this, GA 400 and Kansas Turnpike Highways were the first to put into service of multi-protocol tags which allowed two different standards to be read [2, 4].

Following IBM's early pilot studies in 1990s with Wal-Mart, UHF RFID's popularity enhance in 1999, when the Uniform Code Council, European Article Number (EAN) International, Procter & Gamble and Gillette teamed up to launch the Auto-ID Center at the Massachusetts Institute of Technology. This research paid particular attention on putting a serial number on the tag to keep the price down using a microchip and an antenna. By storing this information in a database, tag tracking was finally comprehended in this imposing networking technology. This was a crucial point in terms of business because now a stronger communication link between the manufacturers and the business partners was established. A business partner would now know when a shipment was leaving the dock at a manufacturing facility or warehouse, and a retailer could automatically let the manufacturer know when the goods arrived [2].

The Auto-ID Center also developed the two air interface protocols (Class 1 and

Class 0), the Electronic Product Code (EPC) numbering scheme, and the network architecture used to inquire about the RFID tag data between 1999 and 2003. The Uniform Code Council licensed this technology in 2003 and EPCGlobal was born as a joint venture with EAN International, to commercialize EPC technology.

Today some of the major retailers in the world such as Albertsons, Metro, Target, Tesco, Wal-Mart, and the U.S. Department of Defense affirmed that they plan to use EPC technology to track their goods. The pharmaceutical (healthcare), tire (automotive), defense and other industries are also pushing towards adaptation of this new technology. EPCGlobal accepted a second generation (Gen-2 ISO 18000-6C ) standard in December 2004. This standard is extensively used in the RFID world today [2, 5].

### 2.3 RFID Transponders and Interrogators

The fundamental components of an RFID system were presented in Figure 2.2. These are primarily a transponder (tag), an interrogator (reader), communication networks and host computers. In this part, detailed explanation of the transponder and interrogator sub-parts of the higher level system will be given [1].

#### 2.3.1 Transponder (Tag)

The RFID tag is a device that consists of an electronic circuit (ASIC) and an antenna integrated into one piece.

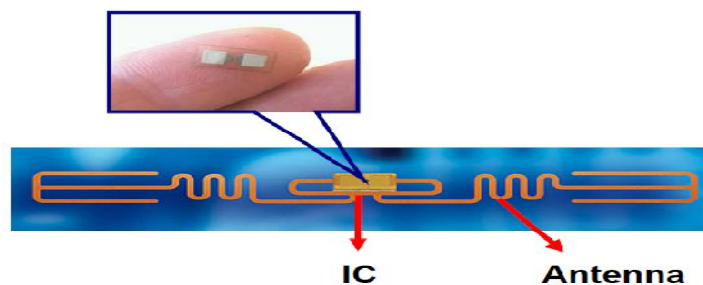


Figure 2.2 RFID Tag picture showing the components.

### **2.3.1.1 RFID Tag Components**

As shown in Figure 2.2 the RFID tag consists of four components (Chip, antenna, strap, and substrate)

#### **Application Specific Integrated Circuit (ASIC)**

The integrated circuit (IC; chip) is mainly comprised of RF front-end, some basic signal processing blocks, logic circuitry (algorithm implementation), and memory for storage (Figure 2.3). These components are crucial for the operational functionality of the tags [8].

#### **Elements:**

- **RF Front-end:**

The RF front-end generally consists of a simple circuit like resistor-inductor circuit. The RF front-end is the core interface between the antenna and signal processing unit. It is responsible of implementing modulators, voltage regulators, resets and connections to the external antenna.

- **Signal Processing:**

Signal processing handles the necessary data acquisition from RF front-end.

- **Control Logic:**

Control logic takes control of functions that include the error and parity/CRC checkers, data encoders, anti-collision algorithms, controllers, command decoders. Data encryption and even tamper-proofing hardware can be included in more complex RFID ICs.

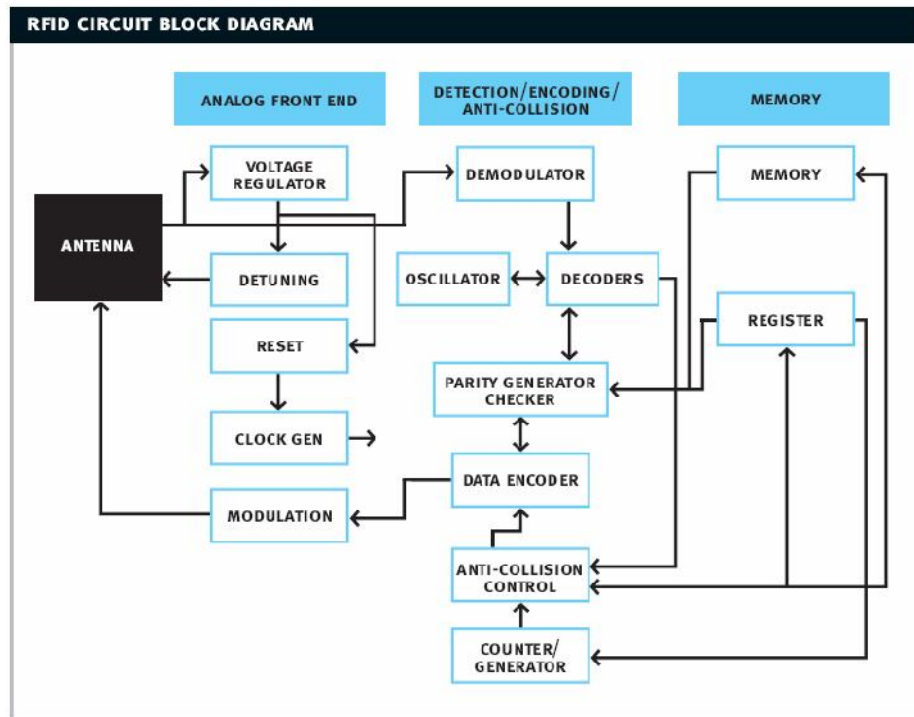


Figure 2.3 Basic RFID IC block diagram [8].

• **EEPROM Storage Memory:**

Electrically Erasable and Programmable Read-only Memory (EEPROM) gives the functionality of tags to be read/write; however, tags that cannot be programmed use state machines or read-only memories (ROM) to store or generate the information [1]. Because of the included programmable feature of EEPROM, it is the memory storage unit in the new Gen 2 RFID standard.

**The Antenna**

RFID Tag antenna receives and reflects radio-frequency (RF) waves coming from the reader antenna. Since it is the largest part of the tag, it determines the size of the tag. Antenna is designed for a particular frequency and customized for the application.

### **The Strap**

The strap is made up of an IC and two conducting pads that can be connected to an antenna to enable high-speed conversion into inlays, labels or packaging materials.

### **The Substrate**

The Substrate holds IC, strap, and antenna together on the tag and inlays. It may have adhesive to attach tags to objects.

## **2.3.1.2 Classification of RFID Tags**

Tags can be categorized according to the power source, frequency, functionality and protocols that they belong to. In this section, tags will be explained in detail according to these criteria.

### **2.3.1.2.1 Power Source**

Depending on the source of the power, tags are classified as:

- Passive
- Semi-active or semi-passive (also called battery assisted passive tags- BAP or battery assisted tag - BAT)
- Active

#### **Passive Tags:**

The passive tag does not have its own power source (no onboard battery) or a radio transmitter. It obtains power from the RF waves emitted by the reader. Therefore, it can communicate only when inside the read zone and is energized by the RF waves. The passive tag's read range is limited by the amount of power that can be obtained

from the RF waves from the reader. Beyond approximately 3-5 m from the reader antenna, the tag cannot collect enough power to turn on its IC and thus cannot communicate with the reader. Some of the advantages of the passive tag are small size, lightweight, inexpensive and longer life (20+ years). These tags, if manufactured in billions will come down in price from \$0.30 to \$0.05 in the next 2 years [8]. The disadvantages of passive tags are a lower read range and high power readers.

### **Semi-Active (Semi-Passive) Tags:**

The semi-active tag has a battery on it but no radio transmitter. The battery powers its integrated circuit (IC), which helps it to modulate the reflected signal. The reflected signal is required because the tag does not have a radio transmitter. The advantage of this type of tag is that you do not need to power the tag from the reader. Therefore, one can use low-power readers and store more data on the tag. This type of tag is used to get longer read range (up to 50m) or to couple the tag with environment sensors such as temperature, pressure, relative humidity, Global Positioning System (GPS), etc. Since the sensors require continuous power, the battery is required on the tag. The disadvantages of these tags are higher cost, larger and heavier tag and limited life due to battery [1].

### **Active Tags:**

Active tags have their own battery and transmitters. This tag communicates at a longer distance because it is not dependent on a reflected signal. Its communication distance ranges from 100m to 225m. It has more memory, up to 128Kbytes. However, the cost is high, the size is larger, and the weight is higher. So, the same advantages and disadvantages of semi-active tags also apply to the active tag [1]. The Table 2.3 below provides an overview of the tag parameters and related data for passive and active tags.

**Table 2.3 Active vs. Passive Tag**

<b>Parameters</b>	<b>Passive Tags</b>	<b>Active Tags</b>
Tag power source	RF energy from reader	Internal to tag
Tag battery	No	Yes
Availability of power	Only in the RF field of reader	Continuous
Cost	\$0.20 to \$0.5	\$20+
Size	Small	Limited by battery size
Tag life	20+ years	2 to 5 years
Reader signal strength	High	Low
Ranges	10cm to 6m	100m to 225m
Multi-tag reading	Few hundred per second with slow moving speed	Thousands of tags recognized up to 160 kmh
Data Storage	Up to 128Kb or read/write with sophisticated search and access	128 bytes of read/write

The Table 2.4 below points out the primary tradeoff between active and passive tags is range versus cost.

**Table 2.4 Active vs. passive tag tradeoffs**

<b>Active</b>	<b>Passive</b>
<ul style="list-style-type: none"> <li>• Box, pallet, or container level tracking</li> <li>• High-value or critical assets</li> <li>• People tracking (such as patients)</li> <li>• Real-time location</li> <li>• Long-range monitoring</li> </ul>	<ul style="list-style-type: none"> <li>• Item, box, or case level tracking</li> <li>• Low-value assets</li> <li>• Identification (passports, badges, etc.)</li> <li>• DVDs, documents, etc.</li> <li>• Library checkout</li> <li>• Apparel</li> </ul>

<ul style="list-style-type: none"> <li>• Area monitoring</li> <li>• Security</li> <li>• Sensor monitoring</li> <li>• Vehicles</li> </ul>	<ul style="list-style-type: none"> <li>• Baggage tracking</li> <li>• Point of sale</li> <li>• Blood supply, drug packages, etc.</li> <li>• Livestock, pets, etc.</li> <li>• Computers, printers, televisions, camcorders</li> <li>• Company assets</li> </ul>
--	---

### 2.3.1.2.2 RFID Tag Characteristics

As pointed out in the following chapters, tags are designed to operate at different frequency bands to communicate with the interrogator because of:

- Government regulatory requirements
- Type of host material (such as metal, water, etc.)
- Read range and speed required

Four frequency bands are used in tag design:

- 125, 135 KHz (low frequency - LF)
- 13.56 MHz (high frequency - HF)
- 860-960 MHz (ultra high frequency - UHF)
- 2.45 and 5.8 GHz (microwave)

Different frequency tags have different characteristics. They behave differently when tagged to different types of material. The read range varies from a few centimeters to few meters. Because of government regulations and customer mandates, certain frequency tag may be selected.

- **Low Frequency Tags: 125 to 134 KHz (LF)**

LF tags require a coil antenna with several hundred turns around a ferrite core. They are expensive to manufacture. Attenuation of water is less compared to high frequency tags. These tags are first to be used and are still being used for animal tracking. LF does not penetrate or transmit around metals and LF tags are well suited for applications requiring reading small amounts of data at slow speeds and minimal distances.

- **High Frequency Tags: 13.56 MHz (HF)**

HF tags have simpler antenna design with fewer turns of coil (five to seven turns) and are therefore thinner and cheaper to manufacture than LF tags. HF like LF is not affected by water. HF tags are well suited for applications requiring small read distances or where the tagged objects contain water like pharmaceuticals, humans, and animals. They have higher data rate than LF and HF readers cost less than the LF and the UHF readers. HF is used in Smart Cards popular in Europe and the typical read range of HF tag is about 30-70 cm. HF reader antennas fill the volume surrounding antenna and are not directional.

- **Ultra High Frequency Tags: 860-960 MHz (UHF)**

UHF tags have good non-line-of-sight communication (except for “lossy” materials) capability. They have higher data rate and a typical read range of up to 5m. UHF reader antennas are directional providing a controlled read zone. This is the most talked about frequency range for supply chain applications. UHF does not penetrate water/tissue, UHF readers are more expensive than HF and the technology is less matured than HF. Also regulations regarding UHF use are different in different parts of the world. Different countries allow different frequencies, number of channels, maximum power, and duty cycle.

- **Microwave Frequency Tags: 2.45, 5.8 GHz**

Microwave tags also have good non-line-of-sight communication (except for “lossy” materials) capability. They have higher data rate and a typical read range of up to 15m. These tags are also effective around metals with tuning/design adaptations. Microwave reader antennas are directional providing a controlled read zone. Table 2.5 below summarizes the RFID frequencies and related applications.

**Table 2.5 List of the RFID frequencies and related applications [1]**

Frequency band	Data and speed	Read range	Usage	Advantages	Disadvantages
Low frequency (LF): 125 to 134 KHz	<ul style="list-style-type: none"> <li>• Low-read speed</li> <li>• Small amount of data</li> </ul>	Vey short; up to 40 cm	<ul style="list-style-type: none"> <li>• Access control</li> <li>• Animal tagging</li> <li>• Inventory control</li> <li>• Car immobilizer</li> </ul>	<ul style="list-style-type: none"> <li>• Good in environment with water</li> </ul>	<ul style="list-style-type: none"> <li>• Small range, data and speed</li> <li>• No anti-collision</li> <li>• Costly tags</li> </ul>
High frequency (HF): 13.553 to 13.567 MHz	<ul style="list-style-type: none"> <li>• Medium-read speed</li> <li>• Small/medium amount of data</li> </ul>	Short to medium; 30 cm to 1m	<ul style="list-style-type: none"> <li>• Smart Cards</li> <li>• Item or Case level tagging</li> </ul>	<ul style="list-style-type: none"> <li>• Sufficient data amount</li> <li>• Most standards in place</li> <li>• Good in moist environment</li> <li>• Anti-collision 10-40 tags/sec</li> </ul>	Poor in metal environment
Ultra-high frequency (UHF): 860 to 960 MHz	<ul style="list-style-type: none"> <li>• High-read speed</li> <li>• Small/medium amount of data</li> </ul>	Medium; 60 cm to 6m	<ul style="list-style-type: none"> <li>• Pallet or Case level tagging</li> <li>• Wal-mart, Dod mandates</li> </ul>	<ul style="list-style-type: none"> <li>• Good range, high speed</li> <li>• Many standards in place</li> <li>• Good in metal environment</li> <li>• Anti-collision 500 tags/sec</li> </ul>	High tag cost
Microwave frequency: 2.45 GHz	<ul style="list-style-type: none"> <li>• High-read speed</li> <li>• Medium amount of data</li> </ul>	Medium; 60 cm to 15m	<ul style="list-style-type: none"> <li>• Container or rail car</li> <li>• Toll collection</li> <li>• Pallet or level tagging</li> </ul>	<ul style="list-style-type: none"> <li>• Long range, high speed</li> <li>• Good in metal environment</li> <li>• Anti-collision 50 tags/sec</li> </ul>	<ul style="list-style-type: none"> <li>• High tag cost</li> <li>• Poor in moist environment</li> </ul>

### 2.3.1.2.3 RFID Tag Functionality

The EPCGlobal tag classes categorize tags by implemented functionality. EPCGlobal distinguishes RFID tags in six classes (numbered 0 through 5) according to their:

- Read and write capabilities
- Power sources
- Communications capabilities
- Memory capacities

Tags are classified from classes zero to five, with zero being the class with the least functionality [5]. The Table 2.6 below lists the various classifications and their related functionality.

**Table 2.6 List of the various classifications and their related functionality [5]**

<b>Class</b>	<b>Functionality</b>
0	<ul style="list-style-type: none"><li>• Passive</li><li>• Data written once during manufacture</li><li>• Read only</li></ul>
1	<ul style="list-style-type: none"><li>• Passive</li><li>• Factory or field programmable only once</li><li>• Read-only functionality after initial programming</li></ul>
2	<ul style="list-style-type: none"><li>• Passive</li><li>• Read/write functionality</li><li>• User memory and encryption</li></ul>
3	<ul style="list-style-type: none"><li>• Semi-passive</li><li>• On-board sensors</li><li>• Read/write functionality</li><li>• User memory</li></ul>
4	<ul style="list-style-type: none"><li>• Active</li><li>• On-board sensors</li><li>• Read/write functionality</li><li>• Peer-to-peer communication with other active tags in the same frequency band with readers.</li></ul>
5	<ul style="list-style-type: none"><li>• Readers and read/write functionality can power class 0, 1, and 2 tags.</li><li>• Can communicate with class 0 to 5 tags and devices.</li></ul>

#### 2.3.1.2.4 RFID Tag-Reader Protocols

A protocol is the tag-to-reader wireless air interface scheme. Basically, it is a language that allows the tag and the reader to communicate with each other. Protocols are defined by the manufacturers of the tags and readers or by various standards setting organizations and may be proprietary or open. Open standardized protocols help readers and tags from different manufacturers work together. The reader and tag must use the same protocols to communicate [1].

Tag reader protocols are specified by:

- Air interface
  - Frequency
  - Maximum emission power
  - Modulation and encoding
  - Data rate
  - Packet structures
- Data structure
  - 64 bit
  - 96bit
  - 128 bit
- Command and control
  - Reader-to-tag communication
  - Tag-to-reader communication
  - Anti-collision algorithm used to isolate tag one by one

#### Example of protocols:

Protocols are independently developed and generally do not interoperate since the user needs transparency (that is, multiprotocol and multiband readers). Protocols preceded by a company name are proprietary protocols. The followings are the examples of protocols [1]:

- ISO 14443 (A/B) [51]
- Philips I-Code
- ISO 15693 [52]
- TI Tag-It

- Matrics electronic product code (EPC) Class 0
- Alien electronic product code (EPC) Class 1
- ISO 18000-4 (A/B) [53]
- ISO 18000-6 (A/B/C) [54]
- EM Micro
- Philips I-Code HSL
- Intermec Intellitag

### 2.3.2 Interrogator (Reader)

Another important part in a RFID system is the reader sub-system. It is possible to divide an RFID reader system into two differentiated groups, namely the high frequency interface and the control system. These groups interact among each other and with an external host system as can be seen in Figure 2.4.

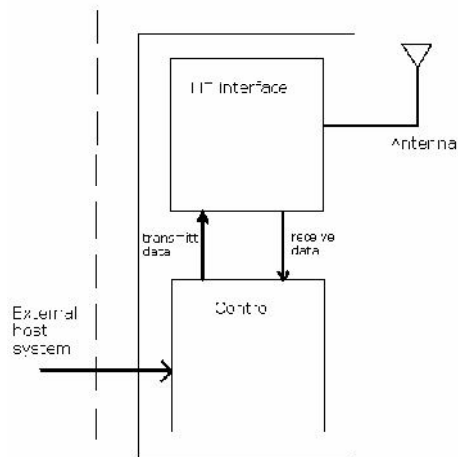


**Figure 2.4 General RFID reader block diagram.**

The main functions performed by a reader are demodulating the data retrieved from the tag, decoding the received data, and energizing in the case of passive and semi-passive tags. Readers are designed for various frequencies or protocols [1]. A more detailed diagram of the reader can be found in Figure 2.5.

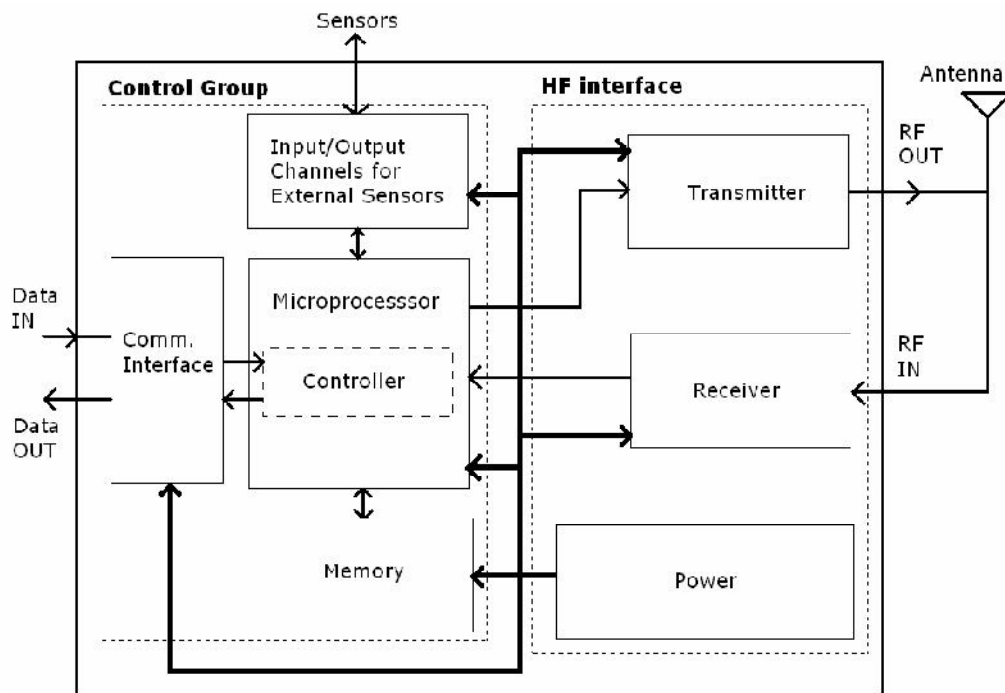


Figure 2.5 RFID reader sub-block diagram

### 2.3.2.1 The HF Interface

The HF interface carries out the principle functions listed below:

- Demodulates and decodes the information retrieved from the tag.
- Supply power to passive tags to communicate with them.

#### Elements:

##### • Antenna:

A reader antenna is a converter between radiated waves and wired voltage. It is the biggest and the most obvious component of system and is most vulnerable to obstruction by metallic objects. With UHF and microwave, antenna polarization is important and the choice depends on the circumstances of use [1]. For example:

- In a controlled tag orientation environment, using linearly polarized antenna to provide the longest range with the least amount of power is more efficient.

- In an uncontrolled tag orientation environment, using circularly polarized antenna to provide the best tag readability is more efficient.

- **Transmitter:**

The main task of this element is to transmit power and the clock cycle to the tags. It is part of the transceiver module.

- **Receiver:**

This component is responsible for receiving signals from the tag via the antenna. Afterwards, it sends these signals to a microprocessor where the digital information is extracted.

- **Power:**

This module supplies the adequate power levels to all components in the reader.

### **2.3.2.2 The Control Group**

To allow the functions of decoding, error checking and communication with an external system the control unit makes use of a microprocessor, a controller, a communication interface, memory and input/output channels.

- **Microprocessor:**

The reader protocol is implemented in the microprocessor. The microprocessor will interpret the received commands, and then seek the memory for the corresponding program code and will execute it depending on the protocol required by the particular standard. At this is the point error checking is performed [1].

- **Controller:**

In order to allow joint operation with an external system, a system called the controller, responsible for converting external orders to understandable

microprocessor binary code, is needed to enable communication. The controller may be either in a software or hardware form.

- **Communication Interface:**

By using the controller, the communication interface is able to interact with an external host system by transferring data, passing or responding to instructions. The communication interface can be a part of the controller or an independent entity depending on the integration level and speed requirements.

- **Memory:**

The memory is responsible for storing the data retrieved from the tags. The data will be transmitted to the host system when demanded.

- **Input/output Channels for External Sensors:**

While operating a reader it might happen that when the tags are not in its read range, making continuous operation is a waste of energy. For instance; in a conveyor belt passing in front of the reader, it is likely to efficiently run the reader by activating it at the required times by using external sensors that is capable of detecting the presence of an item nearby.

Additionally, it is possible to classify the readers by the communication interface in use or by its mobility. A brief description of each category is given as follows:

### **Communication Interface:**

- **Serial Reader:**

This reader uses a RS232 serial port to communicate with the host system and transfer data or commands executed by the user or application. These readers have a lower data transfer rate compared with others such as a wired network reader and have a cable length limitation. On the other hand, serial port connections are more reliable.

- **Network Reader:**

This reader can be connected wired or wirelessly to a computer, therefore it appears as a network device. In this case, the cable length is not a limitation, but the connection is not as reliable as in serial readers.

**Mobility of Readers:**

- **Stationary Reader:**

These readers are mounted on a wall, portal or suitable structure in the read zone. They can be mounted on moving objects such as trucks. These readers usually are connected to one or more external antennas. Usually more common varieties of UHF fixed readers have four antenna ports to connect external antennas. Agile readers are able to operate in different frequencies (reader and tag frequencies must match) and use different communications protocols (reader and tag protocols must match). An RFID printer is a type of stationary reader able to print a barcode and write on its RFID tag.

- **Handheld Reader:**

This type of reader has an integrated antenna on it and can operate as a handheld unit.

## **2.4 RF in RFID and Coupling Mechanisms**

The RFID systems may be divided into two broad categories, near-field and far-field coupled systems. There is a fundamental difference between them that dictates how they operate and how they can be used. In this part, the major difference between these two technologies and the coupling mechanisms between the reader and the tag will be explained in detail.

### **2.4.1 RF in RFID**

The antenna of the transponder is the only radiating element which provides the

RF communication link from the transponder to the interrogator and vice versa. The general expression for the fields from a radiating sinusoidal current filament source is given below as [6]:

$$E_{\theta} = \frac{I_o dz}{4\pi} \left[ \frac{j\omega\mu}{r} + \sqrt{\frac{\mu}{\epsilon}} \frac{1}{r^2} + \frac{1}{j\omega\epsilon r^3} \right] \epsilon^{-jkr} \sin(\theta) \quad (1)$$

$$E_r = \frac{I_o dz}{2\pi} \left[ \sqrt{\frac{\mu}{\epsilon}} \frac{1}{r^2} + \frac{1}{j\omega\epsilon r^3} \right] \epsilon^{-jkr} \cos(\theta) \quad (2)$$

$$H_{\phi} = \frac{I_o dz}{4\pi} \left[ \frac{jk}{r} + \frac{1}{r^2} \right] \epsilon^{-jkr} \sin(\theta) \quad (3)$$

where;

$I_o$  = the amplitude of the sinusoidal current filament source

$dz$  = the sinusoidal current filament source length

$k = \frac{2\pi}{\lambda}$ ,  $\lambda$  is the wavelength

$r$  = radial distance from the sinusoidal current filament source

$\omega = 2\pi f$ ,  $f$  is the frequency

$\mu$  = permeability of the medium

$\epsilon$  = permittivity of the medium

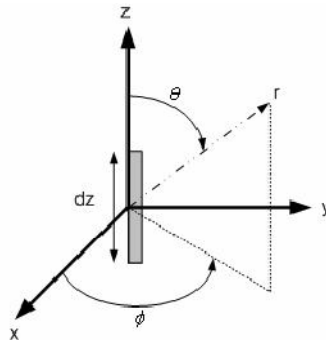


**Figure 2.6 Geometrical representation of the sinusoidal current filament source**

The geometry of the sinusoidal current filament source is displayed in Figure 2.6. Using the equations in (1, 2, 3), the three regions surrounding the radiating element can be identified. These regions are namely (a) reactive near-field, (b) radiating near-field (Fresnel) and (c) far-field (Fraunhofer) regions as shown in Figure 2.7 [7].

**Regions:**

• **Reactive Near-field Region:**

It is the part of the field in the vicinity of the antenna (distance  $R < 0.62\sqrt{D^3/\lambda}$ ) is predominantly reactive and  $1/r^3$  terms in the equations (1, 2) define this field.  $D$  is the largest dimension of the antenna and  $D \gg \lambda$  [7]. For a very short dipole, the outer boundary of this region is generally taken to exist at a distance  $\lambda / 2\pi$  from the antenna surface [7]. The waves in this field do not travel; on the other hand standing waves are stored this field. The tags at LF and HF frequencies are mostly loop or inductive coil antennas and operate in this region.

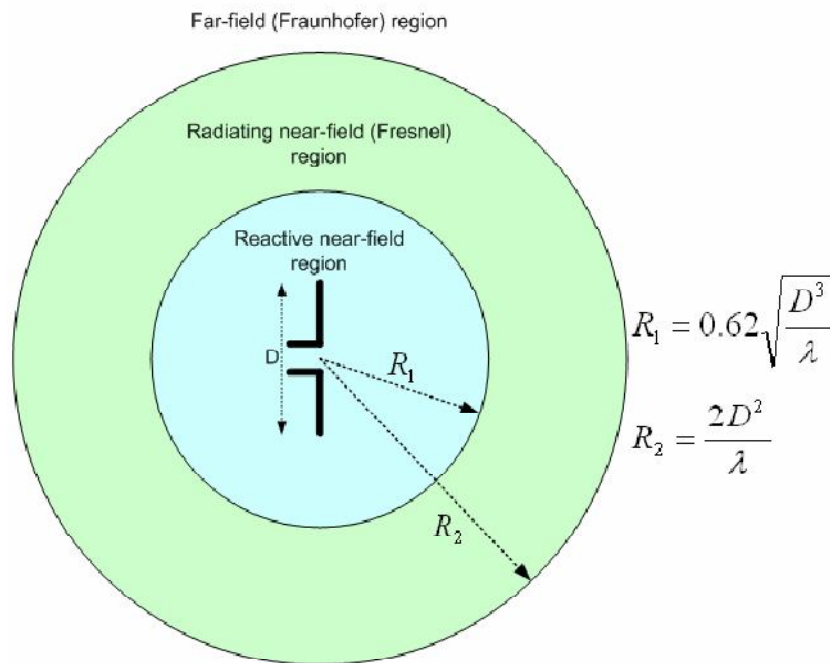


**Figure 2.7 Field regions of an antenna**

• **Radiating Near-field (Fresnel) Region:**

Standing waves and traveling waves of both near-field and far-field regions are included in the Fresnel region. It is present from just outside the boundary of reactive near-field region to the far-field region boundary. These fields are dominated by the  $1/r^2$  term in the equations (1, 2, and 3) and reach to  $2D^2/\lambda$  [6]. This region may not exist, if the antenna's maximum dimension is not large compared to the wavelength, [7].

• **Far-field (Fraunhofer) Region:**

It is defined as the field region of an antenna where the angular field distribution is essentially independent of the distance from the antenna. This is the region outside of the radiating near-field boundary. The traveling waves dominate in this region where they decay with a rate of  $1/r$ . These traveling waves carry the electromagnetic power to the passive and semi-passive UHF and microwave transponders.

In the far-field (Fraunhofer) region for a dipole antenna as shown in Figure 2.7,  $E_\theta$  and  $H_\phi$  take the form of

$$E_\theta = j\eta \frac{I_o}{2\pi r} \left[ \frac{\cos(\frac{kl}{2} \cos(\theta)) - \cos(\frac{kl}{2})}{\sin(\theta)} \right] \epsilon^{-jkr} \quad (4)$$

$$H_\phi = \frac{E_\theta}{\eta} = j \frac{I_o}{2\pi r} \left[ \frac{\cos(\frac{kl}{2} \cos(\theta)) - \cos(\frac{kl}{2})}{\sin(\theta)} \right] \epsilon^{-jkr} \quad (5)$$

where  $\eta$  is the intrinsic impedance ( $\sqrt{\frac{\mu}{\epsilon}} = 377 = 120\pi$  ohms for free space) and  $l$  is the length of the dipole antenna. Figure 2.8 shows the normalized  $E_\theta$  radiation for different lengths. As it can be seen from the figure, the directivity of the antenna increases when the length of the antenna increases. However; for some applications in RFID such as tags are attached to the boxes in large storage areas, omni-directionality is needed. In that case the increase in directivity could be a problem. When the length is increased to  $l > \lambda$ , another major problem occurs. The side lobes begin to increase as shown in Figure 2.9.

These side lobes cause nulls which mean no electric field radiation. For instance, the plotted pattern in Figure 2.9 has six nulls compared to only two in Figure 2.8. Current distribution plays an important role in the characterization of the previously shown radiation patterns.

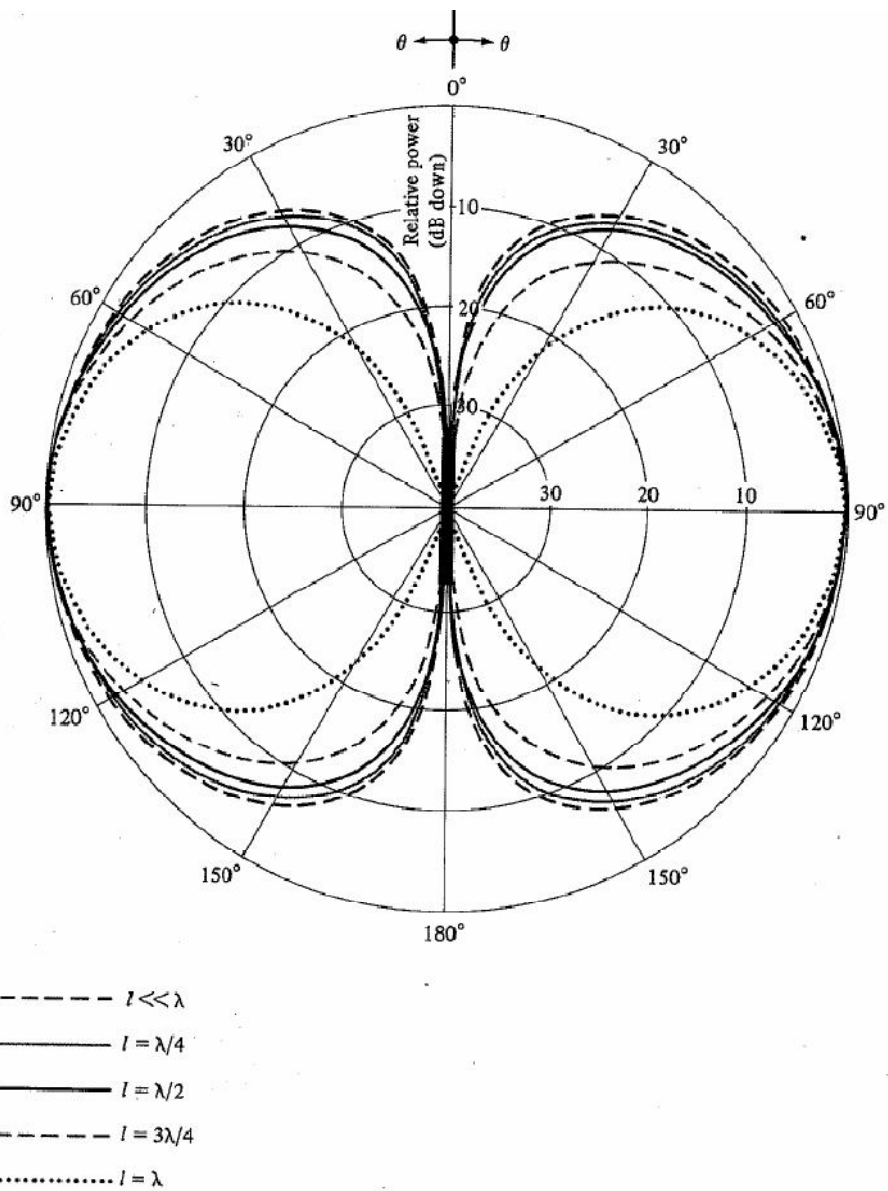


Figure 2.8 Elevation plane amplitude patterns for a thin dipole with sinusoidal current distribution ( $l = \lambda/4, \lambda/2, 3\lambda/4, \lambda$ ) [7].

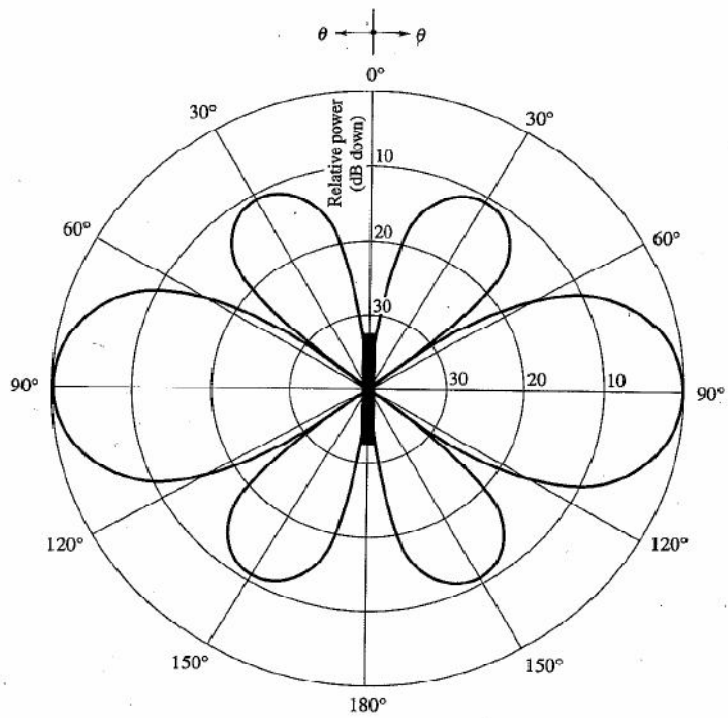
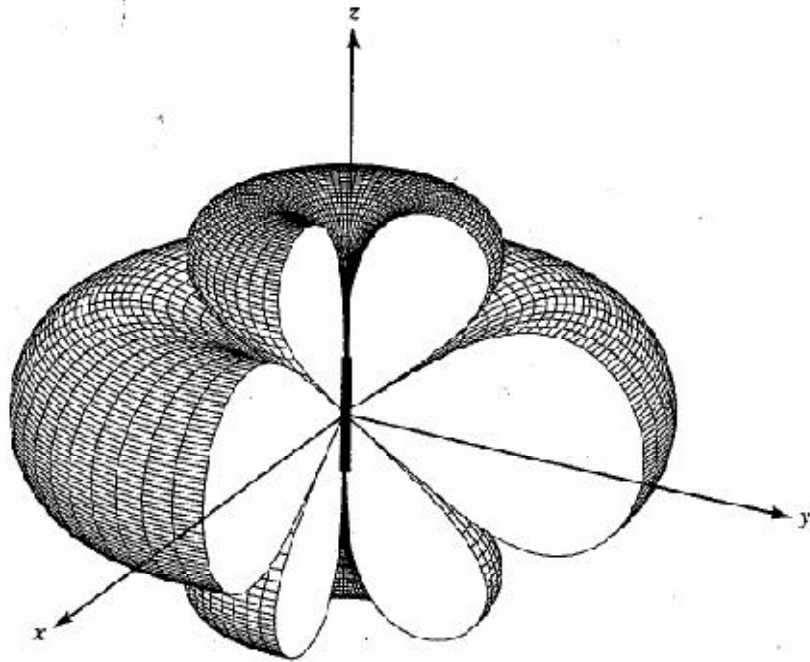


Figure 2.9 Three and Two-dimensional amplitude patterns for a thin dipole of  $l = 1.25\lambda$  and sinusoidal current distribution [7].



While determining the operating range of a UHF RFID transponder, both the distance at which the transponder receives enough power to turn the chip on and the distance at which the interrogator will be able to detect the reflected signal have to be considered. Generally, the transponder's receive sensitivity determines the reading range since the interrogator's receive sensitivity is lower than that of transponder's. The following maximum read range equation can be derived by using the Frii's free space formula:

$$r_{\max} = \frac{\lambda}{4\pi} \sqrt{\frac{P_t G_t G_r \tau}{P_{th}}} \quad (6)$$

Or received power in decibel form

$$P_r = P_t - L_{\text{sys}} + G_t + G_r + \tau - 20\log_{10}\left(\frac{4\pi}{\lambda}\right) - 20\log_{10}(r_{\max}) \quad (7)$$

where  $\lambda$  is the wavelength,  $P_t$  is the transmitted power from the reader,  $G_t$  is the gain of the transmitter antenna,  $G_r$  is the gain of the receiver tag antenna,  $P_{th}$  is the minimum threshold power of the transponder's chip (receive sensitivity) and  $\tau$  is the power transmission coefficient (a design factor which takes into account the amount of energy transferred from the antenna to the transponder's chip).  $L_{\text{sys}}$  is the system losses that need to be taken into account during the measurement which includes the cable and connector losses, temperature differences that cause internal losses in the instruments (i.e. antenna + transceiver of reader and tag).

## 2.4.2 Coupling Mechanisms

In this part, the differences in operation between passive/semi-passive and active transponders are introduced in order to understand each coupling mechanism.

Passive transponders obtain power from an interrogation pulse which was sent from the reader. They use this power to send the requested information message, a reply. Since these transponders have no built in battery, they basically last forever, and they do not wear out. A passive RFID transponder is little more than an antenna with some basic circuitry. It has a read range up to about 10 meters. Active transponders have built in battery; hence they are capable of sending a signal that can travel perhaps as much as 150 meters or more to a remote interrogator. The semi-active tag has a battery on it but no radio transmitter. The battery powers its integrated circuit (IC), which helps it to modulate the reflected signal. The reflected signal is required because the tag does not have a radio transmitter. This type of tag is used to get longer read range (up to 50m) or to couple the tag with environment sensors such as temperature, pressure, relative humidity, Global Positioning System (GPS), etc.

There are four types of coupling mechanisms between the tag (transponder) and the reader according to the tag type (passive/active/semi-active):

- Inductive Coupling
- Modulated Backscatter Coupling
- Transmitter (Beacon) Type
- Transponder Type

#### **2.4.2.1 Near-Field Coupling**

The transfer of information is managed using inductive coupling for passive and semi-active transponders. Inductively coupled transponders are always operated passively which means that all the energy needed for the operation of the microchip is provided by the interrogator. The generation of the electromagnetic field from the interrogator's antenna coil penetrates the cross-section of the transponder's coil area and the area around the coil. Since the signal's wavelength is several times greater than the distance between the interrogator's antenna and

the transponder (for instance, a signal of 135 KHz in the Low Frequency band (LF) has a wavelength of 2221 meters, and a signal of 13.56 MHz in the High Frequency band (HF) has a wavelength of 22.2 meters), the electromagnetic field behaves like a simple alternating magnetic field with regard to the distance between the transponder and the antenna. This is called "near-field coupling" as discussed mathematically earlier and shown in Figure 2.7.

In the near-field, the electromagnetic energy lines are formed moving outwards from the radiating element and then back into the radiating element as shown in Figure 2.11. Near-field coupling takes place within approximately one wavelength of a radiating element. Near-field coupling takes place for RFID applications operating in the LF and HF bands with relatively short reading

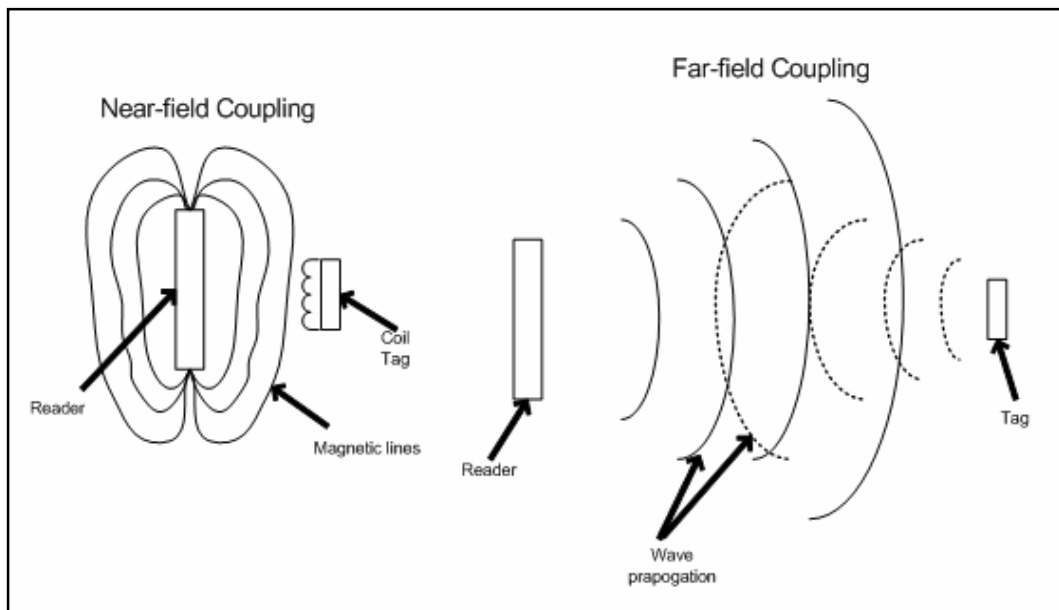


**Figure 2.11 Near-field (LF and HF) and far-field (UHF) coupling mechanisms**

distances well within the radian sphere,  $R$ , defined by  $\lambda/2\pi$  ( $\lambda$ = wavelength in free space), because of the relationship  $\lambda = 2\pi R$  [1].

#### **2.4.2.1.1 Inductive Coupling**

The partial penetration of the emitted field from the antenna coil of the transponder creates current on the coil of the interrogator. To understand this completely, it is compulsory to define the term electromagnetic induction. Electromagnetic induction is a phenomenon through which a change in the magnetic field of a source such as an interrogator creates a voltage level in a remote circuit such as a transponder. A parallel circuit used to adjust the transponder's operating frequency to that of the interrogator is formed by a capacitor in parallel to the transponder's antenna coil which behaves as an inductor. At a definite frequency, the interrogator's antenna interchanges energy at a particular rate, called resonant frequency, which depends on several design parameters such as number of turns, size of the coil, or distance between the capacitance plates, among others. At this point, high currents are generated in the interrogator's antenna coil by the method known as *resonance step-up* [1].

When the frequency of the transmitted signal becomes similar to the designed resonant frequency of the circuit resonance step-up occurs. At this point, a portion of the energy accumulated as magnetic form in the inductor is converted into electrical form in the capacitor. Before reaching a steady state, a temporary tuning in the energy levels at the transponder's inductor and capacitor take places; this whole process explains the before mentioned resonance step-up effect. After reaching the steady state at resonant frequency, the received energy is "stored" in the transponder by transfer back and forth from the capacitance to the inductance, in accordance with the required field strengths for the operation of the remote transponder. A constant current is required for microchip's operations; this can be attained by using a rectifier, a built-in component which converts the alternating energy arriving at the tag into a constant current. As a general rule, it is possible to say that inductively-coupled systems are based upon a transformer-type coupling between the primary coil in the interrogator and the secondary coil in the transponder. This definition is correct when the space between the two

coils does not go beyond  $\lambda/2\pi$ , which identifies the near-field of the interrogator antenna [1].

#### **2.4.4.2 Far-Field Coupling**

Outside the near-field region the far-field starts and the electromagnetic energy basically propagates outwards. UHF and microwave (2.4GHz and 5.8GHz) RFID systems make use of far-field coupling; hence they have long read range. Information is transferred by means of modulated backscatter coupling for passive and semi-active transponders, on the other hand, transmitter and transponder type coupling for active transponders [1]. The occurrence of modulated backscatter, transmitter type and transponder type coupling takes place in the “far-field coupling” region as previously shown mathematically and displayed in Figure 2.7.

##### **2.4.2.2.1 Modulated Backscatter Coupling**

The interrogation signal created from the interrogator propagates outside the near-field of the reader antenna. While this RF signal propagates outwards, it may hit transponder’s antenna. According to the radar technology, an electromagnetic wave reflects from an object if the dimension of the object is greater than half the wavelength of the electromagnetic wave. The “reflection cross-section” (RCS) can then be defined as the parameter that determines the strength of the returned signal. An electromagnetic field propagates outwards from the interrogator's antenna and a small proportion of that field (reduced by free space attenuation) reaches the transponder's antenna. By using a rectifier circuitry in the IC, the captured signal by the antenna is transferred from AC to DC power which is then supplied to deactivate or activate the power saving "power-down" mode [6].

The antenna of the transponder captures a portion of the incoming RF energy and this energy is then reflected by the antenna of the tag and travels outwards. By altering the load connected to the antenna terminals, the reflection characteristics (i.e., reflection cross-section) of the antenna can be changed. A load resistor (or

capacitor) connected in parallel with the antenna is switched on and off synchronously with the data stream to be transmitted which makes the transmission of data from the transponder to the interrogator. The strength of the signal reflected and re-radiated from the transponder to the reader can be modulated by changing the load of the transponder antenna.

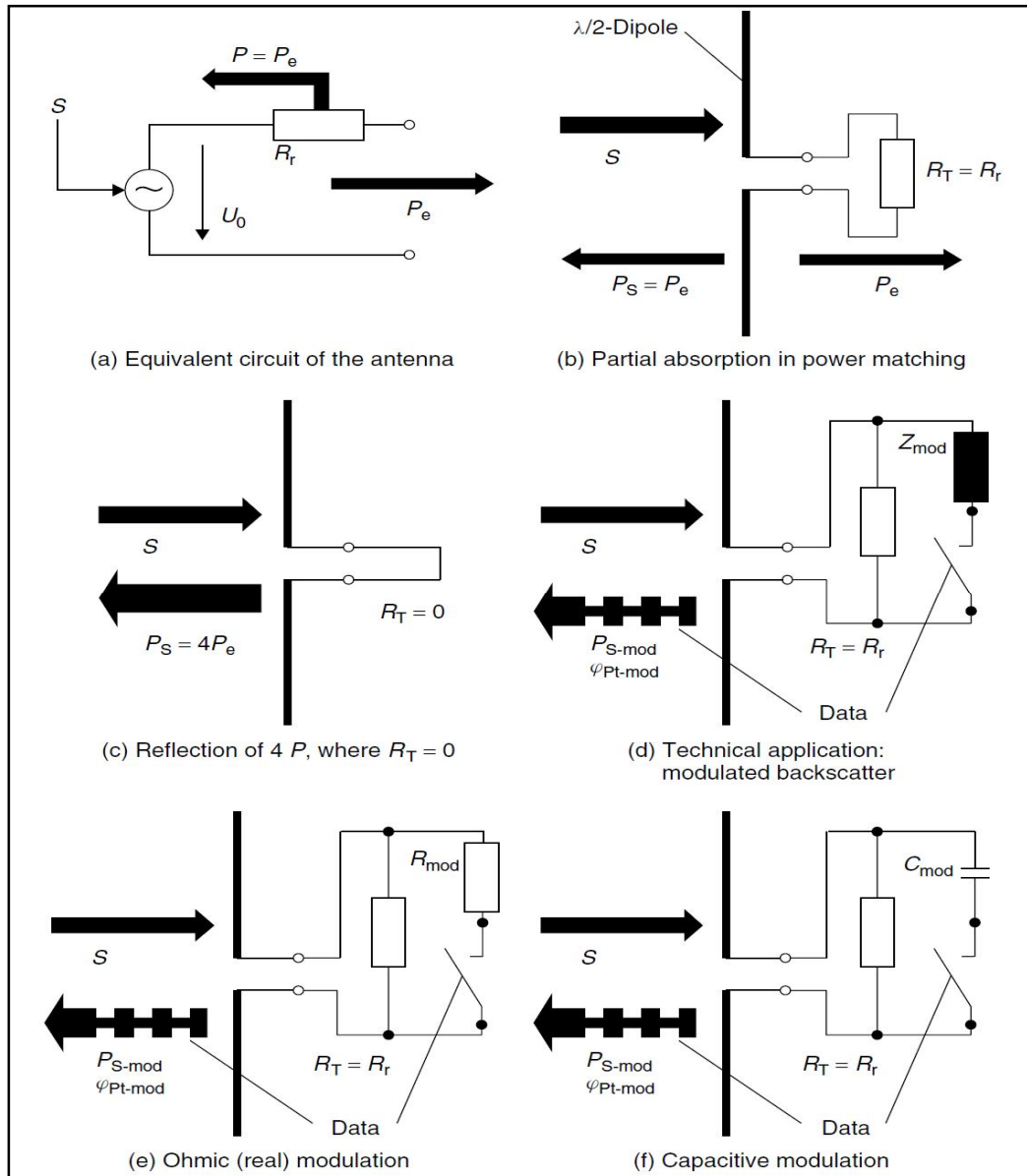


Figure 2.12 Generation of the modulated backscatter by the modulation of the transponder impedance  $Z_T (=R_T)$  [1].

In electromagnetic terms, this is referred to as modulated backscatter (Figure 2.12). When the modulated and encoded data stream in the ASIC reaches the interrogator, it is then decoded and subsequently demodulated allowing the user to retrieve the required information [1].

#### **2.4.2.2.2 Beacon (Transmitter) Type**

Beacons are used in most real-time locating systems (RTLS), as the approximate location of an asset needs to be tracked. Active transponders are used in this type of communication. In this type of coupling, a beacon transmits a signal with its unique identification number at pre-defined periods. Depending on how often it is needed to know the location of an asset, the query time could be set at many different times; could so frequent as every five seconds or once a day. Minimum three reader antennas positioned around the outside of the area where assets are being tracked, detect the beacon's signal. By this way, the precise location of the asset can be found. Real-time location systems are generally used in a large open area; however, automakers use the systems in large manufacturing facilities to track parts' bins.

#### **2.4.2.2.3 Transponder Type**

While in receipt of a signal from an interrogator, active transponders are awakened. For example, in checkpoint control, toll payment collection, and port security systems, transponder type active tags are utilized. In toll payment collection, an interrogator at the gate send outs a signal that turns on the transponder mounted on the car's windshield.

When a vehicle with an active tag comes very close to the tollbooth, the transponder then transmits its unique ID to the interrogator. By having the tag communicate with the interrogator just it is within the read zone of that interrogator, battery life protection can be accomplished.

## **2.5 Chapter Summary**

In this chapter, the necessary concepts to realize the operational principles of the RFID technology with a concise historical overview have been presented. The differences between the three types of tags namely passive, semi-passive and active tags were discussed. Moreover, the crucial elements such as the reader, the tag (antenna + IC), and the coupling mechanisms in the overall RFID system were explained comprehensively. UHF (i.e. 860-960 MHz) band applications were also explained to lay the fundamentals for the following chapters in this document.

## CHAPTER 3

### RFID TAG ANTENNA DESIGN

#### PROCEDURES AND PROBLEMS

In this chapter, procedures to realize a general passive RFID antenna type possessing desired characteristics will be described briefly. Tag performance issues, various design requirements, generic design process, prototyping and validation including range measurement techniques will be discussed.

#### 3.1 Performance Criteria

The most significant tag performance criteria is read range which is defined as the maximum distance at which RFID interrogator is able to detect the backscattered signal from the transponder. The read range is generally defined by the transponder response threshold since the reader sensitivity is typically high compared to the transponder. Read range also depends on the tag orientation, the material the tag is attached, and the loss in propagation environment [10].

The read range can be calculated using Friis free-space formula as;

$$r_{\max} = \frac{\lambda}{4\pi} \sqrt{\frac{P_t G_t G_r \tau}{P_{th}}} \quad (1)$$

where  $\lambda$  is the wavelength,  $P_t$  is the power transmitted by the reader,  $G_t$  is the gain of the transmitting antenna,  $G_r$  is the gain of the receiving tag antenna,  $P_{th}$  is the minimum threshold power necessary to activate the RFID tag chip, and  $\tau$  is the power transmission coefficient given by

$$\tau = \frac{4R_c R_a}{|Z_c + Z_a|^2}, \quad \text{and} \quad 0 \leq \tau \leq 1 \quad (2)$$

where  $Z_c = R_c + jX_c$  is chip impedance and  $Z_a = R_a + jX_a$  is antenna impedance [10].

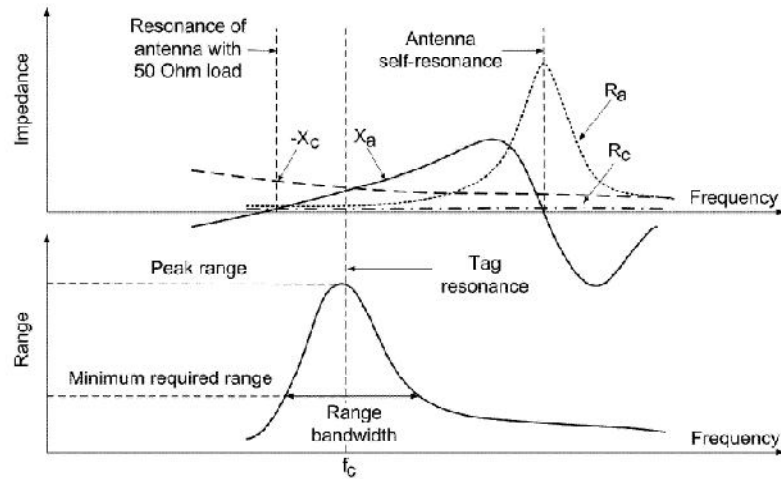


**Figure 3.1 Antenna impedance, chip impedance, and range as a function of frequency for a typical RFID tag [10].**

Qualitative behavior of antenna impedance, chip impedance, and read range as a function of frequency for a typical RFID transponder is shown above in Fig. 3.1. The frequency of the maximum range is defined as the tag resonance frequency. The tag range bandwidth can be defined as the frequency band in which the tag offers an acceptable minimum read range over that band. From (1) one can see that read range is determined by the product  $P_t G_t$  of the reader (transmitter EIRP), tag antenna gain  $G_r$ , and transmission coefficient  $\tau$ . Typically  $\tau$  is

dominant in frequency dependence and primarily determines the tag resonance which happens at the frequency of the best impedance match between chip and antenna. This frequency is different from the resonant frequency of antenna loaded with 50 Ohm and the antenna self-resonance [10].

### **3.1.1 Tag Characteristics**

Transponder performance in an RFID system is mostly determined as how well the transponder read range is in different environments. This depends mainly on the transponder (chip and antenna) properties as well as the propagation environment. The tag characteristics can be classified as chip sensitivity, antenna gain and polarization, and impedance match [11]. The propagation environment limitations are the path loss and tag detuning [11].

- **Chip Sensitivity:**

It is defined as the minimum threshold power to turn the chip of the transponder on. It is mainly determined by the RF Front end architecture and fabrication process [11, 12]. Low threshold power chips (tags) are high sensitive and they have higher read range when compared with the low sensitive ones.

- **Antenna Gain and Polarization:**

Antenna gain is a measure of how directive the antenna and if it is radiating efficiently. The size and geometrical structure (single or array of antennas) of the antenna at the frequency of operation determines how much gain can be achieved. Polarization of the tag is important considering RFID system level performance. Maximum power transfer is achieved when the polarization of the tag is matched to the reader's. When the polarization of the reader's antenna is circular (generally it is) and tag's antenna is linear then only half of the power will be transferred to the tag due to polarization mismatch and vice versa.

- **Impedance Match:**

The complex impedance (i.e.  $12 - j140$  for Alien Higgs-2 Chip at 910 MHz) of the chip requires a complex conjugate impedance match at the antenna terminals. This becomes a real problem because the chip impedance changes at different power levels and frequencies [13]. In order to maximize the transponder operating range, impedance should be matched at various IC power levels such as at minimum threshold power. As it can be seen from Figure 3.1, if the transponder antenna complex reactance  $X_a$  is equal to the negative complex reactance  $-X_c$  of the chip then the peak read range can be achieved at resonant frequency. The RFID tag antenna design process involves inevitable tradeoffs between antenna gain, impedance, and bandwidth.

### 3.1.2 Propagation Environment Limitations

- **Path Loss:**

The path loss is dependent on the surrounding environment [14, 15]. The type of scattering around the tag affects the read performance of the tag and defines the path loss. Since multiple reflections occur with the main line-of-sight signal, the ideal  $(\lambda/4\pi d)^2$  for free space propagation can be altered significantly in a room [16].

- **Tag Detuning:**

Resonant frequency of the antenna shifts from the designed frequency when the tags are located on or contained in lossy materials (i.e. detergent, liquid or human bodies) and in the proximity of metal [17, 18]. This effect makes the tag detuning. Tag detuning also affects the antenna performance such as antenna gain and the radiation pattern, hence gives rise to a lower operating range. Multiple tags also reveals this kind of performance degradation if the tags are very close to each other. The parasitic coupling between the antennas causes the tags to detune since

it varies the antenna impedance. Simultaneous multiple tag identification and the position analysis of these tags are pointed out in [14, 15]. Antenna curving can also detune the tag due to the changes of the radiation pattern and impedance of the antenna [19].

### 3.2 Design Requirements

Several common RFID tag design requirements whose relative significance depends on tag application are reviewed in the following part. These requirements largely determine the criteria for choosing an RFID tag antenna.

**Frequency band:** Regulations of the country where the tag will be used determines the tag's operation frequency band [10].

**Size and form:** The size of the tag becomes a main problem when tags are used on items that are restricted in size. The main factor affecting the dimension of a tag is antenna size which depends on the operating frequency. For example, resonance is attained for an optimum performing antenna length around  $\lambda/2$  for a variety of antenna types such as folded printed dipole, printed patch, log-spiral [17]. Therefore, the price and dimension of the tag increases for low LF and HF ( $\lambda/2=1111\text{m}$  and  $10.5\text{m}$  respectively) frequency applications as well as for UHF ( $\lambda/2 \approx 16\text{ cm}$ ) tags. For HF frequency, printed inductive loop antennas in the coil form are used [20, 21]. For the UHF frequencies, printed dipole antenna size reductions are generally attained by means of meandering topologies [22, 23]. It has to be stated that the main trade-off is between size reduction and efficiency including gain [22]. These topics will also be addressed later in this thesis.

**Read range:** Minimum required read range is generally defined for different [10]:

- **EIRP:** EIRP is determined by local country regulations.

- **Objects:** Tag performance decreases when it is attached on various objects (e.g. cardboard boxes with different content), or when other objects are present in close proximity of the tagged object. Tag antenna can be designed or tuned for optimum performance on a particular object or designed to be less sensitive to the content on which the tag is placed.
- **Orientation:** Antenna orientation is important and affects the read range. Some applications require a tag to have an omni-directional or hemispherical coverage radiation pattern.

**Applications with mobility:** RFID tag may be used in circumstances where tagged objects like pallets or boxes travel on a conveyor belt at speeds up to either 18 m/min or 16 kmh. The Doppler shift in this case is not important and does not affect RFID operation. Nevertheless, the tag spends less time in the read zone of RFID reader, requiring high read rate capability. In such cases, RFID system must be carefully planned to make sure reliable tag identification [10].

**Cost:** RFID tag must be a cheap device; hence, both the antenna structure and the choice of materials for its construction including the chip are restricted. Typical conductors used in tags are copper, aluminum, and silver ink. The dielectrics include flexible polyester PET and rigid PCB substrates like FR4 [10].

**Reliability:** RFID tag must be a reliable device that can sustain in harsh environments like temperature, humidity, stress, and endure its normal operation after such processes as label insertion, printing and lamination.

### 3.3 Design Process

RFID tag antenna performance strongly relies on the frequency-dependent complex impedance of the chip. Tag read range must be carefully examined in the design process in order to meet the design requirements. Since antenna size

and frequency of operation limits the maximum attainable gain and bandwidth [24], [25] compromises have to be made to obtain optimum tag performance to satisfy design requirements. Generally, a tunable antenna design is desirable to provide tolerance for tag fabrication deviations and for optimizing antenna performance on various materials in different frequency bands [10].

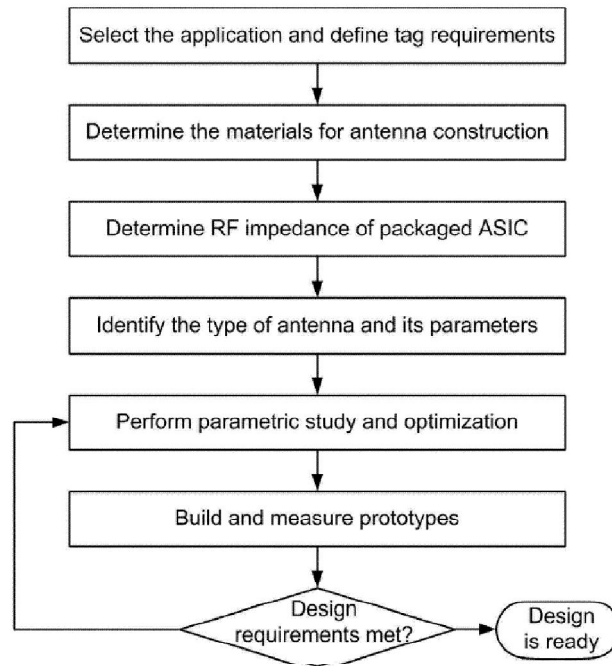


**Figure 3.2 RFID tag antenna design process [10].**

RFID tag antenna design process is demonstrated on a flow chart shown in Figure 3.2. When the RFID application is chosen, system requirements can be interpreted to the tag requirements. These requirements specify the materials for tag antenna construction and chip to be used. The impedance of the selected ASIC in a chosen RF package (like flip-chip, etc.) to which antenna will be matched can be learned from the manufacturer datasheet or measured with a network analyzer.

Antenna parametric study and optimization is performed in simulation until design requirements are met. Tag antennas are usually analyzed with electromagnetic modeling and simulation tools (computer software), typically with method of moments (MoM; for instance, ADS) for planar designs (e.g. thin flexible tags) and with finite-element method (FEM; for example, HFSS) or finite-difference time-domain method (FDTD) for more complex three-dimensional designs (e.g. thick metal mounted tags). Fast EM analysis tools are important for efficient tag design. In a usual design process, modeling and simulation tools can be referred against measurements. Some parameters such as antenna gain, impedance and read range can be simulated and analyzed directly in EM software to observe the antenna behavior in various circumstances [10].

In the final step of the design process, prototypes are built and their performance is measured extensively. If design requirements are satisfied, the antenna design is ready. Otherwise, the design is further modified and optimized until requirements are met.

### **3.4 Prototyping and Validation**

After the prototypes are implemented, it comes to the validation of the designs to observe if the desired requirements are met. The most important criterion to be observed is the operation range of the tag.

Precise tag range measurement can be carried out in a controlled environment, such as anechoic chamber or transverse electromagnetic (TEM) cell. In both methods tag position can be fixed and transmitter output power can be altered by means of controlled attenuation [10]. This allows one to carry out accurate tag range measurements and avoid using large and expensive chambers or cells. Compact TEM cell is a suitable tool for measuring small tags while larger anechoic chamber can be used to measure tag performance on different objects.

In anechoic chamber, the tag is located at a predetermined distance from the reader antenna as illustrated in Figure 3.3.

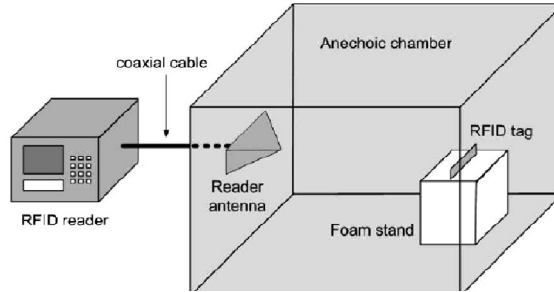


**Figure 3.3 RFID tag range measurement using anechoic chamber [10].**

At each frequency, the minimum power  $P_{min}$  required to communicate with the tag is recorded. Since the loss  $L$  of the connecting cable, the gain  $G_t$  of the transmitting antenna and the distance  $d$  to the tag are known, the tag range for any transmitter EIRP of interest can be determined from (1) as

$$r = d \sqrt{\frac{EIRP}{P_{min} L G_t}} \quad (3)$$

The general guidelines for selecting the tag position in anechoic chamber are the following [10]:

- i) the distance must be such that the tag will respond and will be in far field and
- ii) the tag must be placed in a quiet zone of the anechoic chamber where multipath is minimal.

### **3.5 Chapter Summary**

With the exception of higher level problems in RFID applications; tag design brings about different lower level problems. These problems consist of current high cost of tags, size limitations and optimization and tag performance issues. From a system point of view, problems at the lower level must be eliminated before moving up on the RFID system hierarchy for an optimized overall performance. This thesis also proposes on how to deal with some of these challenges.

## CHAPTER 4

### FOLDED DIPOLE ANTENNA DESIGNS

In this chapter, three folded dipole antennas (two 2-wire folded and one 3-wire folded) are presented for 915 MHz passive tags that are designed to be used for supply chain and security applications. The necessary power required to energize and activate the tag's microchip is drawn from the electromagnetic field provided by the reader unit's antenna. The transponder IC stores the item's unique ID, which can be associated with the product identification number. The chip also stores information about when and where the product was made, its expiration date and so on.

Passive ICs are basically highly reactive because of the required power to bias the IC which is delivered by charging up the IC through electromagnetic coupling. Due to the low resistive but high capacitive impedance of the microchip, three folded dipole type RFID antennas proposed comprising of antennas that are lowly resistive (high efficiency) and highly inductive for matching to the input impedance of the transponder IC.

An RFID tag of UHF band employs far-field radiation of the real power contained in free-space propagating electromagnetic plane waves due to its shorter wavelength, while a 13.56 MHz HF tags is utilizing inductive coupling in the near-field region as the wavelength is much longer. The main difference is that in UHF systems the resistive part of the radiating power is used to communicate with the passive tag where in HF systems the reactive part of the

radiating power is used. The HFSS design tool [26], which is based on Finite Element Method (FEM), is used to optimize and analyze the tag. This tool is used as main platform to design and come up with certain antenna performance parameters such as return loss, gain, directivity, radiation pattern, efficiency and theoretical calculated read range. Three different 10.5cm x 4cm (equal in area or smaller) antenna designs are built to make sure maximum range is obtained. Achieving that range has been a challenge because the lossy items make it harder to get an impedance matching and creates additional power loss in that environment. The tags which are simulated by means of computer yield maximum operational distance ranging from 2.82m to 6.87m which is well beyond the required range (2.5m) for the supply chain applications.

#### **4.1 Design Approach**

The IC input impedances for the supply chain at 915 MHz are  $16-j350 \Omega$  (Philips EPC 1.19),  $12-j140 \Omega$  (Alien Higgs-2) and  $73-j113 \Omega$  (NSC MM9647), which means the load antenna impedance should be  $16+j350 \Omega$ ,  $12+j140 \Omega$  and  $73+j113 \Omega$  respectively for maximum power transfer (conjugate matching). This requires the antenna impedance to be low-resistive but high-inductive. Different antenna designs like 2-wire folded dipole and 3-wire folded dipoles have been proposed as a solution in the past [27, 28]. However, in our research the modified simple version followed to keep the antenna size small and the load impedance to have a low real part (small resistance) and a high positive imaginary part (high inductance). To achieve this, an inductive element required to be incorporated into the antenna. In addition to this, the metal size is preferred to be as big as possible to obtain better radiation parameters such as directivity and efficiency through the larger radiating aperture, however it could increase the metal loss leading to a trade-off in the antenna efficiency. Increasing the metal size also lowers the surface resistance and increases current flow. It is for these above-mentioned reasons, a 2-wire folded dipole antenna with inductive stubs and a

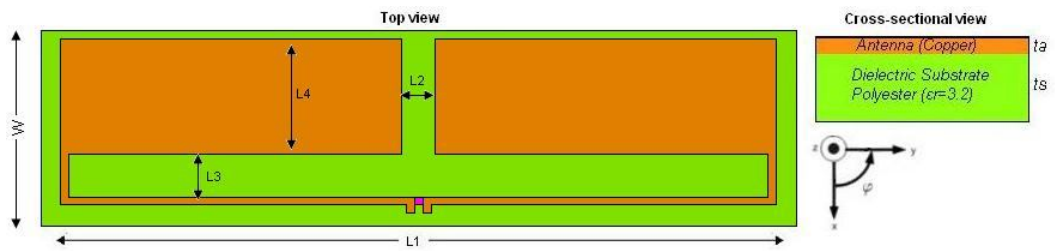
radiating metal patch is used for the first antenna design of this chapter. The stub provides the inductive load impedance meanwhile the radiating metal patch lowers the load resistance. In the second antenna design, 2-wire folded dipole with radiating stubs will be used to achieve low real part and high imaginary part. In the third antenna design, 3-wire folded dipole antenna is used to achieve complex conjugate matching. To accomplish maximum directivity and optimum radiation, the designs are built to achieve half-wavelength ( $\lambda/2 \sim 16.4$  cm at 915 MHz) resonance at first.

In reality, the designs possess similarity to the half-wave dipole antenna; however, there exists a trade-off between antenna-chip matching and resonance. Whenever the antenna size is increased to match for resonance, antenna-chip matching deteriorates. The miniaturization of the antenna size is another issue, which requires the length of the antenna to be smaller than the resonance length.

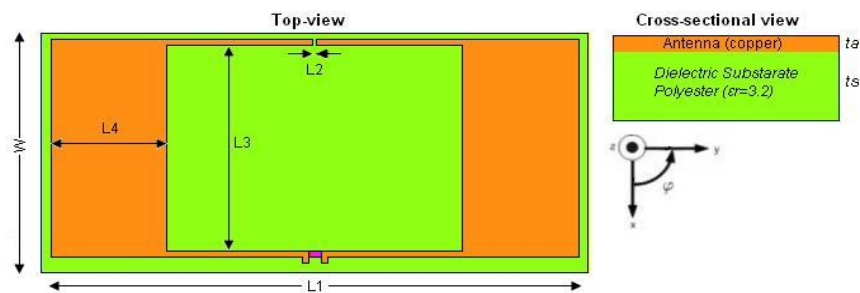
## 4.2 Antenna Designs

The three RFID tag antenna designs are shown in Figure 4.1. These antennas are made of copper metal with a thickness of  $0.02\text{mm}$  and polyester (with  $\epsilon_r=3.2$  and loss tangent  $\delta = 0.003$ ) with a thickness of  $0.1\text{mm}$  as a substrate. In addition to this, one-port differential excitation, which is used to measure the actual antenna-chip configuration, is employed to numerically calculate the antenna parameters such as return loss and antenna load impedance as well as the theoretical read range measurement.

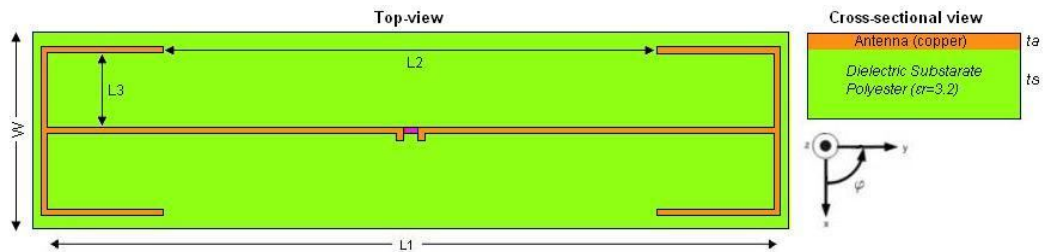
The single inductor stub in Antenna#1 as shown in Figure 4.1a is utilized to obtain the required inductance where the radiating patch is the main radiator for Antenna#2. The 3-wire folded Antenna#3 has no radiating or inductive stubs as the other antenna designs.



- a) Antenna#1 where  $W = 26.4\text{mm}$ ,  $L1 = 87\text{mm}$ ,  $L2 = 3\text{mm}$ ,  $L3 = 5.4\text{mm}$ ,  $L4 = 16\text{mm}$ ,  $t_a = 0.02\text{mm}$ ,  $t_s = 0.1\text{mm}$ , line width ( $w$ ) =  $1\text{mm}$  and port separation of  $1\text{mm}$ .



- b) Antenna#2 where  $W = 39.5\text{mm}$ ,  $L1 = 80\text{mm}$ ,  $L2 = 0.5\text{mm}$ ,  $L3 = 34\text{mm}$ ,  $L4 = 18\text{mm}$ ,  $t_a = 0.02\text{mm}$ ,  $t_s = 0.1\text{mm}$ , line width ( $w$ ) =  $1\text{mm}$  and port separation of  $2\text{mm}$ .



- c) Antenna#3 where  $W = 28.6\text{mm}$ ,  $L1 = 104\text{mm}$ ,  $L2 = 71\text{mm}$ ,  $L3 = 10.8\text{mm}$ ,  $L4 = 1\text{mm}$ ,  $t_a = 0.02\text{mm}$ ,  $t_s = 0.1\text{mm}$ , line width ( $w$ ) =  $1\text{mm}$  and port separation of  $2\text{mm}$ .

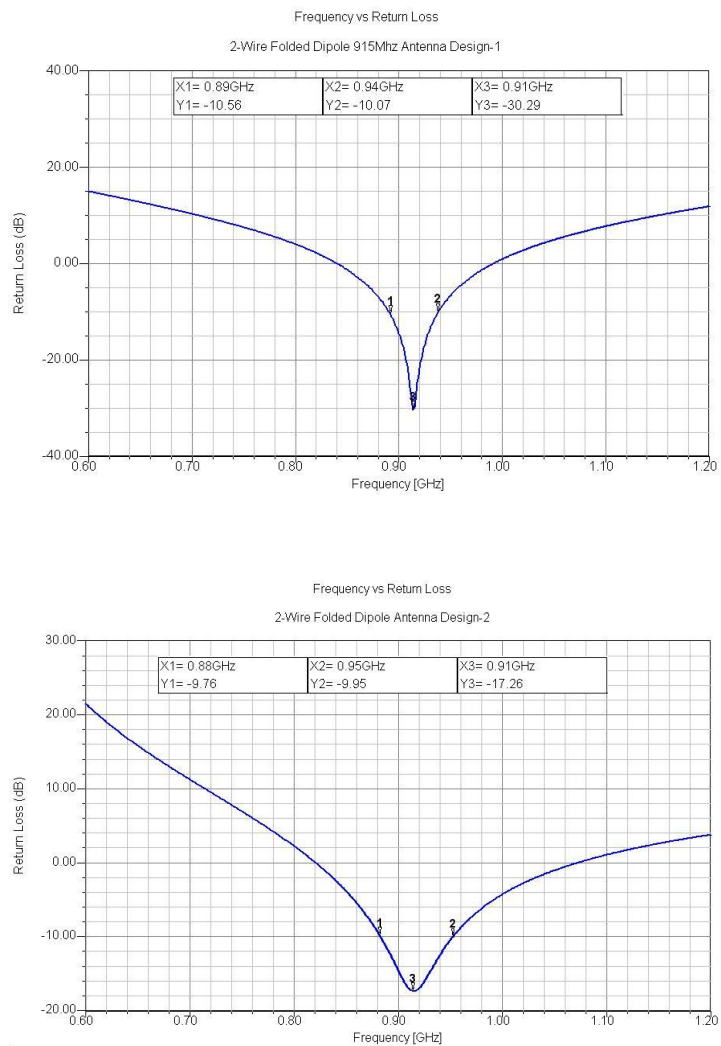
**Figure 4.1 The three different folded dipole RFID antenna designs for supply chain applications.**

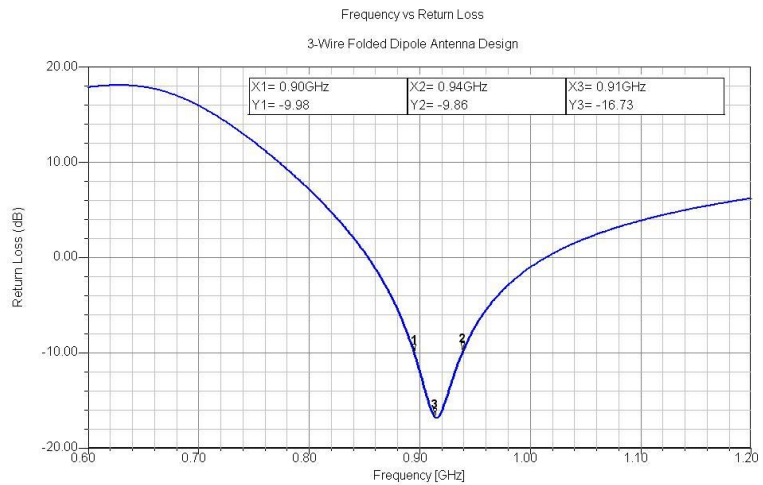
Figure 4.1a is also highly inductive due to the double stubs that are easily integrated into the radiator rectangular patches. This feature is proven to be very

important to enhance radiation because the inductive stub, which is used for antenna-chip reactance matching, becomes more part of the radiating element by creating additional coupling with the radiating element.

### 4.3 Simulation Results and Discussion

The simulated return losses with respect to frequency are illustrated in Figure 4.2.

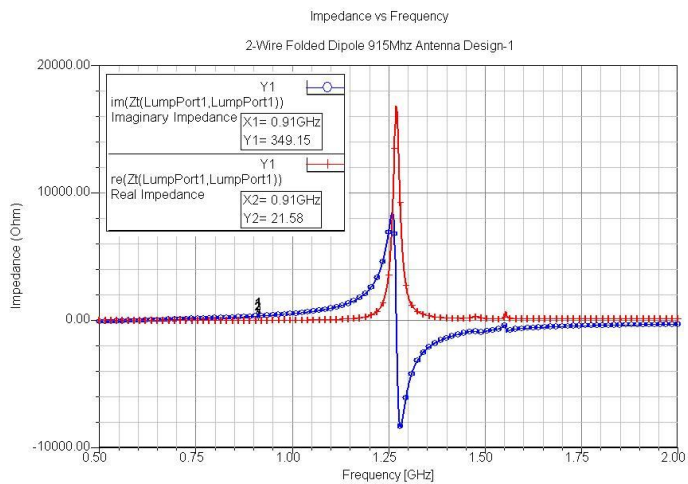




**Figure 4.2 Simulation results showing the return losses of the antennas.**

As seen from the Figure 4.2 the -10 dB bandwidth of the antennas are %5.4 (50 MHz), %7.6 (70 MHz) and % 4.4 (40 MHz) respectively.

Figure 4.3 below shows the simulated antenna input impedances with respect to the frequency verifying that they are high-inductive and low-resistive.



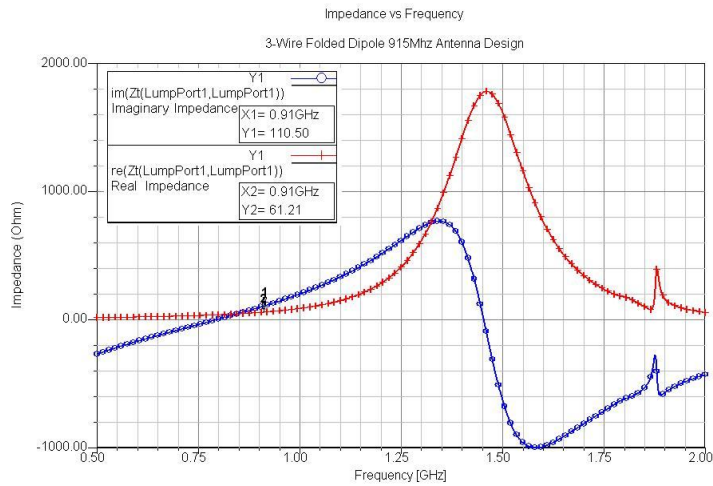
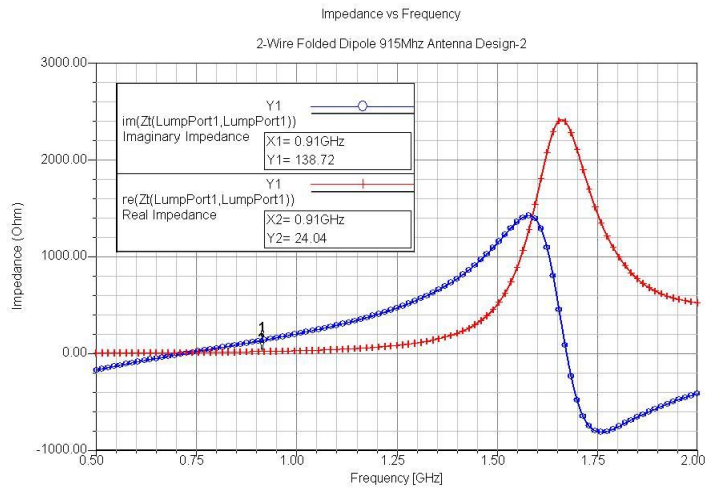


**Figure 4.3 Simulated antenna input impedances with respect to frequency.**

As it can be seen from the plots, the antenna input impedances are achieved to match complex conjugate of the chip impedances at that frequency. It is important to achieve complex conjugate match of the antenna at the frequencies which is distant from the antenna self resonant frequency. That is because, at the antenna self resonant frequency the impedance changes more quickly and antenna-chip matching deteriorates a lot at these regions. In order to achieve maximum operating bandwidth, the frequency of the conjugate matching should be selected where antenna input impedances exhibits slow changes in the real and imaginary parts.

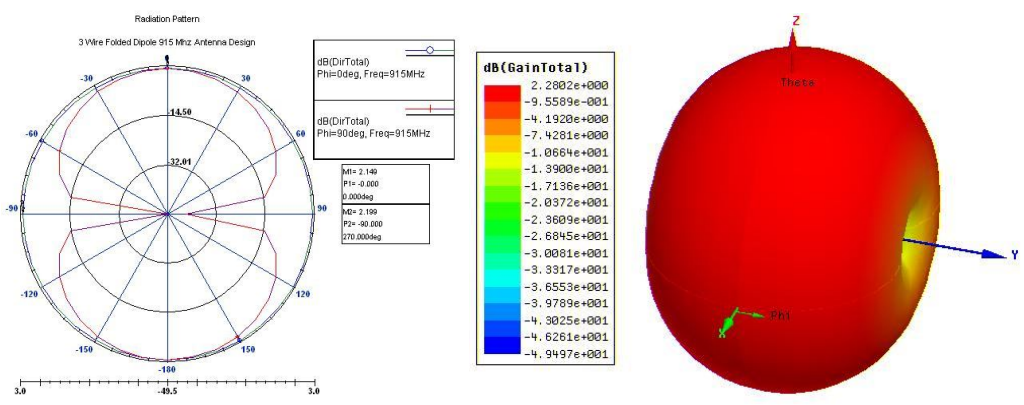
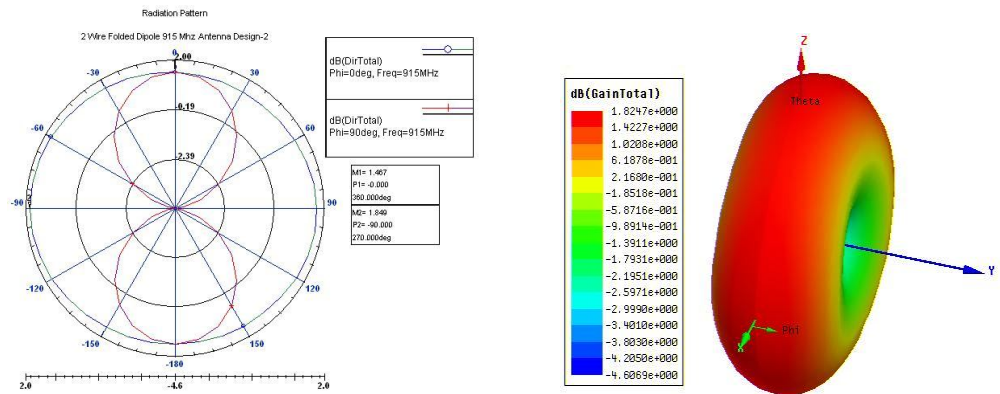
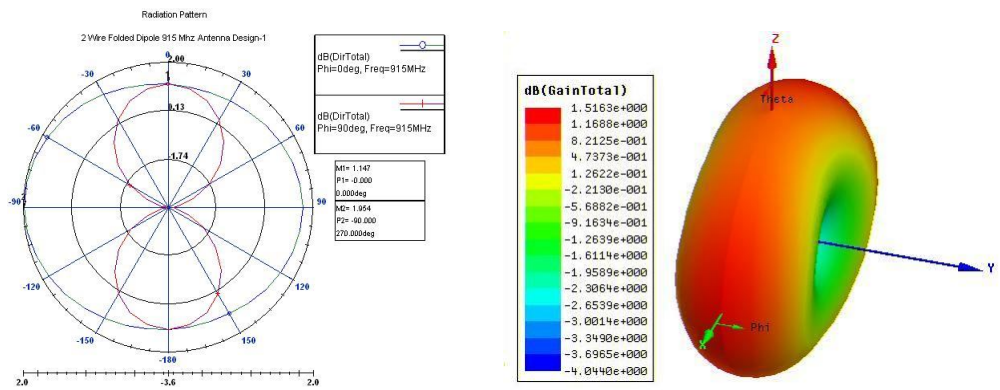


**Figure 4.4 Simulated 2-D radiation patterns (Directivity patterns for  $\phi=0$  (x-z) and  $\phi=90$  (y-z) planes) for the three 915 MHz UHF antenna designs and 3-D gain patterns. Antennas are located in the horizontal plane.**

The radiation patterns for the three designs are shown in Figure 4.4. All of the antenna designs have doughnut-shaped radiation patterns in the  $\phi=0$  deg (x-z plane) and  $\phi=90$  deg (y-z plane) planes as expected since the antennas are dipole type. The antenna#3 has a higher gain and more omni-directional (high HPBW) pattern than the other antenna designs. The creation of nulls in the horizontal plane (x-y plane) with dipole type of antennas is a restrictive factor. It is essentially desired to attain maximum radiation when the tag is read in the plane (x-z or y-z planes) that is perpendicular to the RFID antenna. The horizontal plane radiation is also important in relation to the orientation of the interrogator. The Interrogator (reader) does not essentially have to be positioned on top or bottom with respect to the RFID transponder; however the RFID transponder should also have the functionality to be read from the sides as well. Making use of the two orthogonal transponders (x-y horizontal plane and x-z/y-z vertical planes) would overcome this obstacle in case the application requires effective radiation characteristics in the horizontal plane. The dual polarization (horizontal and vertical) capture will improve the detection in the direction vertical to the antenna (z-axis) where antenna is least likely to be read.

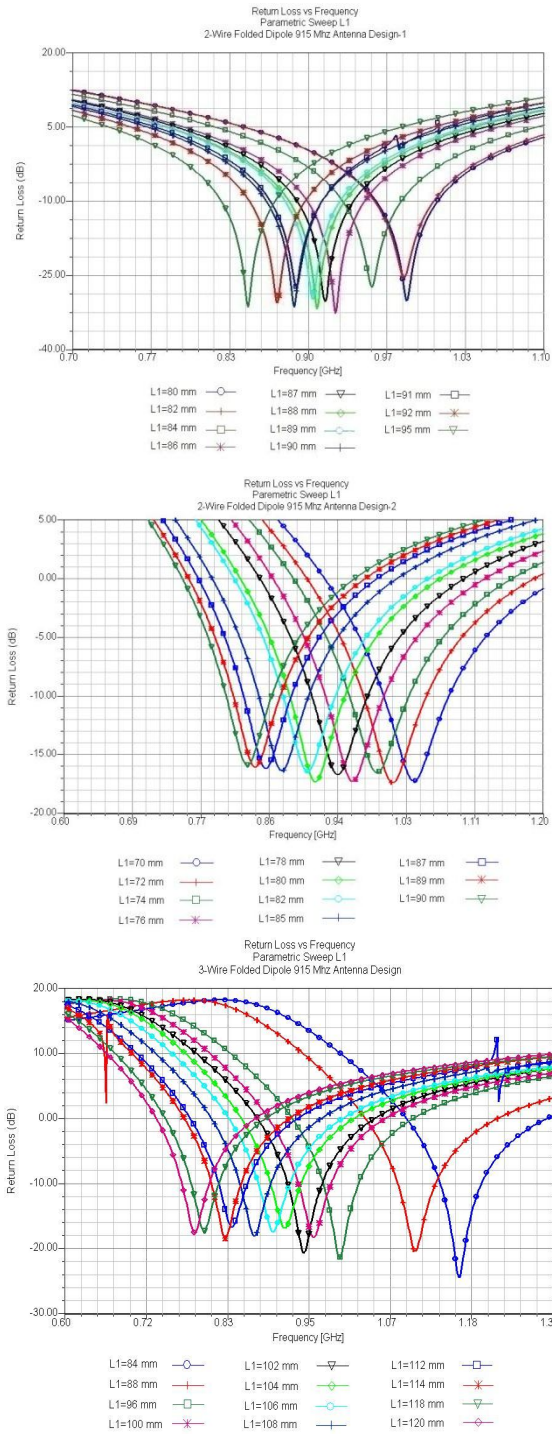
The load impedance values are displayed in Table 4.1 along with other radiation parameters namely return loss, gain, directivity, antenna efficiency, and theoretical read range in free space. As it can be seen from Table 4.1, the antenna efficiency determines how much operational distance is needed for the tag. For example, although the Antenna#1 exhibits the minimum return loss the read range is higher for the other two antenna designs. Therefore, the read range does not only depend on the return loss or the gain of the radiating antenna but also efficiency of the antenna. Antenna#1, #2, and #3 yield maximum theoretical read distances of 2.82m, 4.84m and 6.77m respectively.

**Table 4.1 Simulated antenna parameters and calculated theoretical read range.**

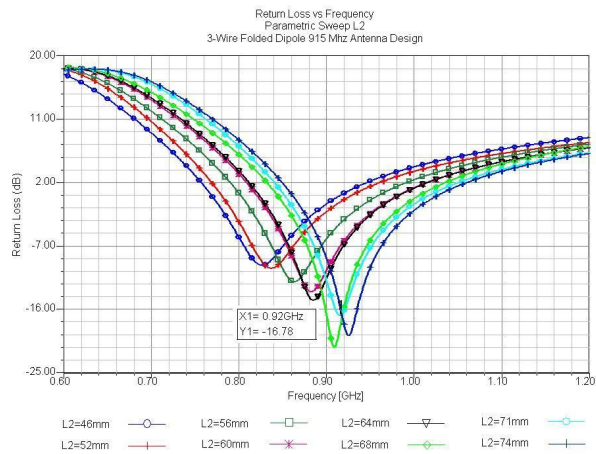
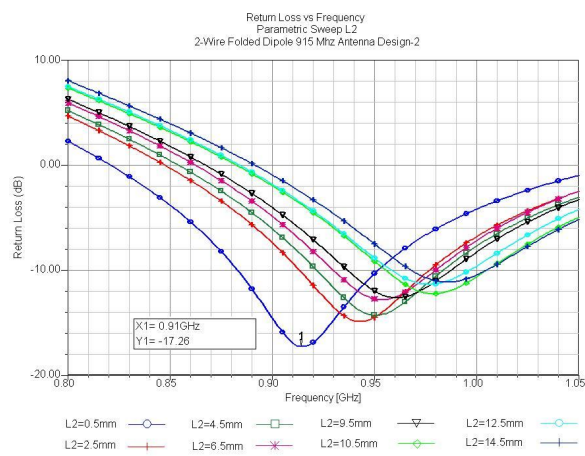
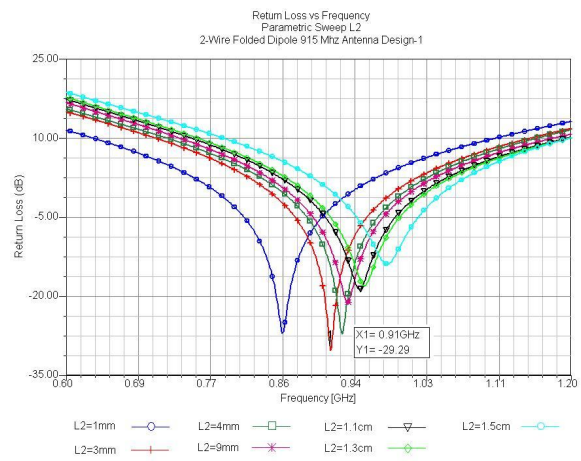
	Impedance (Ohm)	Return Loss (dB)	Gain (dB)	Directivity (dBi)	Antenna Efficiency (%)	Theoretical read range (m)
Ant #1	19.8+ j351.2	-29.9	1.51	1.95	86.8	2.82
Ant #2	24.1+ j139.4	-17.3	1.82	1.84	99.4	4.84
Ant #3	62.1+ j111.6	-16.9	2.28	2.2	100	6.77

### **4.3.1 The Influence on Resonant Frequency**

The resonant frequency of the antenna is mainly determined by the geometry L1, L2 and L3 of the antenna. Other parameters such as L4, substrate thickness and line width (w) also affects the resonant frequency but not as much as L1, L2 and L3 does. Figure 4.5 shows the influence of the parameter L1 on the resonant frequency. As it can be seen from the plots, L1 decides the antenna's resonant frequency and the resonant frequency varies 9.3 MHz/mm, 12 MHz /mm and 10.2 MHz/mm respectively. The resonant frequency drops when L1 increases, and resonates at 915 MHz when L1 are 87mm, 80mm and 104 mm respectively.

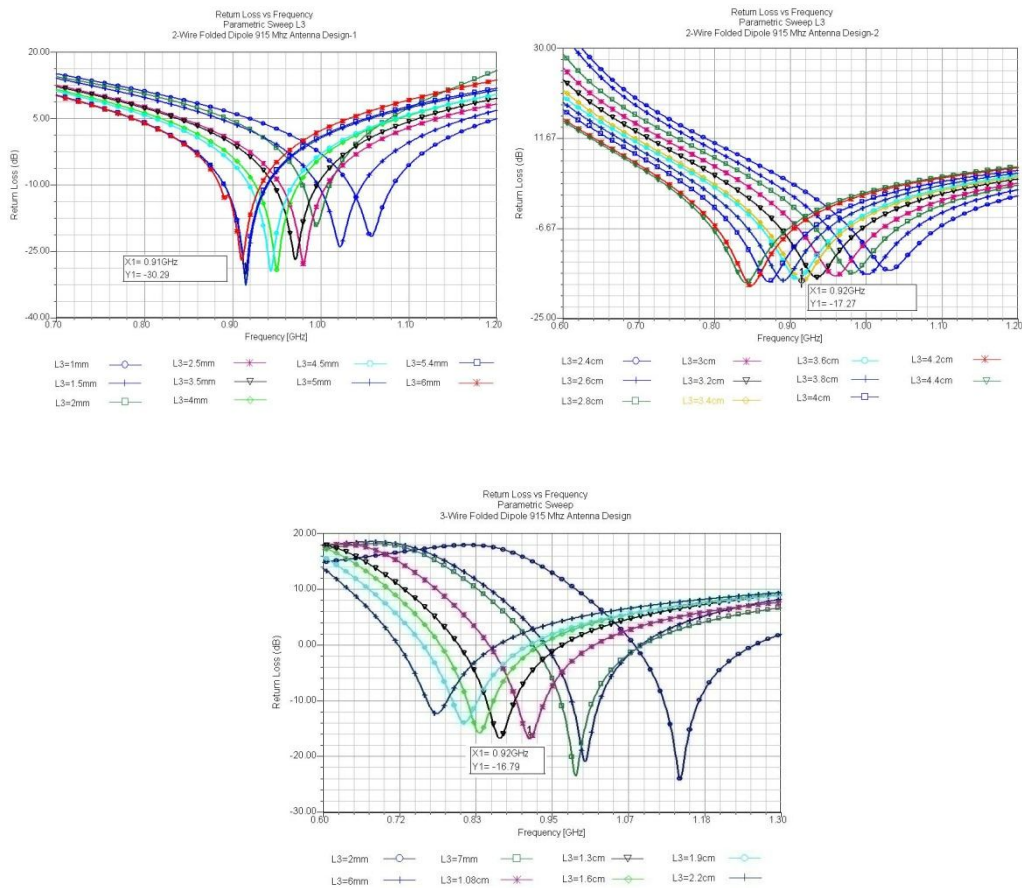


**Figure 4.5 Influence on resonant frequency L1 as a parameter.**



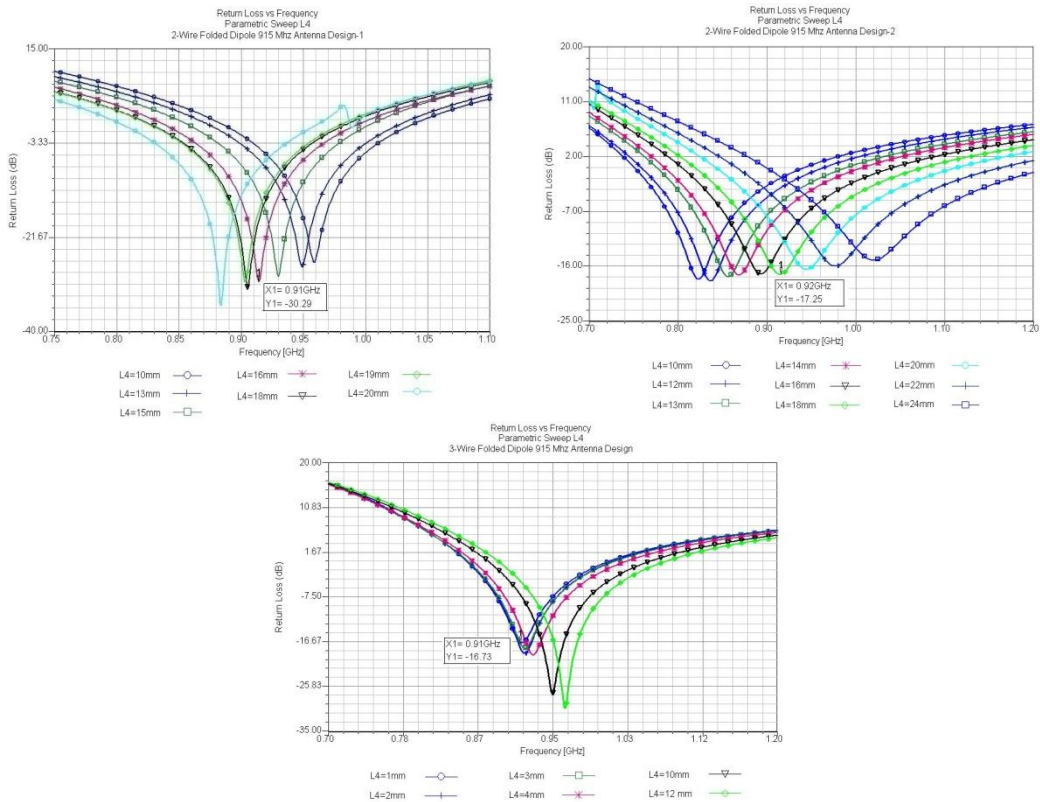
**Figure 4.6 Influence on resonant frequency L2 as a parameter.**

Figure 4.6 shows that the resonant frequency increases as L2 increases, its average variance is about 8.5 MHz/mm, 5 MHz/mm and 3.5 MHz/mm respectively.



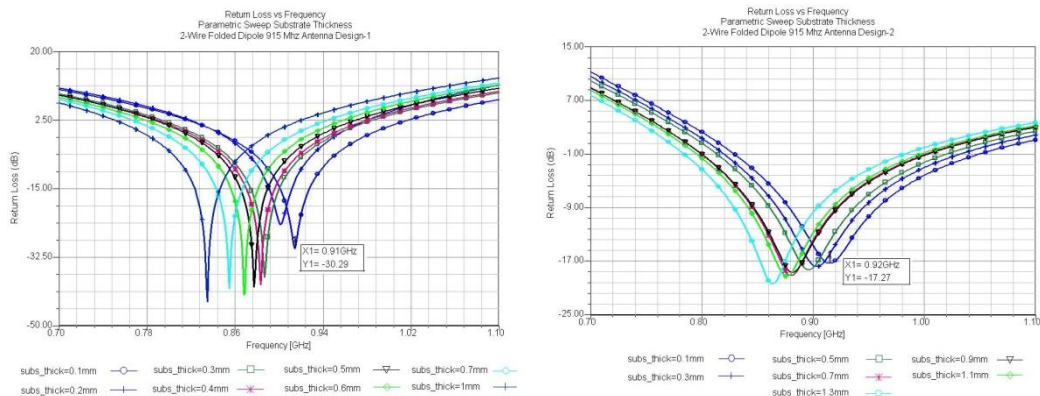
**Figure 4.7 Influence on resonant frequency L3 as a parameter.**

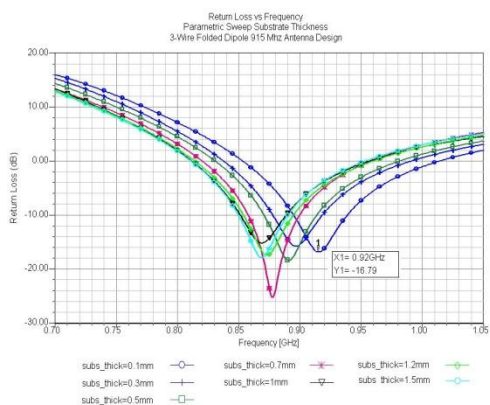
Figure 4.7 shows that antenna's resonant frequency drops as the L3 increases and its variation speed gets slower. Since the L3 is the distance of the folded arms and couple exist between the folded arms, the larger the L3 the less the couple affects on the resonant frequency.



**Figure 4.8 Influence on resonant frequency L4 as a parameter.**

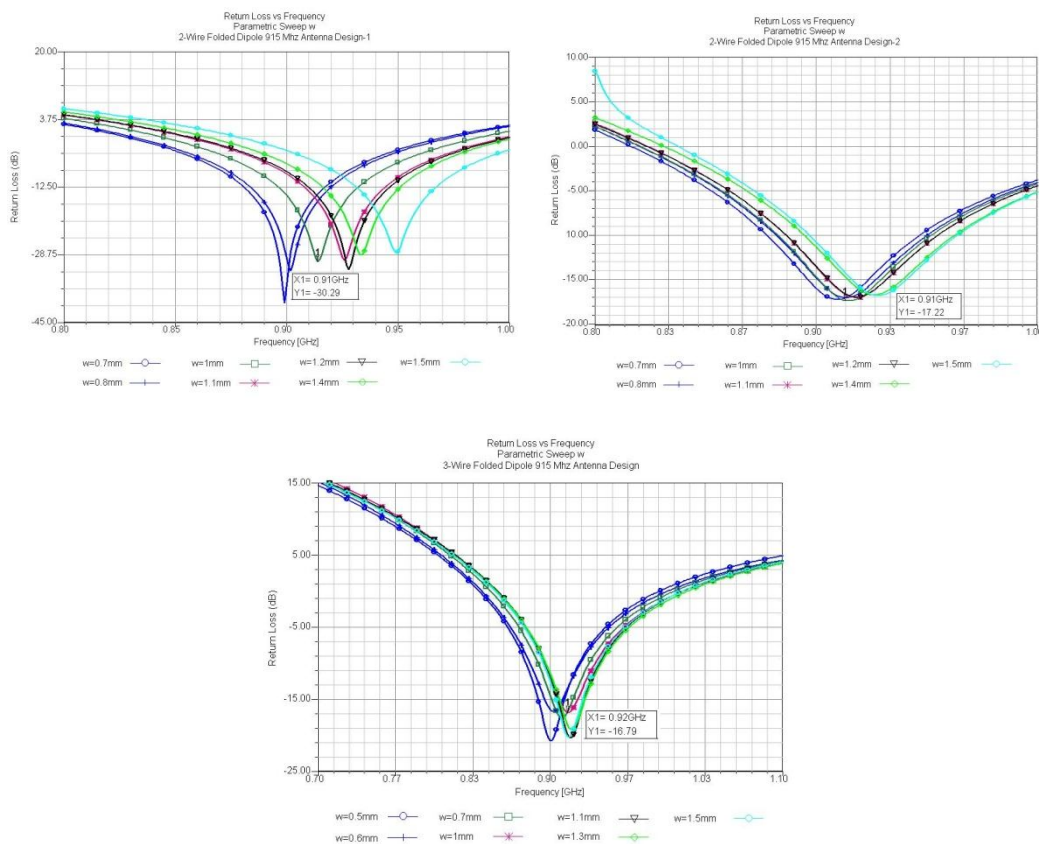
Since the L4 is not defined as the same way in all the three antenna designs the effect on the resonant frequency is different. Figure 4.8 above shows the influence of the L4 on resonant frequency. In the Antenna#1, as the L4 increases the resonant frequency decreases. However, in the Antenna#2 and Antenna#3 the reverse case is true. In addition, its variation speed is higher in the Antenna#2 than the others.





**Figure 4.9 Influence on resonant frequency substrate thickness as a parameter.**

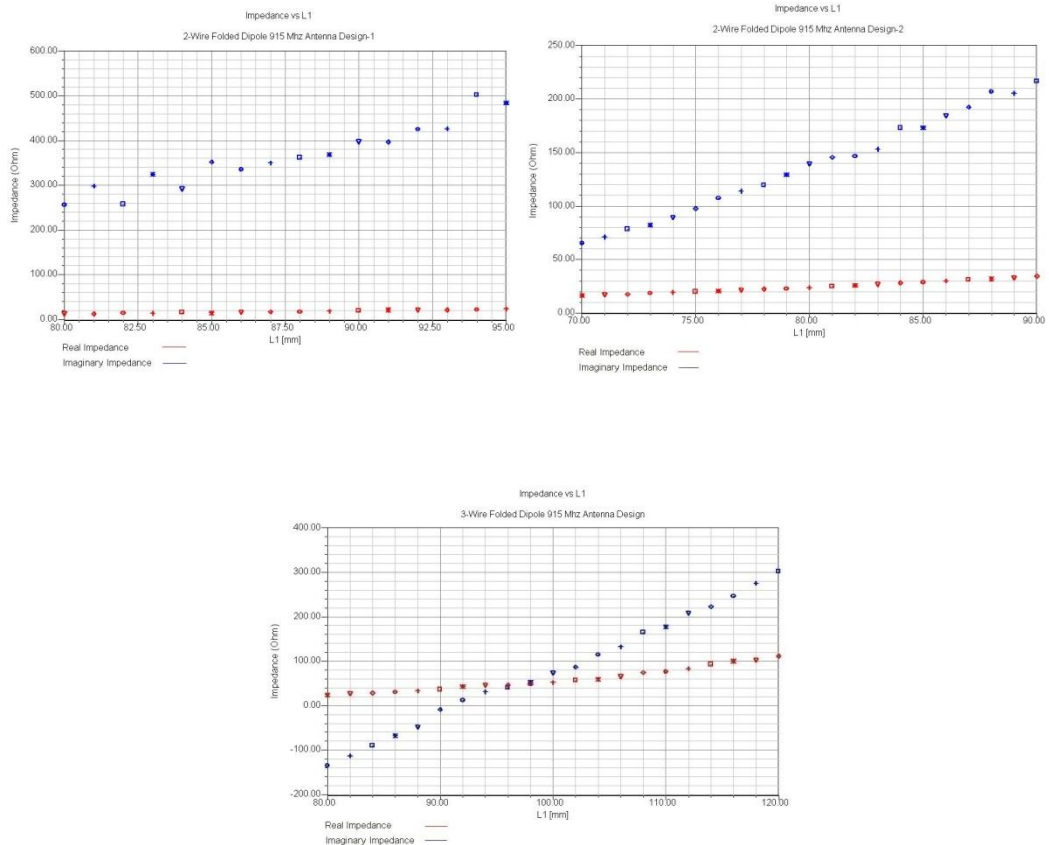
Figure 4.9 shows, as the substrate thickness increases, all of the antenna resonant frequency decreases as expected because lossy materials shifts the antenna frequency to lower. If the substrate thickness is not changed but the lossy dielectric of the substrate increased then we would see the same shift in the frequency to lower values.



**Figure 4.10 Influence on resonant frequency line width (w) as a parameter.**

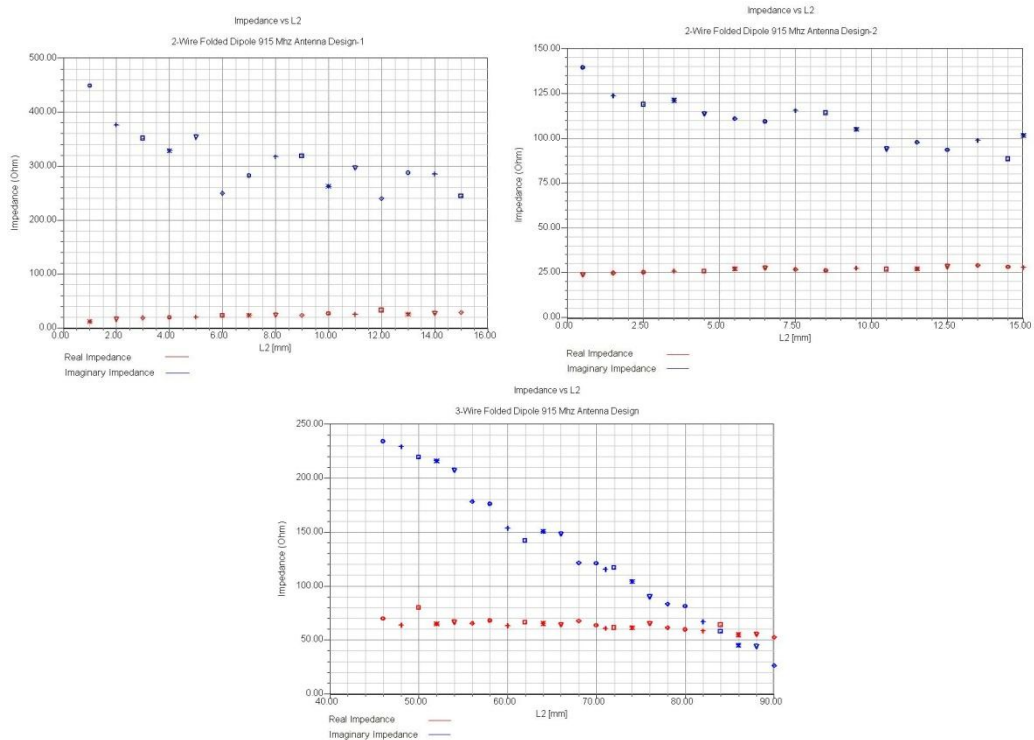
From Figure 4.10 we can interpret that as the line width of the antenna increases the resonant frequency slightly shifts to a higher value.

### 4.3.2 The Influence on Input Impedance



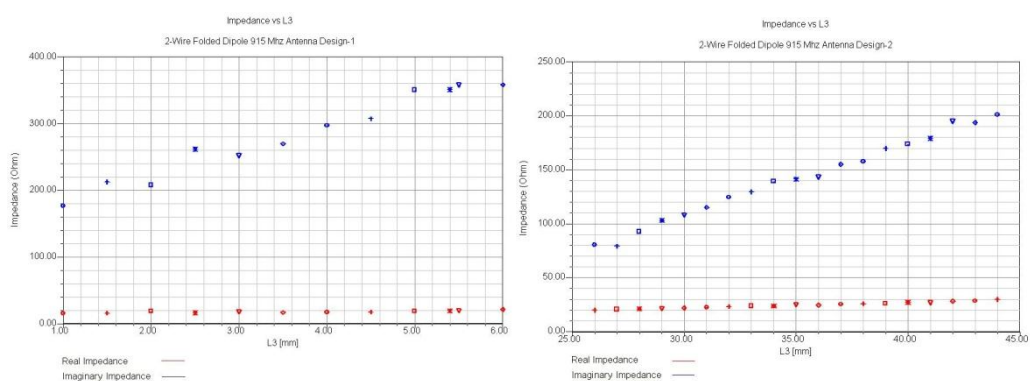
**Figure 4.11 Influence on input impedance L1 as a parameter**

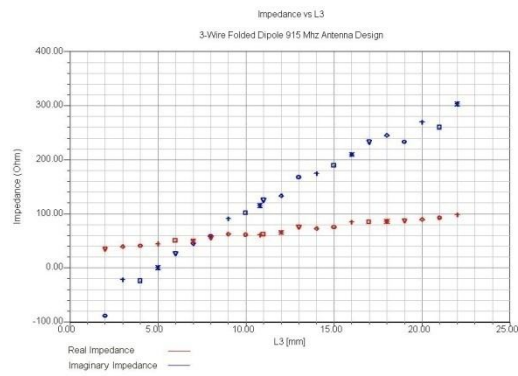
From Figure 4.11 we can see the simulated input impedance as a function of L1.  $R_{in}$  and  $X_{in}$  increase when L1 increases and we can conclude that the length of L1 has a great influence on the antenna's input impedances.



**Figure 4.12 Influence on input impedance L2 as a parameter**

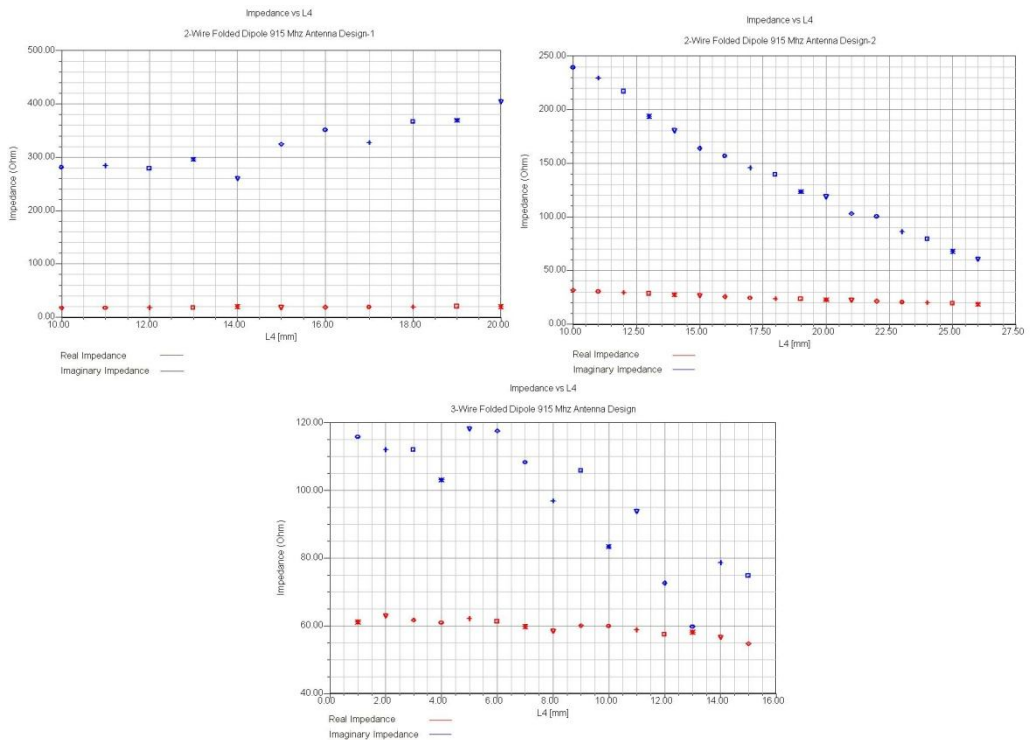
As in the case of L2 parameter, in Figure 4.12 it is obvious that when the L2 increases the reactance drops a lot but the resistance changes a little.





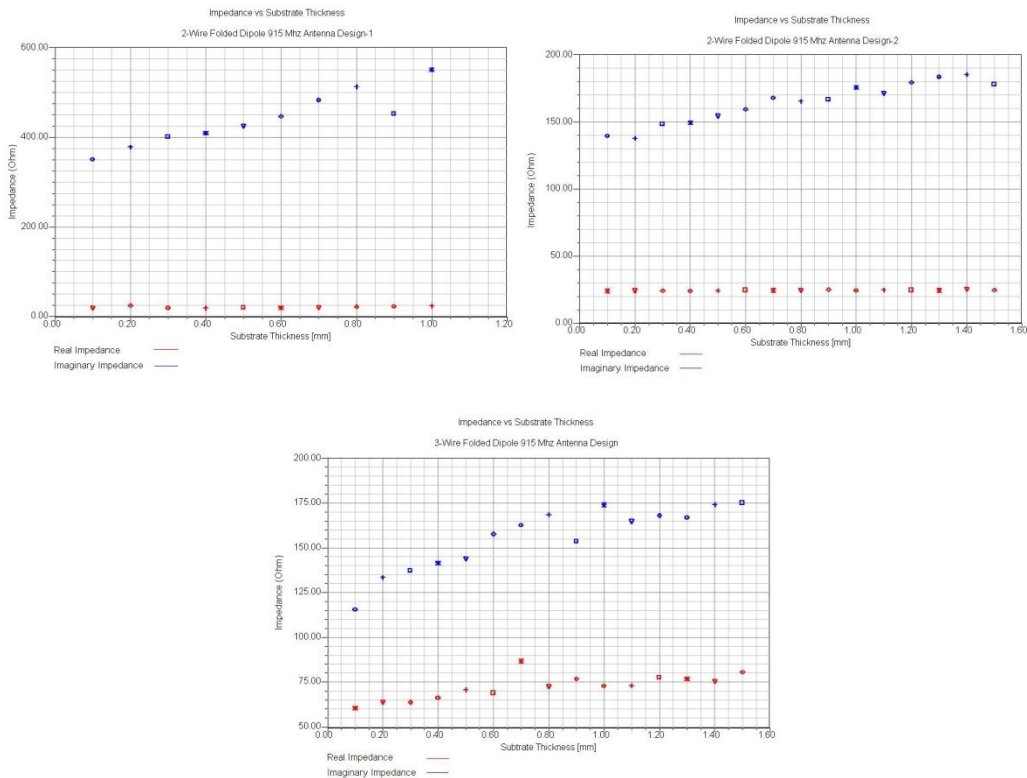
**Figure 4.13 Influence on input impedance L3 as a parameter**

Figure 4.13 shows that as the L3 increases, the resistance and reactance increases but it mainly acts on the reactance. It has influence on resistance less than L1 but more than L2.



**Figure 4.14 Influence on input impedance L4 as a parameter**

In the Figure 4.14, it is seen that increase of L4 increase the reactance of the antenna#1 but decrease the both resistance and the reactance of the antenna#2 and antenna#3. That is because of the different L4 interpretation in the antenna designs.



**Figure 4.15 Influence on input impedance substrate thickness as a parameter**

When the substrate thickness of the antennas are increased the reactance increases mainly but the resistance remains unchanged or changes a little (Figure 4.15).

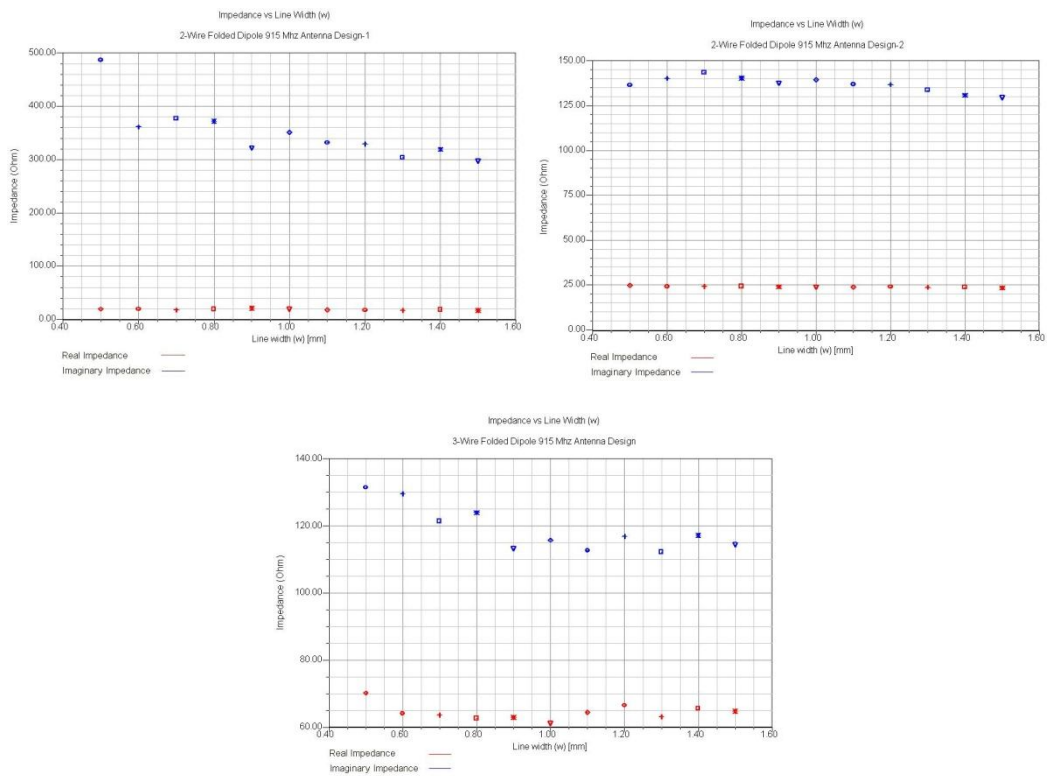


**Figure 4.16 Influence on input impedance, line width (w) as a parameter**

Finally, as the line thickness increased the antennas reactances are usually decreased but the resistances remains stable or exhibit a little variation.

## 4.4 Chapter Summary

Three different folded dipole type antennas have been designed for 915 MHz UHF RFID applications for supply chain applications. Analysis of these antennas with low resistance and high inductance for the input impedance provide a good example of a design procedure especially for the transponders which have specified load impedance. The required impedance can be achieved easily by simply changing the appropriate L1, L2, L3, L4, substrate width and line width. The tag size plays a major role in determining the read range. The smaller the tag, the smaller the energy capture area, therefore the shorter the read range. A proper

design of the system and a careful optimization of the interrogator power, antenna positioning and orientation, and an optimum tag positioning helps to alleviate this limitation. Multiple tagging can be used to improve the detection of the tags in both the horizontal and vertical planes.

## CHAPTER 5

### OTHER IMPEDANCE MATCHING TECHNIQUES

This chapter presents different methodologies for the design of UHF (915 MHz) passive tag antennas.

The necessary power required to energize and activate the passive transponder's microchip is drawn from the electromagnetic field supplied by the reader unit's antenna. Passive ICs are basically highly reactive because of the required power to bias the IC which is delivered by charging up the IC through electromagnetic coupling. Due to the low resistive but high capacitive impedance of the microchip, three different feeding type RFID antennas proposed comprising of antennas that are lowly resistive (high efficiency) and highly inductive for matching to the input impedance of the transponder IC.

The HFSS design tool [26], which is based on Finite Element Method (FEM), is used to optimize and analyze the tag. This tool is used as main platform to design and come up with certain antenna performance parameters such as return loss, gain, directivity, radiation pattern, efficiency and theoretical calculated read range. One T-Match (16.5cm x 2cm), one proximity coupled loop (16.5cm x 3.5cm) and one nested-slot (16.3cm x 16.3cm) antenna designs are built to make sure maximum range is obtained. Achieving that range has been a challenge because the lossy items make it harder to get an impedance matching and creates additional power loss in that environment. The tags which are simulated by

means of computer yield maximum operational distance of 4.53m which is well beyond the required range (2.5m) for the UHF RFID applications.

The rest of the chapter is organized into three sections which introduce different techniques for achieving complex impedance matching such as the T-match, the proximity-loop, and the nested-slot antenna layouts that are designed to be used for RFID applications.

## 5.1 T-Match Antenna Design

According to Figure 5.1, the input impedance of a (planar) dipole of length  $l$  can be altered by establishing a centered short-circuit stub, as explained in detail in the old book [29], and more recently in [7]. The antenna source is attached to a second dipole of length  $a \leq l$ , positioned at a close distance,  $b$ , from the first and larger dipole. The electric current distributes along the two main radiators according to the size of their transverse sections. It can be confirmed [7, 29] that the impedance at the source point is given by

$$Z_{in} = \frac{2Z_t(1+\alpha)^2Z_A}{2Z_t+(1+\alpha)^2Z_A}, \quad (1)$$

where  $Z_t = jZ_0 \tan ka/2$  is the input impedance of the short-circuit stub produced by the T-match conductors and piece of the dipole;  $Z_0 \cong 276 \log_{10} (b/\sqrt{r_e r_e'})$  is the characteristic impedance of the two-conductor transmission line with spacing  $b$ ;  $Z_A$  is the dipole impedance taken at its center in the absence of the T-match connection;  $r_e = 0.25w$  and  $r_e' = 8.25w'$  are the equivalent radii of the dipole and of the matching stub, supposed to be planar traces; and  $\alpha = \ln(b/r_e')/\ln (b/r_e)$  is the current division factor between the two conductors.

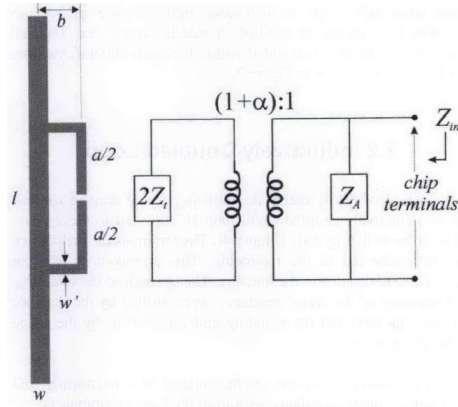


**Figure 5.1** The T-match configuration for planar dipoles and the equivalent circuit, where the impedance step-up ratio  $(1+\alpha)$  is related to the conductors' cross sections.

### 5.1.1 Design Approach

The IC input impedance to be used in this layout at 915 MHz is  $12-j140 \Omega$  (Alien Higgs-2) which means the load antenna impedance should be  $12+j140 \Omega$  for maximum power transfer (conjugate matching). This requires the antenna impedance to be low-resistive but high-inductive (large impedance phase angle,  $\arctan(Z_A) > 45^\circ$ ). Different T-match antenna designs like embedded T-match design within the main radiator [30], multi-conductor antenna with double T-match [31] or multi-conductor meander-line tag with a circular-shaped double T-match [32] have been proposed as a solution in the past. However, in my research the simplest generic version is investigated to keep the antenna size small and the load impedance to have a low real part (small resistance) and a high positive imaginary part (high inductance). To achieve this, the geometrical parameters,  $a$ ,  $b$ , and the trace's width,  $w'$  can be adjusted to match the complex chip impedance,  $Z_{chip}$ . To accomplish maximum directivity and optimum radiation, the designs are built to achieve half-wavelength ( $\lambda/2 \sim 16.4$  cm at 915 MHz) resonance at first.

In reality, the designs possess similarity to the half-wave dipole antenna; however, there exists a trade-off between antenna-chip matching and resonance.

Whenever the antenna size is increased to match for resonance, antenna-chip matching deteriorates. The miniaturization of the antenna size is another issue, which requires the length of the antenna to be smaller than the resonance length.

### 5.1.2 Antenna Design

The T-match RFID tag antenna design is shown in Figure 5.2. The antenna is made of copper metal with a thickness of  $0.02\text{mm}$  and polyester (with  $\epsilon_r=3.2$  and loss tangent  $\delta = 0.003$ ) with a thickness of  $0.1\text{mm}$  as a substrate. In addition to this, one-port differential excitation, which is used to measure the actual antenna-chip configuration, is employed to numerically calculate the antenna parameters such as return loss and antenna load impedance as well as the theoretical read range measurement.

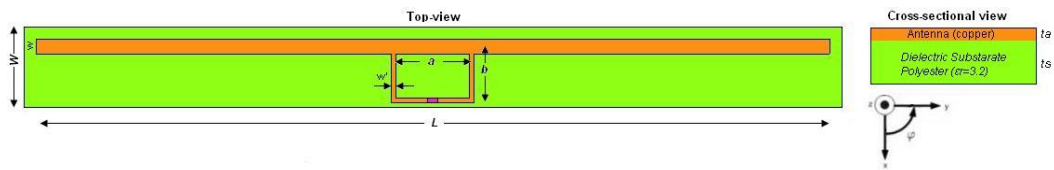


**Figure 5.2** The T-match RFID antenna design layout.

The short-circuit stub in the layout as shown in Figure 5.2 is utilized to obtain the required impedance. The designed antenna shown above has geometrical parameters of  $W = 16.5\text{mm}$ ,  $L = 163\text{mm}$ ,  $a = 15\text{mm}$ ,  $b = 8\text{mm}$ ,  $w = 3\text{mm}$ ,  $w' = 1\text{mm}$ ,  $ta = 0.02\text{mm}$ ,  $ts = 0.1\text{mm}$ , and port separation of  $2\text{mm}$ .

### 5.1.3 Simulation Results and Discussions

The simulated return loss with respect to frequency is illustrated in Figure 5.3.

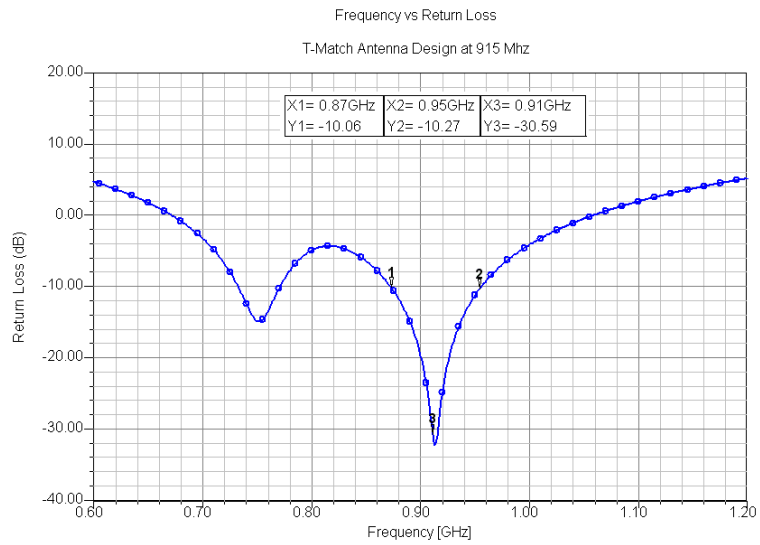


**Figure 5.3 Simulation result showing the return loss of the antenna.**

As seen from the Figure 5.3 the -10 dB bandwidth of the antenna is %8.7 (80 Mhz).

Figure 5.4 below shows the simulated antenna input impedance with respect to the frequency verifying that they are high-inductive and low-resistive.

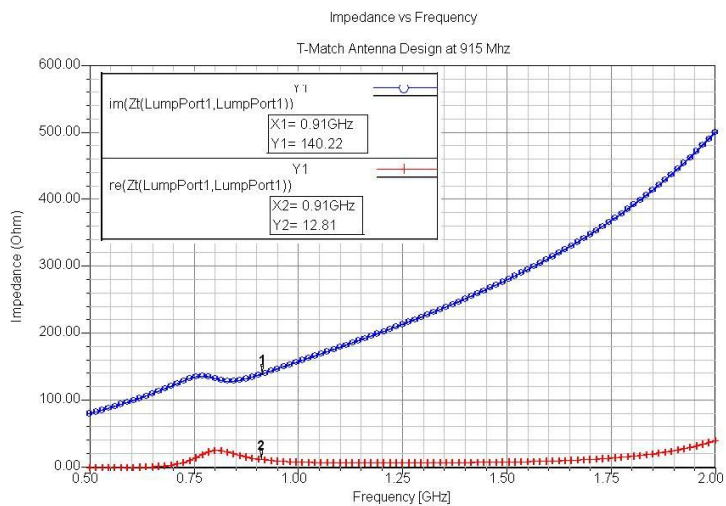


**Figure 5.4 Simulated antenna input impedance with respect to frequency.**

As it can be seen from the plots, the antenna input impedance is achieved to match complex conjugate of the chip impedance at that frequency. It is important to achieve complex conjugate match of the antenna at the frequencies which is distant from the antenna self resonant frequency. That is because, at the antenna self resonant frequency the impedance changes more quickly and antenna-chip matching deteriorates a lot at these regions. In order to achieve maximum operating bandwidth, the frequency of the conjugate matching should be selected where antenna input impedances exhibits slow changes in the real and imaginary parts.

T-match behaves as an impedance transformer (Figure 5.1). For the case of half-wavelength dipoles, the resulting input impedance at the T-match port is inductive, whereas for smaller dipoles, the total input impedance can be both capacitive and inductive.

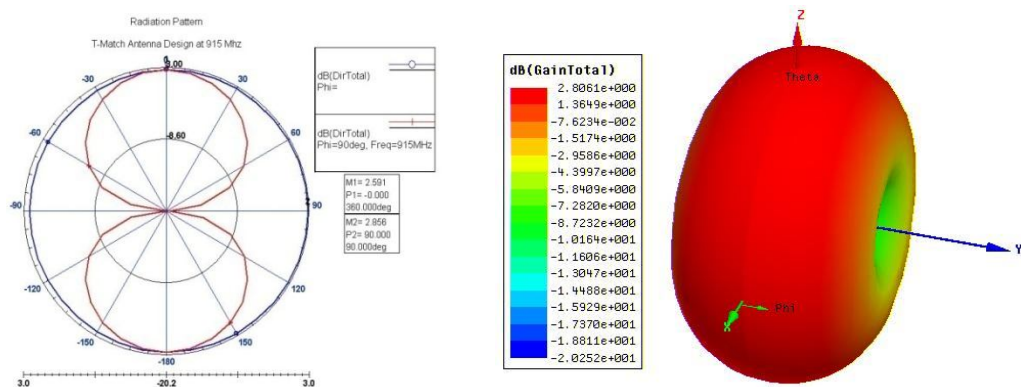


**Figure 5.5 Simulated 2-D radiation pattern (Directivity pattern for  $\phi=0^\circ$  (x-z) and  $\phi=90^\circ$  (y-z) planes) for the T-match 915 MHz UHF antenna design and 3-D gain pattern. Antenna is located in the horizontal plane.**

The radiation patterns for the T-Match design is shown in Figure 5.5. The antenna design has doughnut-shaped radiation patterns in the  $\phi=0$  deg (x-z plane) and  $\phi=90$  deg (y-z plane) planes as expected since the antennas are dipole type. The creation of nulls in the horizontal plane (x-y plane) with dipole type of antennas is a restrictive factor. It is essentially desired to attain maximum radiation when the tag is read in the plane (x-z or y-z planes) that is perpendicular to the RFID antenna. The horizontal plane radiation is also important in relation to the orientation of the interrogator. The interrogator (reader) does not essentially have to be positioned on top or bottom with respect to the RFID transponder; however the RFID transponder should also have the functionality to be read from the sides as well. Making use of the two orthogonal transponders (x-y horizontal plane and x-z/y-z vertical planes) would overcome this obstacle in case the application requires effective radiation characteristics in the horizontal plane. The dual polarization (horizontal and vertical) capture will improve the detection in the direction vertical to the antenna (z-axis) where antenna is least likely to be read.

The load impedance values are displayed in Table 5.1 along with other radiation parameters namely return loss, gain, directivity, antenna efficiency, and theoretical read range in free space.

**Table 5.1 Simulated antenna parameters and calculated theoretical read range.**

	Impedance (Ohm)	Return Loss (dB)	Gain (dB)	Directivity (dBi)	Antenna Efficiency (%)	Theoretical read range (m)
Ant #1	12.8+ j140.2	-30.6	2.8	2.85	98	4.53

## 5.2 Inductively Coupled Loop Antenna Design

Rather than the T-match, the radiating dipole may be excited via an inductively coupled small loop [33], located in close proximity to the radiating body (Figure 5.6). The terminals of the loop are directly connected to the microchip. This arrangement adds a correspondent inductance in the antenna. The strength of the coupling, and therefore of the added reactance, is controlled by the distance between the loop and the radiating body, as well as by the shape factor of the loop. The inductive coupling can be modeled by a transformer, and the resulting input impedance seen from the loop's terminals is

$$Z_{in} = Z_{loop} + \frac{(2\pi fM)^2}{Z_A},$$

where  $Z_{loop} = j2\pi fL_{loop}$  is the loop's input impedance. Whether or not the dipole is at resonance, the total input reactance depends only on the loop inductance,  $L_{loop}$ , while the resistance is related to the sole transformer mutual inductance,  $M$ :

$$R_{in}(f_0) = (2\pi f_0 M)^2 / R_A(f_0),$$

$$X_{in}(f_0) = 2\pi f_0 L_{loop}.$$

Assuming that the radiating body is infinitely long, the loop's inductance and mutual coupling,  $M$ , can be expressed in terms of the loop's size and its distance from the dipole through analytical formulas [33]. It is important to note that the mutual coupling, and therefore the total input resistance, are dependent on both the loop's shape and on the dipole-loop distance, while the reactance,  $L_{loop}$ , is mainly affected only by the loop's aspect ratio.

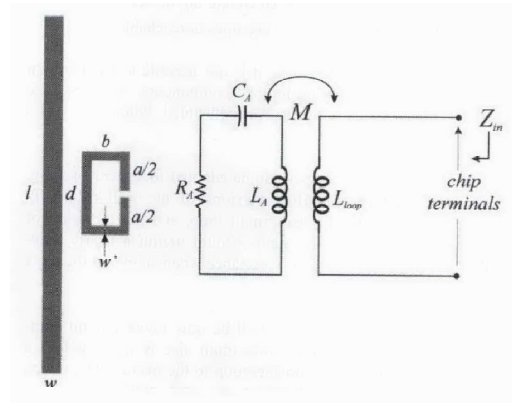


**Figure 5.6** The layout of the inductively coupled feed and its equivalent circuit. The parameters  $R_A$ ,  $C_A$ , and  $L_A$  give the circuit model of the radiating body near its (series) resonance.

### 5.2.1 Design Approach

The IC input impedance to be used in this layout at 915 MHz is  $16-j350 \Omega$  (Philips EPC 1.19) which means the load antenna impedance should be  $16+j350 \Omega$  for maximum power transfer (conjugate matching). This requires the antenna impedance to be low-resistive but high-inductive (large impedance phase angle,  $\arctan(Z_A) > 45^\circ$ ). Different inductively coupled antenna designs like meander-line antenna with inductively coupled feed [34, 35] have been proposed as a solution in the past. However, in my research the simplest generic version is investigated to keep the antenna size small and the load impedance to have a low real part (small resistance) and a high positive imaginary part (high inductance). To achieve this, the geometrical parameters,  $a$ ,  $b$ , and the dipole-loop distance,  $d$  can be adjusted to match the complex chip impedance,  $Z_{chip}$ . To accomplish maximum directivity and optimum radiation, the designs are built to achieve half-wavelength ( $\lambda/2 \sim 16.3$  cm at 915 MHz) resonance at first.

In reality, the designs possess similarity to the half-wave dipole antenna; however, there exists a trade-off between antenna-chip matching and resonance. Whenever the antenna size is increased to match for resonance, antenna-chip

matching deteriorates. The miniaturization of the antenna size is another issue, which requires the length of the antenna to be smaller than the resonance length.

### 5.2.2 Antenna Design

The inductively coupled loop RFID tag antenna design is shown in Figure 5.7. The antenna is made of copper metal with a thickness of  $0.02\text{mm}$  and polyester (with  $\epsilon_r = 3.2$  and loss tangent  $\delta = 0.003$ ) with a thickness of  $0.1\text{mm}$  as a substrate. In addition to this, one-port differential excitation, which is used to measure the actual antenna-chip configuration, is employed to numerically calculate the antenna parameters such as return loss and antenna load impedance as well as the theoretical read range measurement.

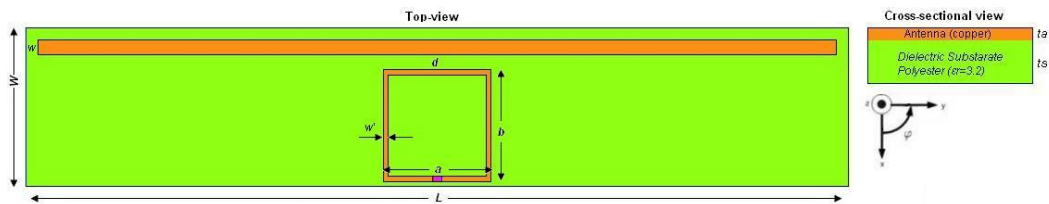
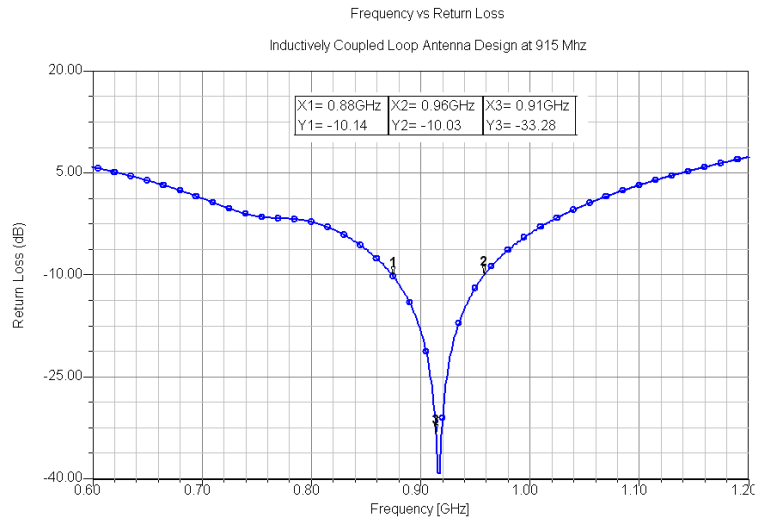


Figure 5.7 The inductively coupled loop RFID antenna design layout.

The inductive small loop in the layout as shown in Figure 5.7 is utilized to obtain the required impedance. The designed antenna shown above has geometrical parameters of  $W = 31.5\text{mm}$ ,  $L = 163\text{mm}$ ,  $a = 20.1\text{mm}$ ,  $b = 20.1\text{mm}$ ,  $d = 3.9\text{mm}$ ,  $w = 3\text{mm}$ ,  $w' = 1\text{mm}$ ,  $t_a = 0.02\text{mm}$ ,  $t_s = 0.1\text{mm}$ , and port separation of  $2\text{mm}$ .

### 5.2.3 Simulation Results and Discussions

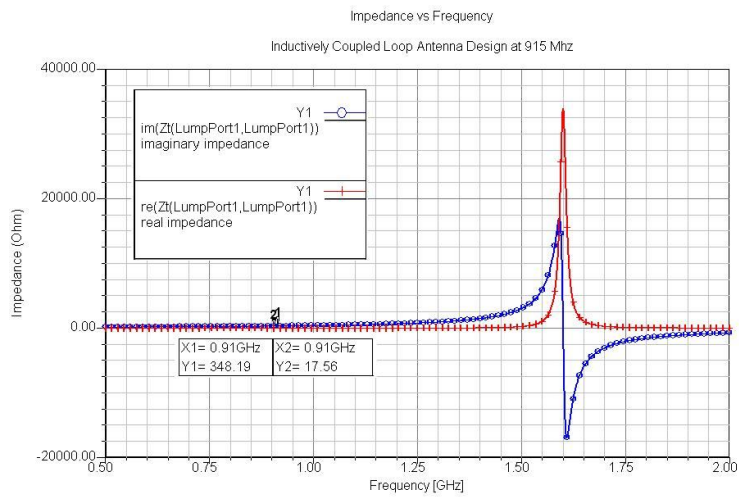
The simulated return loss with respect to frequency is illustrated in Figure 5.8.



**Figure 5.8 Simulation result showing the return loss of the antenna.**

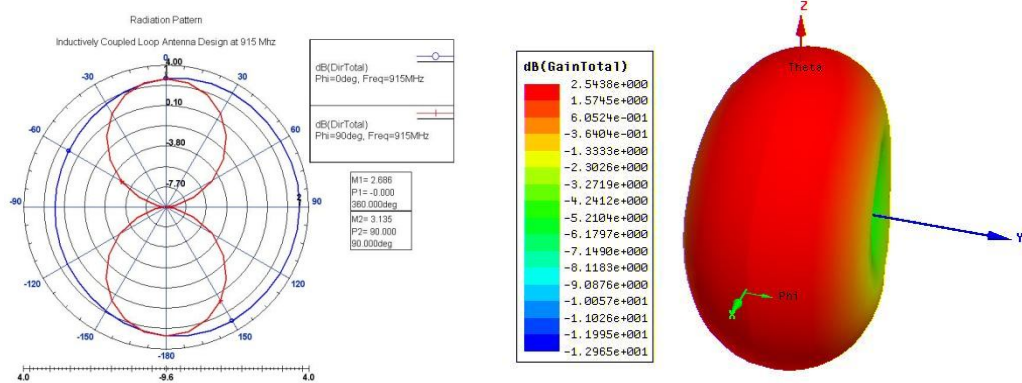
As seen from the Figure 5.8 the -10 dB bandwidth of the antenna is %8.7 (80 Mhz).

Figure 5.9 below shows the simulated antenna input impedance with respect to the frequency verifying that they are high-inductive and low-resistive.



**Figure 5.9 Simulated antenna input impedance with respect to frequency.**

As it can be seen from the plots, the antenna input impedance is achieved to match complex conjugate of the chip impedance at that frequency. It is important to achieve complex conjugate match of the antenna at the frequencies which is distant from the antenna self resonant frequency. That is because, at the antenna self resonant frequency the impedance changes more quickly and antenna-chip matching deteriorates a lot at these regions. In order to achieve maximum operating bandwidth, the frequency of the conjugate matching should be selected where antenna input impedances exhibits slow changes in the real and imaginary parts.



**Figure 5.10 Simulated 2-D radiation pattern (Directivity pattern for  $\phi=0$  (x-z) and  $\phi=90$  (y-z) planes) for the inductively coupled loop 915 MHz UHF antenna design and 3-D gain pattern. Antenna is located in the horizontal plane.**

The radiation pattern for the inductively coupled design is shown in Figure 5.10. The antenna design has doughnut-shaped radiation patterns in the  $\phi=0$  deg (x-z plane) and  $\phi=90$  deg (y-z plane) planes as expected since the antennas are dipole type. The creation of nulls in the horizontal plane (x-y plane) with dipole type of antennas is a restrictive factor. It is essentially desired to attain maximum radiation when the tag is read in the plane (x-z or y-z planes) that is perpendicular to the RFID antenna. The horizontal plane radiation is also important in relation

to the orientation of the interrogator. The Interrogator (reader) does not essentially have to be positioned on top or bottom with respect to the RFID transponder; however the RFID transponder should also have the functionality to be read from the sides as well. Making use of the two orthogonal transponders (x-y horizontal plane and x-z/y-z vertical planes) would overcome this obstacle in case the application requires effective radiation characteristics in the horizontal plane. The dual polarization (horizontal and vertical) capture will improve the detection in the direction vertical to the antenna (z-axis) where antenna is least likely to be read.

The load impedance values are displayed in Table 5.2 along with other radiation parameters namely return loss, gain, directivity, antenna efficiency, and theoretical read range in free space.

**Table 5.2 Simulated antenna parameters and calculated theoretical read range.**

	Impedance (Ohm)	Return Loss (dB)	Gain (dB)	Directivity (dBi)	Antenna Efficiency (%)	Theoretical read range (m)
Ant#2	17.5+ j348.2	-33.2	2.5	3.13	87.2	3.46

### 5.3 Nested Slot Antenna Design

A totally different matching strategy, useful for tags constructed with large planar dipoles or suspended patches [36, 37], may utilize a nested, shaped slot (Figure 5.11a). Due to the inductive reactance of a non-resonant slot, this feeding approach has the significant capability of complex impedance matching, even when the tag is attached onto a high-permittivity substrate (see, for instance, Figure 5.11b). The slot shape can be seen as a slot-line impedance transformer, where each discontinuity (tooth) supplies energy storage and radiation. As the

number of teeth increases, further degrees of freedom are obtained, with the possibility of improving miniaturization and attaining multi-band features [38]. Since the slot sizes may be comparable to the patch surface, the radiation characteristics are related to both objects. Specifically, the maximum antenna gain is fixed primarily by the patch side,  $l$ , while the impedance tuning can be altered by acting on the slot's aspect ratio, dimensions  $a$  and  $b$ . Depending on the shape and on the size of the internal slot, the antenna behaves generally either as an  $H$  slot, a broadband dipole, or as a doubly folded dipole. When the slot width,  $b$ , is much smaller than the external side,  $l$ , a typical RLC behavior can be examined, with strong reactance peaks. When the size  $b$  increases, the resonance shifts towards dc, and the reactance peak is decreased.

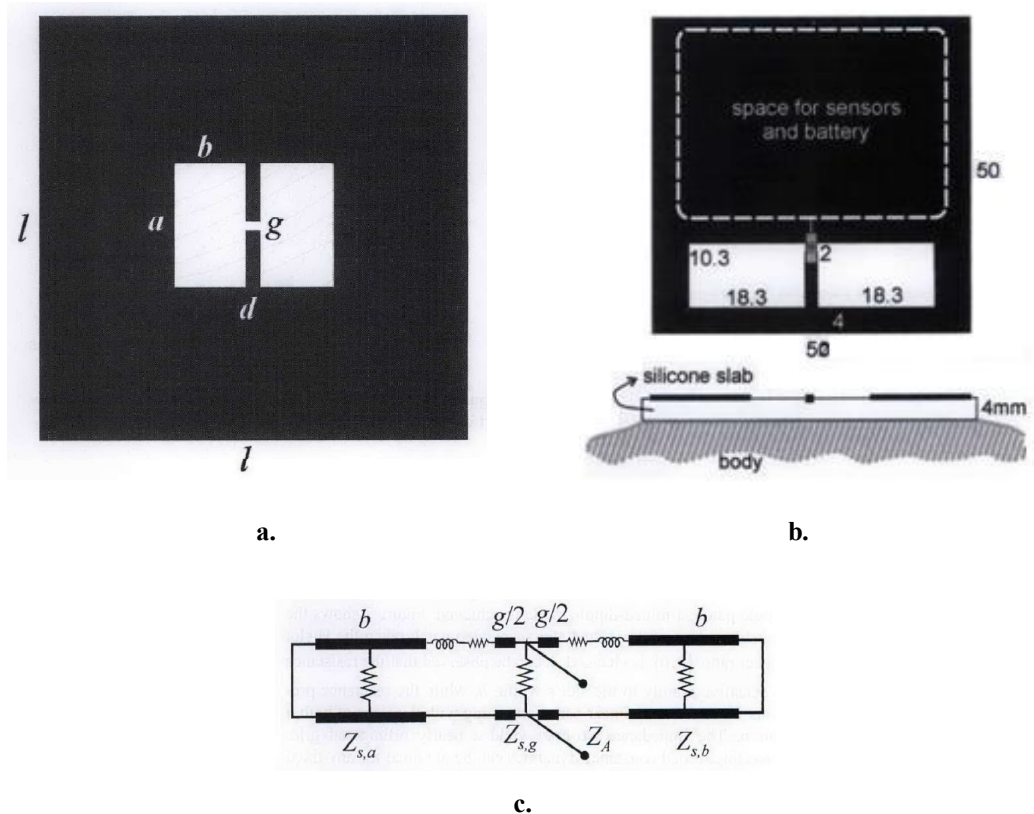


**Figure 5.11 a) The geometry of the nested-slot suspended-patch b) An example of the tag (size in mm) to be attached on to human body and able to host sensors [36] c) The equivalent simplified distributed circuit for the tab of Figure 5.11b.**

### 5.3.1 Design Approach

The IC input impedance to be used in this layout at 915 MHz is  $16-j350 \Omega$  (Philips EPC 1.19) which means the load antenna impedance should be  $16+j350 \Omega$  for maximum power transfer (conjugate matching). This requires the antenna impedance to be low-resistive but high-inductive (large impedance phase angle,  $\arctan(Z_A) > 45^\circ$ ). Different nested-slot antenna designs have been proposed according to the nested slot number (tooth) [38] as a solution in the past. However, in my research the simplest generic version is investigated to keep the load impedance to have a low real part (small resistance) and a high positive imaginary part (high inductance). To achieve this, the geometrical parameters,  $a$ ,  $b$  can be adjusted to match the complex chip impedance,  $Z_{chip}$ . To accomplish maximum directivity and optimum radiation, the designs are built to achieve half-wavelength ( $\lambda/2 \sim 16.3$  cm at 915 MHz) resonance at first.

In reality, the designs possess similarity to the half-wavelength 3-wire folded dipole antenna if the sizes  $a$  and  $b$  increase ( $2b \approx a \approx l$ ) until the slot nearly fills the surface of the whole patch.

### 5.3.2 Antenna Design

The nested slot RFID tag antenna design is shown in Figure 5.12. The antenna is made of copper metal with a thickness of  $0.02mm$  and polyester (with  $\epsilon_r=3.2$  and loss tangent  $\delta = 0.003$ ) with a thickness of  $0.1mm$  as a substrate. In addition to this, one-port differential excitation, which is used to measure the actual antenna-chip configuration, is employed to numerically calculate the antenna parameters such as return loss and antenna load impedance as well as the theoretical read range measurement.

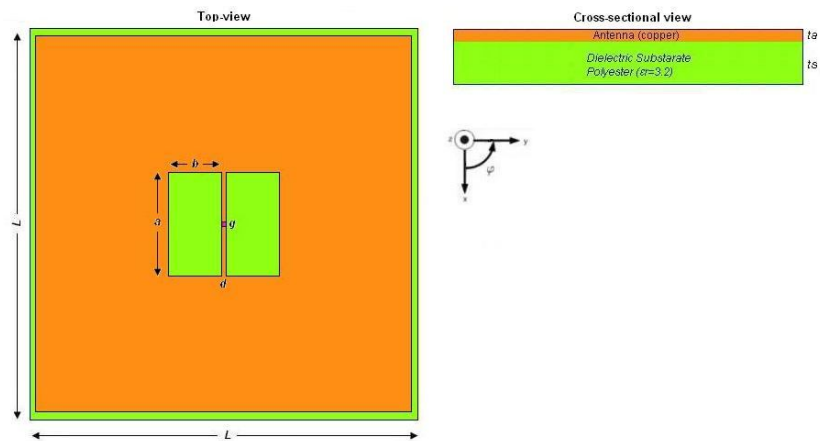


Figure 5.12 The nested-slot RFID antenna design layout.

The nested slot in the layout as shown in Figure 5.12 is utilized to obtain the required impedance. The designed antenna shown above has geometrical parameters of  $L = 163\text{mm}$ ,  $a = 45\text{mm}$ ,  $b = 23\text{mm}$ ,  $d = 2\text{mm}$ ,  $g = 2\text{mm}$ ,  $t_a = 0.02\text{mm}$ ,  $t_s = 0.1\text{mm}$ .

### 5.2.3 Simulation Results and Discussions

The simulated return loss with respect to frequency is illustrated in Figure 5.13.

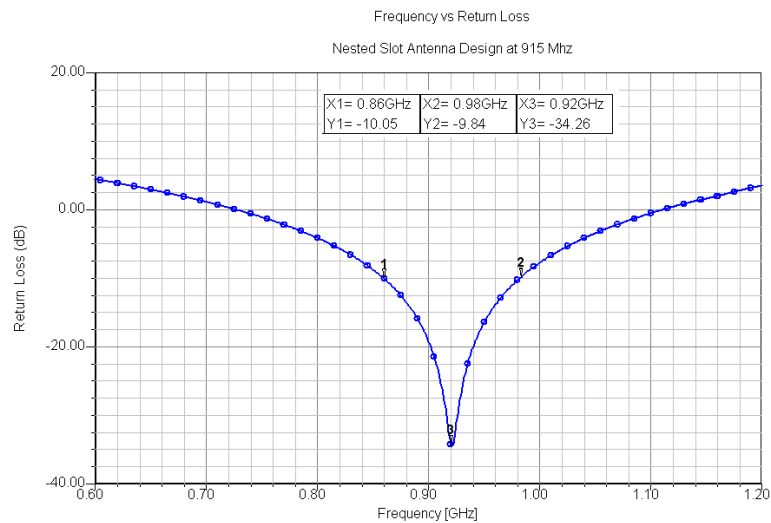
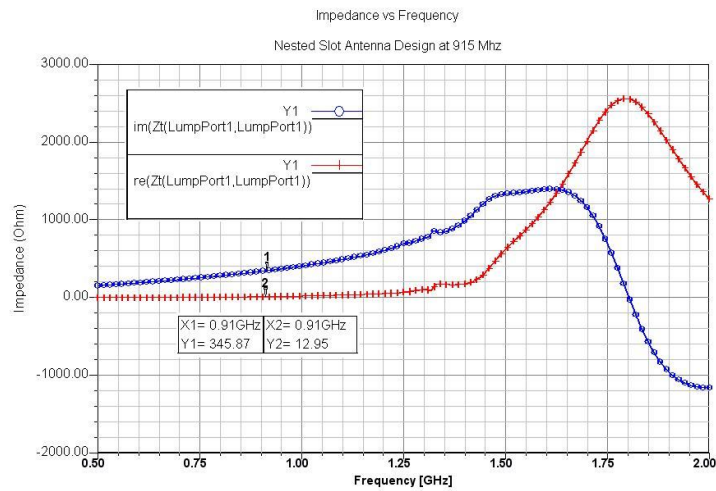


Figure 5.13 Simulation result showing the return loss of the antenna.

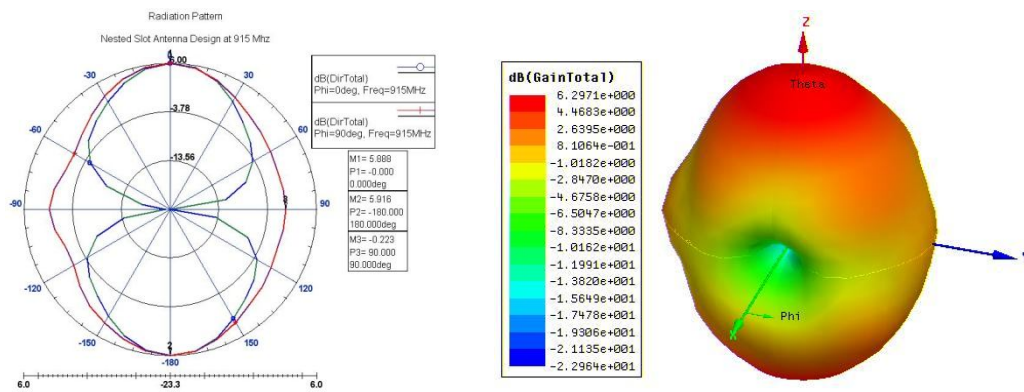
As seen from the Figure 5.13 the -10 dB bandwidth of the antenna is %13.1 (120 Mhz).

Figure 5.14 below shows the simulated antenna input impedance with respect to the frequency verifying that they are high-inductive and low-resistive.



**Figure 5.14 Simulated antenna input impedance with respect to frequency.**

As it can be seen from the plots, the antenna input impedance is achieved to match complex conjugate of the chip impedance at that frequency. It is important to achieve complex conjugate match of the antenna at the frequencies which is distant from the antenna self resonant frequency. That is because, at the antenna self resonant frequency the impedance changes more quickly and antenna-chip matching deteriorates a lot at these regions. In order to achieve maximum operating bandwidth, the frequency of the conjugate matching should be selected where antenna input impedances exhibits slow changes in the real and imaginary parts.



**Figure 5.15 Simulated 2-D radiation pattern (Directivity pattern for  $\phi=0^\circ$  (x-z) and  $\phi=90^\circ$  (y-z) planes) for the nested-slot 915 MHz UHF antenna design and 3-D gain pattern. Antenna is located in the horizontal plane.**

The radiation pattern for the nested-slot antenna design is shown in Figure 5.15. The antenna design has doughnut-shaped radiation patterns in the  $\phi=0^\circ$  deg (H-plane) and  $\phi=90^\circ$  deg (E-plane) planes as expected since the antenna acts as an H-slot. It is essentially desired to attain maximum radiation when the tag is read in the plane (x-z or y-z planes) that is perpendicular to the RFID antenna. The horizontal plane radiation is also important in relation to the orientation of the interrogator. The Interrogator (reader) does not essentially have to be positioned on top or bottom with respect to the RFID transponder; however the RFID transponder should also have the functionality to be read from the sides as well. Making use of the two orthogonal transponders (x-y horizontal plane and x-z/y-z vertical planes) would overcome this obstacle in case the application requires effective radiation characteristics in the horizontal plane.

The load impedance values are displayed in Table 5.3 along with other radiation parameters namely return loss, gain, directivity, antenna efficiency, and theoretical read range in free space.

**Table 5.3 Simulated antenna parameters and calculated theoretical read range.**

	Impedance (Ohm)	Return Loss (dB)	Gain (dB)	Directivity (dBi)	Antenna Efficiency (%)	Theoretical read range (m)
Ant#3	13+ j345.9	-34.26	6.3	5.9	100	4.81

## 5.4 Chapter Summary

Three different feeding type RFID antennas (T-match, proximity-loop and nested-slot) which are lowly resistive (high efficiency) and highly inductive for matching to the input impedance of the transponder IC have been proposed for 915 MHz UHF RFID applications. Analysis of these antennas with low resistance and high inductance for the input impedance provide a good example of a design procedure especially for the transponders which have a specified load impedance. The required impedance can be achieved easily by simply changing the appropriate antenna geometries. The tag size plays a major role in determining the read range. The smaller the tag, the smaller the energy capture area, therefore the shorter the read range. A proper design of the system and a careful optimization of the interrogator power, antenna positioning and orientation, and an optimum tag positioning helps to alleviate this limitation. Multiple tagging can be used to improve the detection of the tags in both the horizontal and vertical planes.

## **CHAPTER 6**

### **MEANDERED LINE DIPOLE**

#### **ANTENNA DESIGNS**

This chapter presents six different meandered-line dipole antenna designs and implementations for the type of UHF (868 MHz) passive tag antennas.

As proposed in [22], by folding the arms of a dipole antenna along a meandered path (Figure 6.1), a wire configuration is produced with distributed capacitive and inductive reactances that globally affect the antenna's input impedance. Up to the first antenna resonance, the currents on the adjacent vertical segments of meandered-line antennas (MLA) have opposite phases. These transmission-line currents do not give a valuable contribution to the radiated power, but nevertheless produce losses. Resonances are achieved at much lower frequencies than in the case of a straight dipole of the same height, at the expense of a narrow bandwidth and a low efficiency.

The HFSS design tool [26], which is based on Finite Element Method (FEM), is used to optimize and analyze the tag. This tool is used as main platform to design and come up with certain antenna performance parameters such as return loss, gain, directivity, radiation pattern, efficiency and theoretical calculated read range. Two meander-line antennas with loading bar which are 10.7cm x 1.6cm (equal in area or smaller) and four meander-line antennas having multiple

unequal turns which are 4.8cm x 4.1cm (equal in area or smaller) antenna designs are built to make sure maximum range is obtained. Achieving that range has been

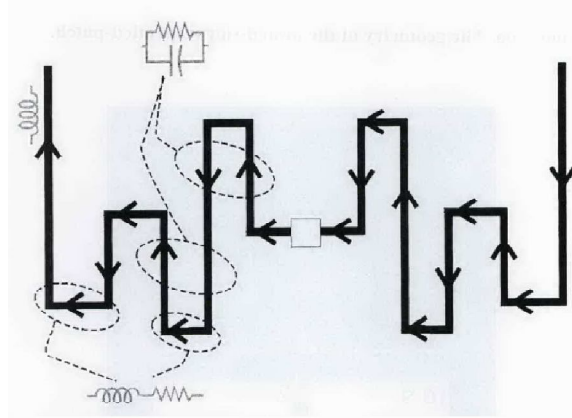


**Figure 6.1** The geometry of a meandered-line antenna (MLA) having multiple unequal turns. The horizontal lines mainly control the radiation resistance, the adjacent vertical lines (transmission-line current mode) give storage of electric energy and loss, and the overall conductor length affects the inductance.

a challenge because the lossy items make it harder to get an impedance matching and creates additional power loss in that environment. The tags which are measured by means of RFID reader yield minimum operational distance of 2.8m which is well beyond the required range (2.5m) for the UHF RFID applications.

## 6.1 Design Approach

The IC input impedance to be used in these layouts at 868 MHz are  $15-j151\Omega$  (Alien Higgs-2 Chip used in designs 1, 3 and 5) and  $30-j211\Omega$  (Alien Higgs-3 Chip used in designs 2, 4 and 6) which means the load antenna impedance should be  $15+j151\Omega$  and  $30+j211\Omega$  for maximum power transfer (conjugate matching). This requires the antenna impedance to be low-resistive but high-inductive (large impedance phase angle,  $\arctan(Z_A) > 45^\circ$ ). Different antenna designs like meander-line antenna with inductively coupled feed [34,35] or equi-

spaced meander-line with T-match feed [39] have been proposed as a solution in the past. However, in my research the simplest generic versions which are equi-spaced meander-line antenna with loading bar and meander-line antennas having multiple unequal turns are investigated to keep the antenna size small and the load impedance to have a low real part (small resistance) and a high positive imaginary part (high inductance). To achieve this, the geometrical parameters of the antennas can be adjusted to match the complex chip impedance,  $Z_{chip}$ . To accomplish maximum directivity and optimum radiation, the designs are built to achieve smaller than half-wavelength ( $\lambda/2 \sim 17.3$  cm at 868 MHz) resonance at first. In reality, the total length of the turns in the designed antenna is longer than that of the half-wave dipole antenna.

## 6.2 Antenna Designs

Six meander-line antenna designs are simulated and implemented. The meander-line RFID tag antenna with loading bar design#1 is shown in Figure 6.2. The antenna is made of copper metal with a thickness of 0.035mm and FR4 (with  $\epsilon_r=4.4$  and loss tangent  $\delta=0.02$ ) with a thickness of 0.8mm as a substrate. In addition to this, one-port differential excitation, which is used to measure the actual antenna-chip configuration, is employed to numerically calculate the antenna parameters such as return loss and antenna load impedance as well as the theoretical read range measurement.

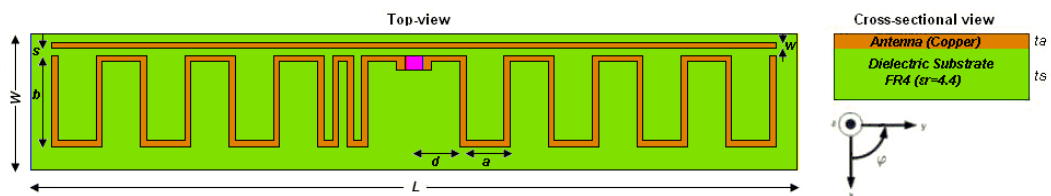
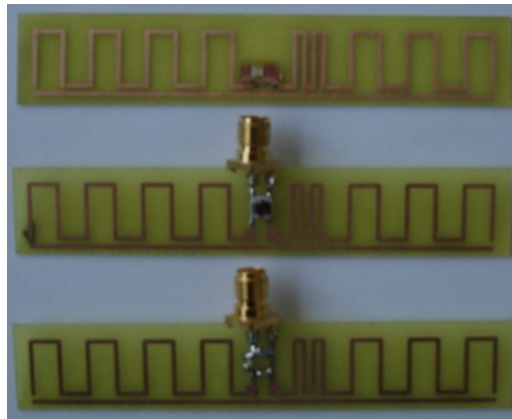


Figure 6.2 The meander-line RFID antenna with loading bar design#1 layout.

The loading bar in the layout as shown in Figure 6.2 is utilized to obtain the required impedance. The designed antenna#1 shown above has geometrical parameters of  $W = 15.7mm$ ,  $L = 88.4mm$ ,  $a = 5.1mm$ ,  $b = 10.5mm$ ,  $d = 5.3mm$ ,  $w = 0.7mm$ ,  $ta = 0.035mm$ ,  $ts = 0.8mm$ , and port separation of  $2mm$ .

The implemented design#1 meander-line antennas with loading bar are shown in Figure 6.3. In order to match the antenna complex input impedance  $Z_A$  to the SMA connector ( $50\Omega$ ) impedance, matching circuit and/or coil transformer is inserted to the design for measurements.



**Figure 6.3 The implemented meander-line RFID antenna with loading bar design#1 layout. Implemented chip inserted antenna, coil impedance transformer inserted with SMA connector and matching circuit inserted with SMA connector antennas are shown from top to bottom.**

The meander-line RFID tag antenna with loading bar design#2 is shown in Figure 6.4. The antenna is made of copper metal with a thickness of  $0.035mm$  and Rogers4003 (with  $\epsilon_r=3.38$  and loss tangent  $\delta=0.0027$ ) with a thickness of  $1mm$  as a substrate.

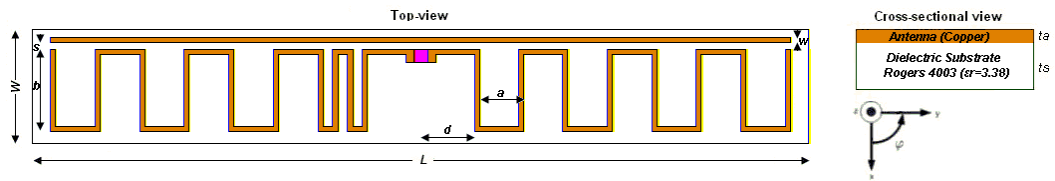


**Figure 6.4** The meander-line RFID antenna with loading bar design#2 layout.

The loading bar in the layout as shown in Figure 6.4 is utilized to obtain the required impedance. The designed antenna#2 shown above has geometrical parameters of  $W = 15.6\text{mm}$ ,  $L = 106.4\text{mm}$ ,  $a = 6.1\text{mm}$ ,  $b = 11.2\text{mm}$ ,  $d = 7.3\text{mm}$ ,  $w = 0.7\text{mm}$ ,  $t_a = 0.035\text{mm}$ ,  $t_s = 1\text{mm}$ , and port separation of  $2\text{mm}$ .

The implemented design#2 meander-line antennas with loading bar are shown in Figure 6.5. In order to match the antenna complex input impedance  $Z_A$  to the SMA connector ( $50\Omega$ ) impedance, matching circuit and/or coil transformer is inserted to the design for measuring antenna parameters.

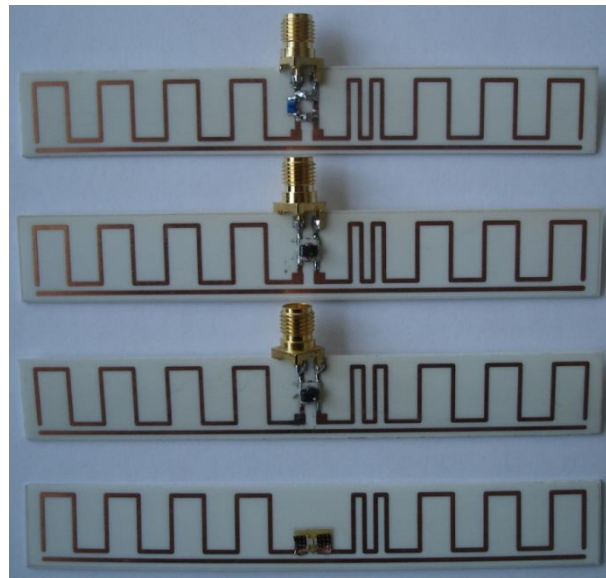


**Figure 6.5** The implemented meander-line RFID antenna with loading bar design#2 layout. Implemented chip inserted antenna, coil impedance transformers inserted with SMA connector and matching circuit inserted with SMA connector antennas are shown from bottom to top.

The meander-line RFID tag antenna with unequal turn design#3 is shown in Figure 6.6. The antenna is made of copper metal with a thickness of 0.035mm and FR4 (with  $\epsilon_r=4.4$  and loss tangent  $\delta=0.02$ ) with a thickness of 0.8mm as a substrate.

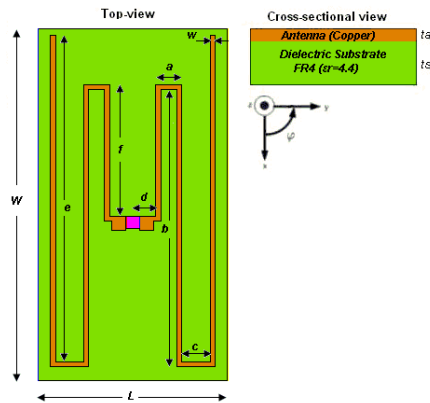


**Figure 6.6 The meander-line RFID antenna with unequal turn design#3 layout.**

The unequal turn in the layout as shown in Figure 6.6 is utilized to obtain the required impedance. The designed antenna#3 shown above has geometrical parameters of  $W = 50mm$ ,  $L = 27mm$ ,  $a = 3mm$ ,  $b = 39.3mm$ ,  $c = 4mm$ ,  $d = 3.3mm$ ,  $e = 46.3mm$ ,  $f = 18.65mm$ ,  $w = 0.7mm$ ,  $ta = 0.035mm$ ,  $ts = 0.8mm$ , and port separation of  $2mm$ .

The implemented design#3 meander-line antennas having unequal turn are shown in Figure 6.7. In order to match the antenna complex input impedance  $Z_A$  to the SMA connector ( $50\Omega$ ) impedance, matching circuit and/or coil transformer is inserted to the design for measurements.

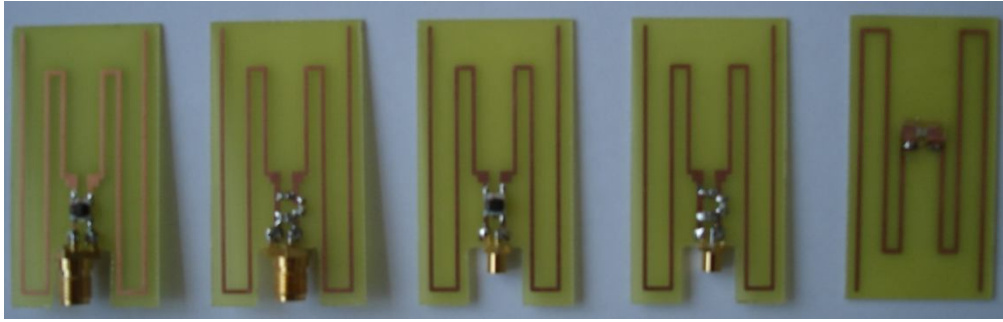


**Figure 6.7** The implemented meander-line RFID antenna having unequal turns design#3 layout. Implemented coil impedance transformer and matching circuit inserted with SMA connector, coil impedance transformer and matching circuit inserted with MMCX connector and chip inserted antennas are shown from left to right.

The meander-line RFID tag antenna with unequal turn design#4 is shown in Figure 6.8. The antenna is made of copper metal with a thickness of 0.035mm and Rogers4003 (with  $\epsilon_r=3.38$  and loss tangent  $\delta=0.0027$ ) with a thickness of 1mm as a substrate.

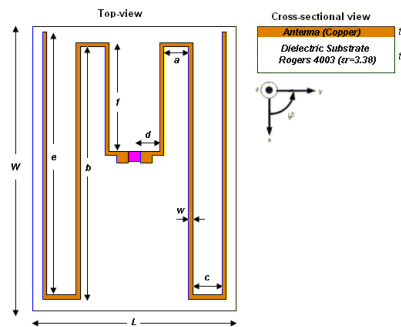


**Figure 6.8** The meander-line RFID antenna with unequal turn design#4 layout.

The unequal turn in the layout as shown in Figure 6.8 is utilized to obtain the required impedance. The designed antenna#4 shown above has geometrical parameters of  $W = 48.8mm$ ,  $L = 35mm$ ,  $a = 3mm$ ,  $b = 39.3mm$ ,  $c = 4mm$ ,  $d = 3.3mm$ ,  $e = 46.3mm$ ,  $f = 18.65mm$ ,  $w = 0.7mm$ ,  $ta = 0.035mm$ ,  $ts = 0.8mm$ , and port separation of  $2mm$ .

The implemented design#4 meander-line antennas having unequal turn are shown in Figure 6.9. In order to match the antenna complex input impedance  $Z_A$  to the

SMA connector ( $50\Omega$ ) impedance, matching circuit and/or coil transformer is inserted to the design for measurements.

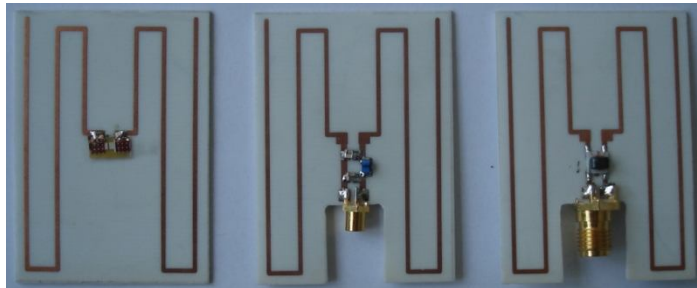


**Figure 6.9** The implemented meander-line RFID antenna having unequal turns design#4 layout. Implemented chip inserted antenna, matching circuit inserted and coil impedance transformer with SMA connector antennas are shown from left to right.

The meander-line RFID tag antenna having multiple unequal turns design#5 is shown in Figure 6.10. The antenna is made of copper metal with a thickness of  $0.035\text{mm}$  and FR4 (with  $\epsilon_r=4.4$  and loss tangent  $\delta=0.02$ ) with a thickness of  $0.8\text{mm}$  as a substrate.

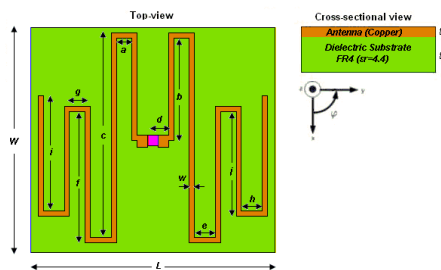


**Figure 6.10** The meander-line RFID antenna having multiple unequal turns design#5 layout.

The multiple unequal turns in the layout as shown in Figure 6.10 is utilized to obtain the required impedance. The designed antenna#5 shown above has geometrical parameters of  $W = 43\text{mm}$ ,  $L = 47\text{mm}$ ,  $a = 3\text{mm}$ ,  $b = 19.5\text{mm}$ ,  $c = 38.95\text{mm}$ ,  $d = 3\text{mm}$ ,  $e = 4\text{mm}$ ,  $f = 25\text{mm}$ ,  $g = 3\text{mm}$ ,  $h = 4\text{mm}$ ,  $i = 22\text{mm}$ ,  $j = 20\text{mm}$ ,  $w = 1\text{mm}$ ,  $t_a = 0.035\text{mm}$ ,  $t_s = 0.8\text{mm}$ , and port separation of  $2\text{mm}$ .

The implemented design#5 meander-line antennas having multiple unequal turns are shown in Figure 6.11.

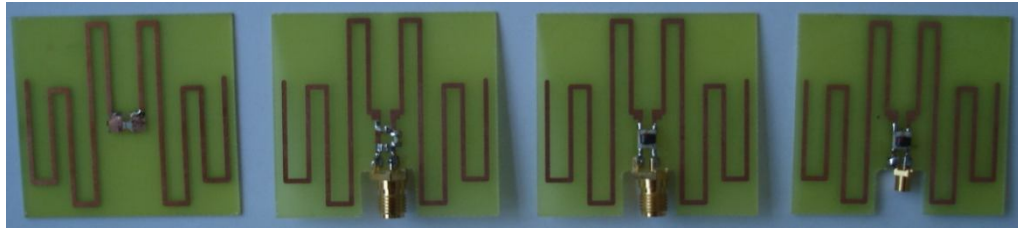


**Figure 6.11** The implemented meander-line RFID antenna having multiple unequal turns design#5 layout. Implemented chip inserted antenna, matching circuit inserted and coil impedance transformer with SMA and MMCX connector antennas are shown from left to right.

The meander-line RFID tag antenna having multiple unequal turns design#6 is shown in Figure 6.12. The antenna is made of copper metal with a thickness of 0.035mm and Rogers4003 (with  $\epsilon_r=3.38$  and loss tangent  $\delta=0.0027$ ) with a thickness of 1mm as a substrate.

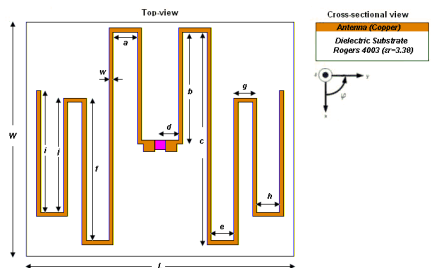


**Figure 6.12** The meander-line RFID antenna having multiple unequal turns design#6 layout.

The multiple unequal turns in the layout as shown in Figure 6.12 is utilized to obtain the required impedance. The designed antenna#6 shown above has geometrical parameters of  $W = 41mm$ ,  $L = 47mm$ ,  $a = 4.3mm$ ,  $b = 19.65mm$ ,  $c = 37.3mm$ ,  $d = 3.3mm$ ,  $e = 4mm$ ,  $f = 25mm$ ,  $g = 4mm$ ,  $h = 4mm$ ,  $i = 21.3mm$ ,  $j = 20mm$ ,  $w = 0.7mm$ ,  $ta = 0.035mm$ ,  $ts = 1mm$ , and port separation of 2mm.

The implemented design#6 meander-line antennas having multiple unequal turns are shown in Figure 6.13.

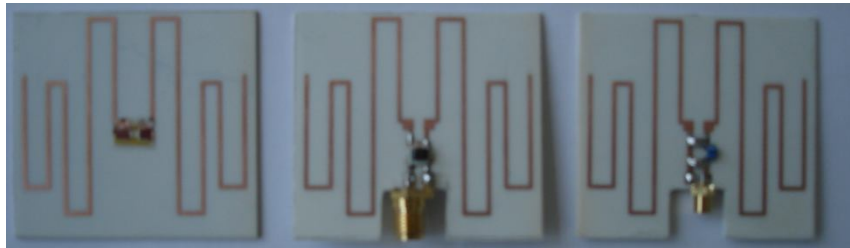


**Figure 6.13** The implemented meander-line RFID antenna having multiple unequal turns design#6 layout. Implemented chip inserted antenna, coil impedance transformer with SMA and matching circuit inserted with MMCX connector antennas are shown from left to right.

### 6.3 Simulation Results and Discussions

The simulated and measured return losses with respect to frequency are illustrated in the following figures.

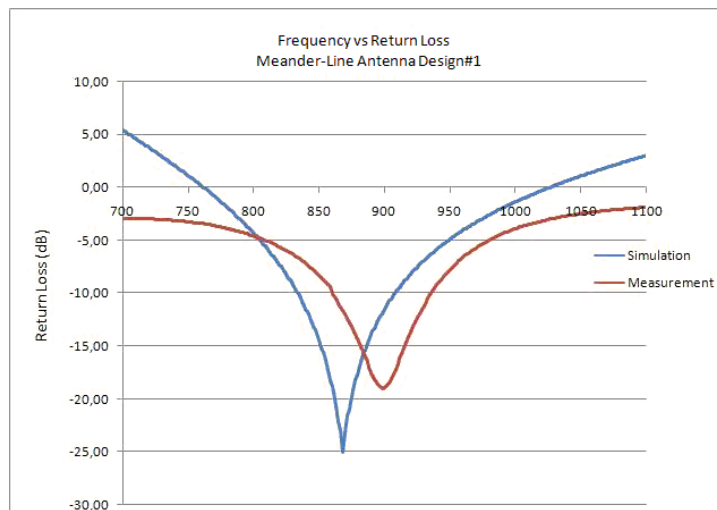


**Figure 6.14** Results showing the return loss of the meander-line antenna design#1

As seen from Figure 6.14, -10 dB bandwidth of the antennas are 74 Mhz and 75 Mhz for the simulation and measurement respectively which is %8.6 of 868 Mhz.

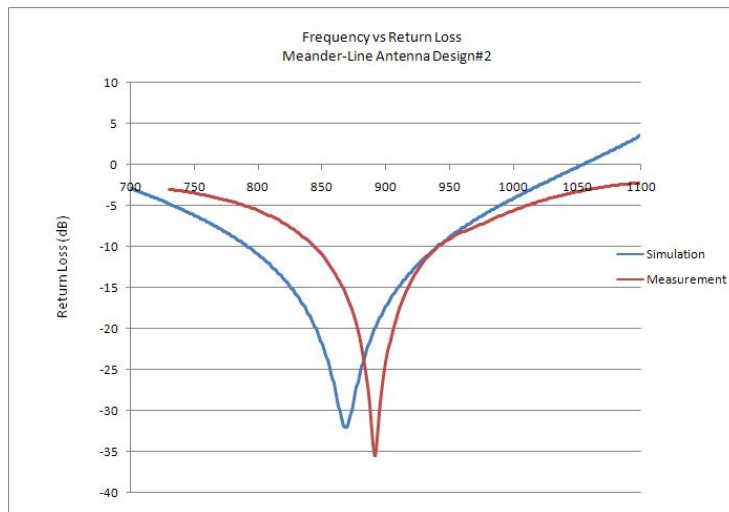


**Figure 6.15 Results showing the return loss of the meander-line antenna design#2**

As seen from Figure 6.15, -10 dB bandwidth of the antennas are 148 Mhz and 97 Mhz for the simulation and measurement respectively which is %11.1-17 of 868 Mhz.

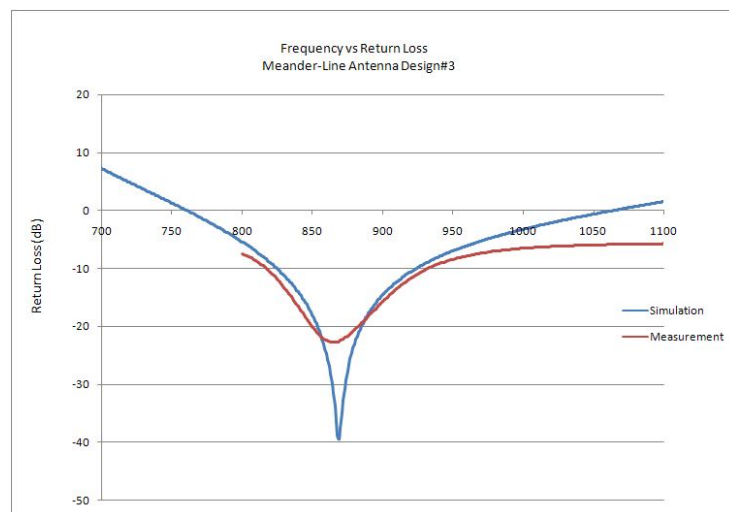


**Figure 6.16 Results showing the return loss of the meander-line antenna design#3**

As seen from Figure 6.16, -10 dB bandwidth of the antennas are 99 Mhz and 113 Mhz for the simulation and measurement respectively which is %11.4-13 of 868 Mhz.

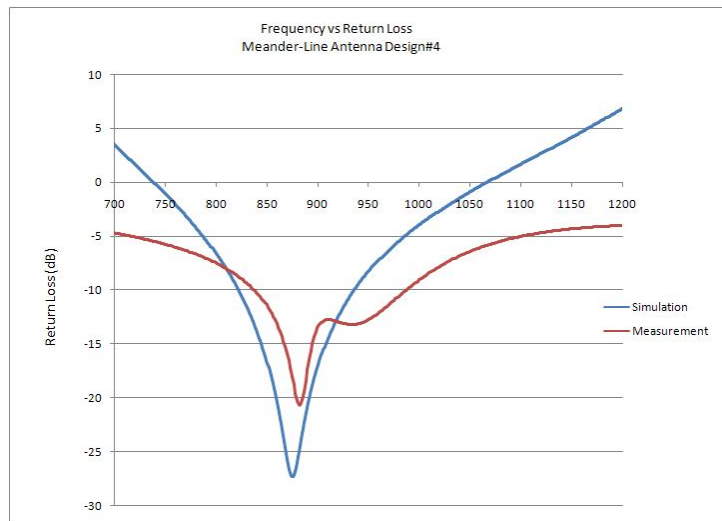


**Figure 6.17 Results showing the return loss of the meander-line antenna design#4**

As seen from Figure 6.17, -10 dB bandwidth of the antennas are 113 Mhz and 149 Mhz for the simulation and measurement respectively which is %13-17 of 868 Mhz.

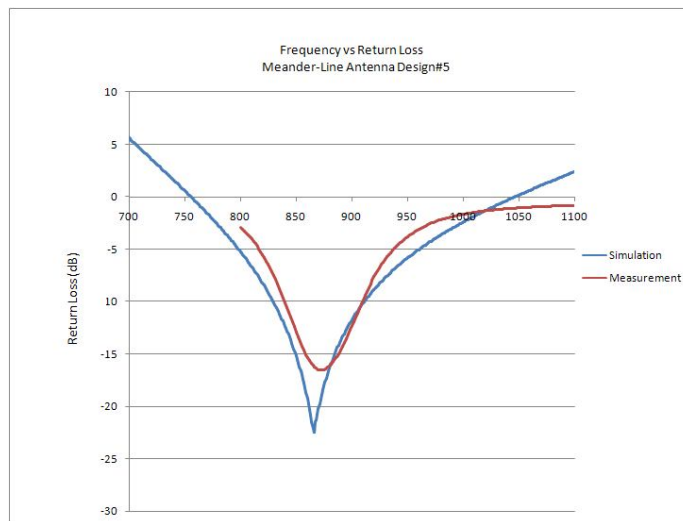


**Figure 6.18 Results showing the return loss of the meander-line antenna design#5**

As seen from Figure 6.18, -10 dB bandwidth of the antennas are 81 Mhz and 68 Mhz for the simulation and measurement respectively which is %7.8-9.3 of 868 Mhz.

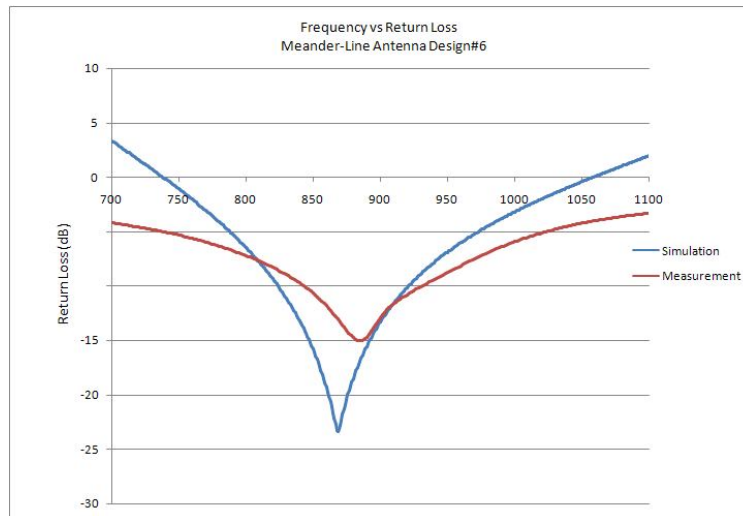


**Figure 6.19 Results showing the return loss of the meander-line antenna design#6**

As seen from Figure 6.19, -10 dB bandwidth of the antennas are 97 Mhz and 85 Mhz for the simulation and measurement respectively which is %9.7-11.1 of 868 Mhz.

When examining the figures above, the resonance frequency of the implemented antennas is seen to slightly shifted to a higher frequencies. This is due to the matching circuits and/or coil impedance transformers, since the simulated designs lack of these circuitries.

Figures below shows the simulated antenna input impedance with respect to the frequency verifying that they are high-inductive and low-resistive.

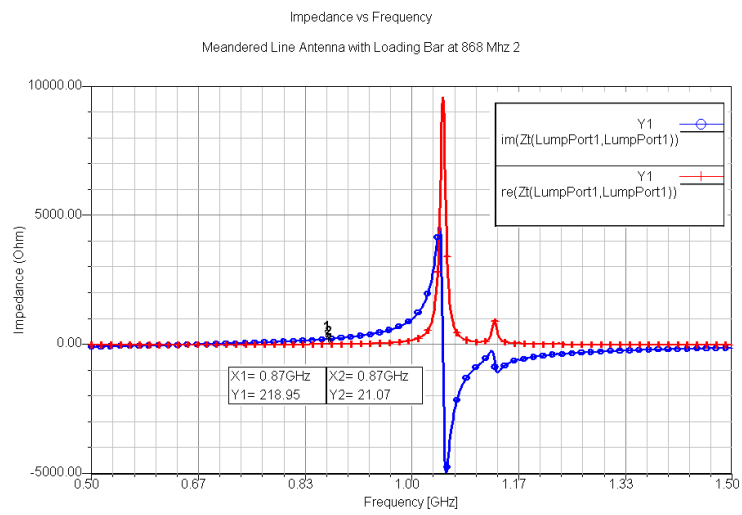
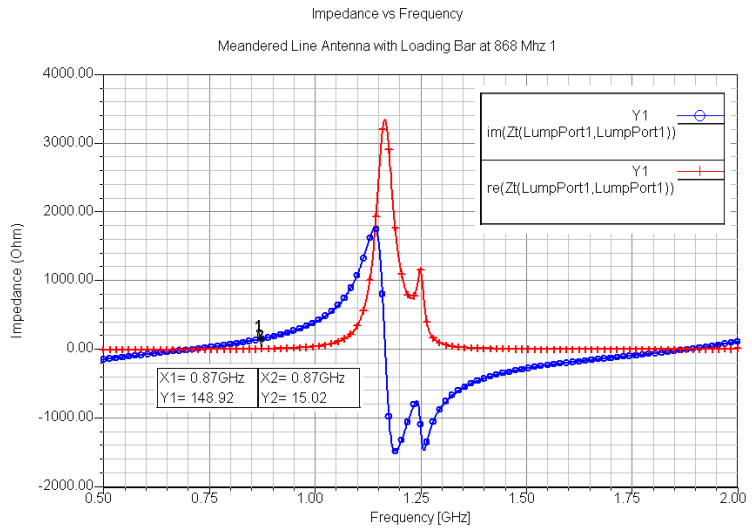


**Figure 6.20 Simulated meander-line antenna designs input impedance with respect to frequency.**

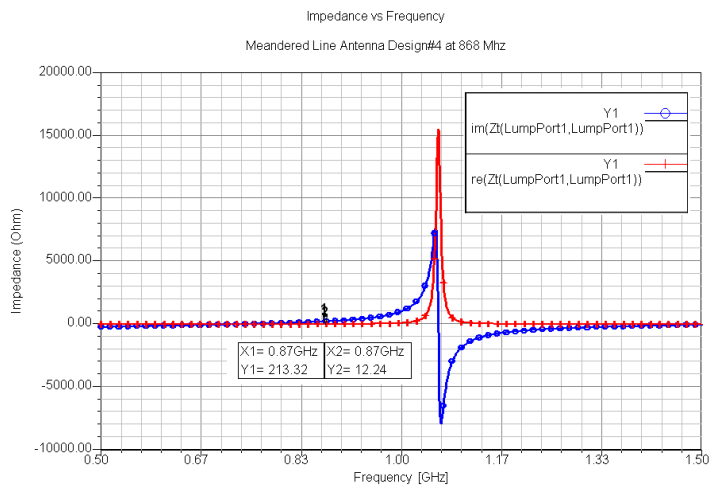
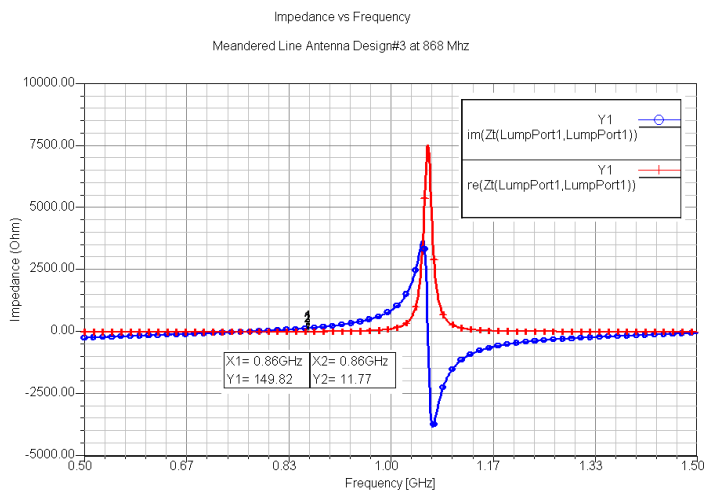


**Figure 6.21 Simulated meander-line antenna designs input impedance with respect to frequency.**

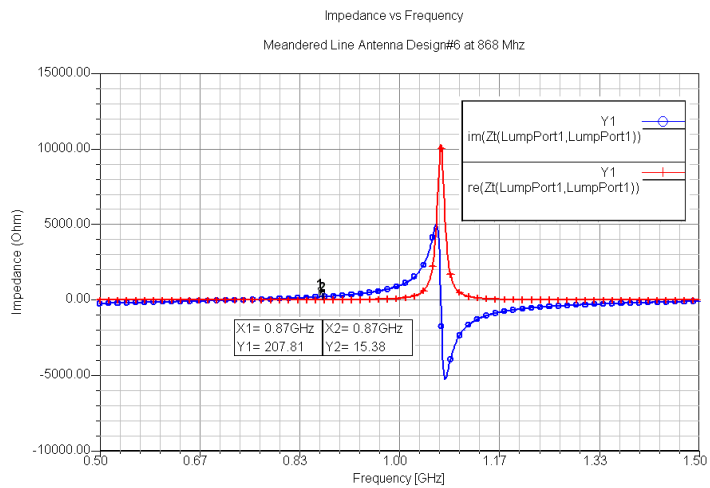
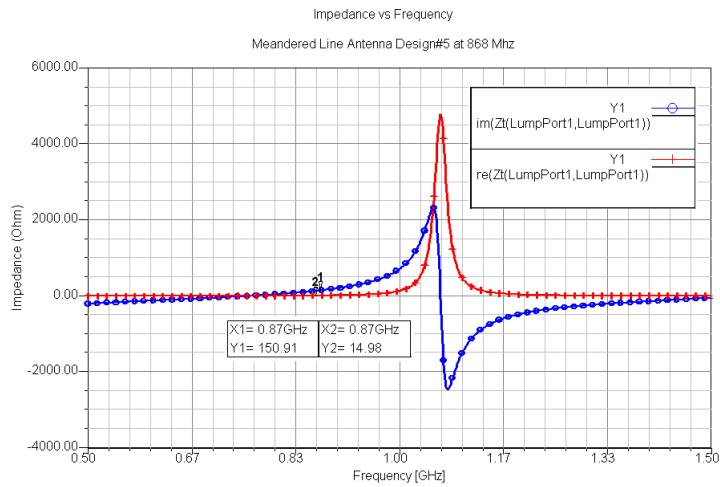
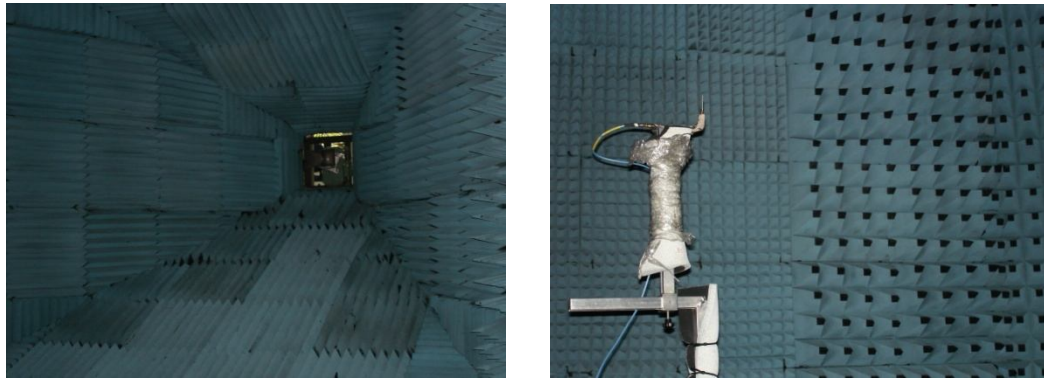


**Figure 6.22 Simulated meander-line antenna designs input impedance with respect to frequency.**

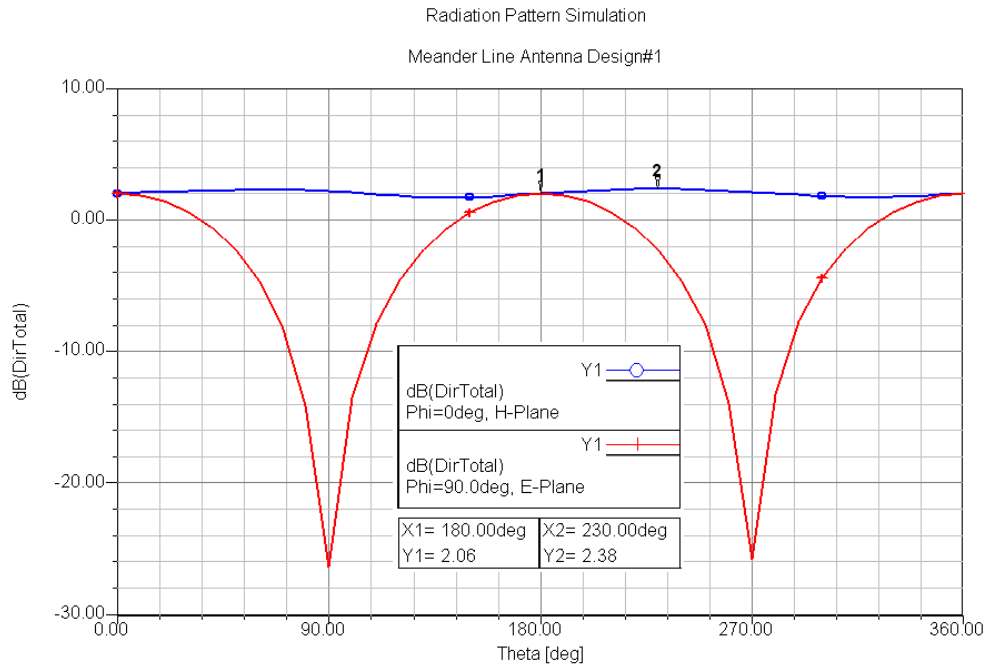
As it can be seen from the above plots, the antenna input impedance is achieved to match complex conjugate of the chip impedance at that frequency. It is important to achieve complex conjugate match of the antenna at the frequencies which is distant from the antenna self resonant frequency. That is because, at the antenna self resonant frequency the impedance changes more quickly and antenna-chip matching deteriorates a lot at these regions. In order to achieve maximum operating bandwidth, the frequency of the conjugate matching should

be selected where antenna input impedances exhibits slow changes in the real and imaginary parts.

The radiation patterns of the implemented antennas are measured in an anechoic chamber illustrated in the Figure 6.23.



**Figure 6.23 Test environment for measuring radiation patterns of the implemented antennas.**



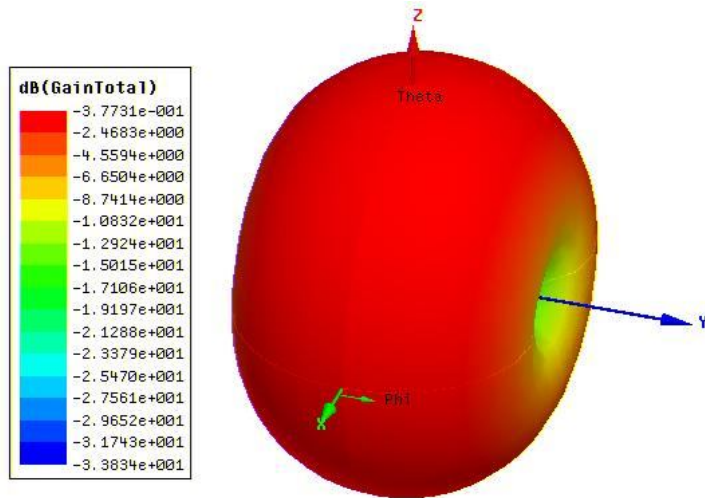
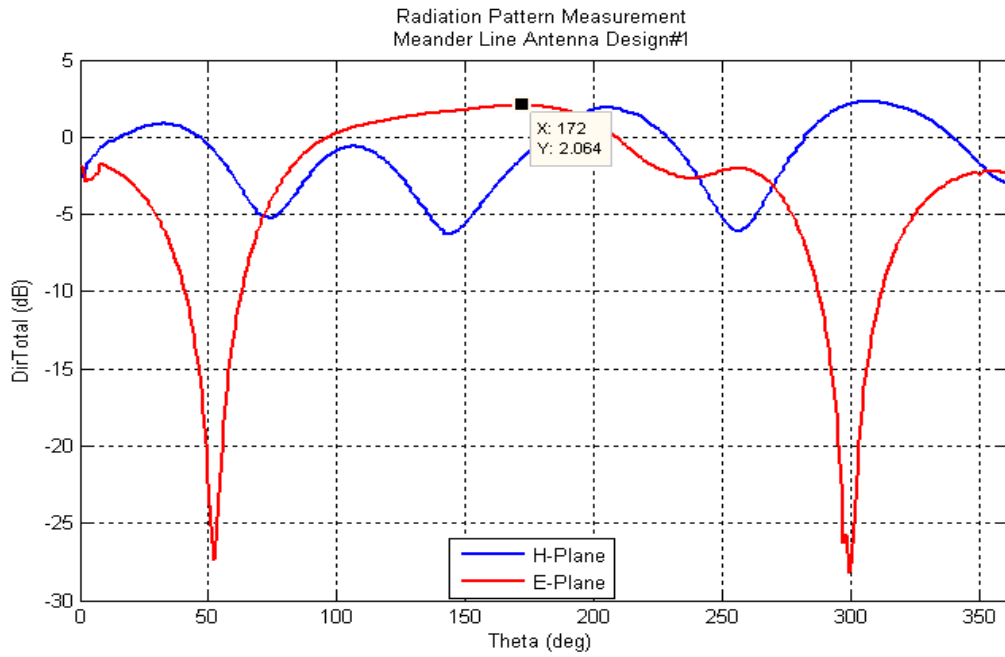


**Figure 6.24 Simulated and measured 2-D radiation pattern (Directivity pattern for  $\phi=0$  (x-z) and  $\phi=90$  (y-z) planes) for the MLA 868 MHz UHF antenna design#1 and 3-D gain pattern. Antenna is located in the horizontal plane.**

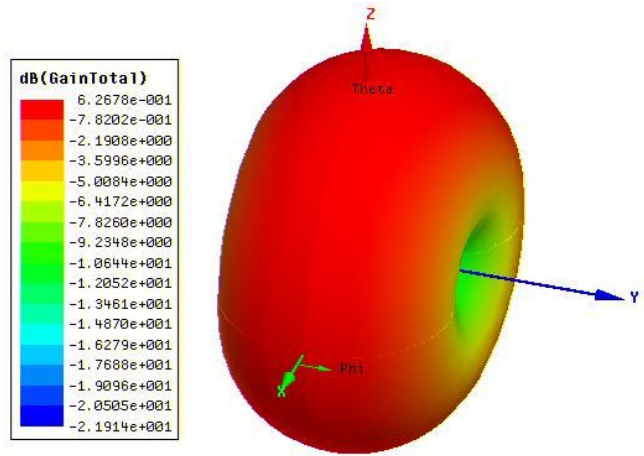
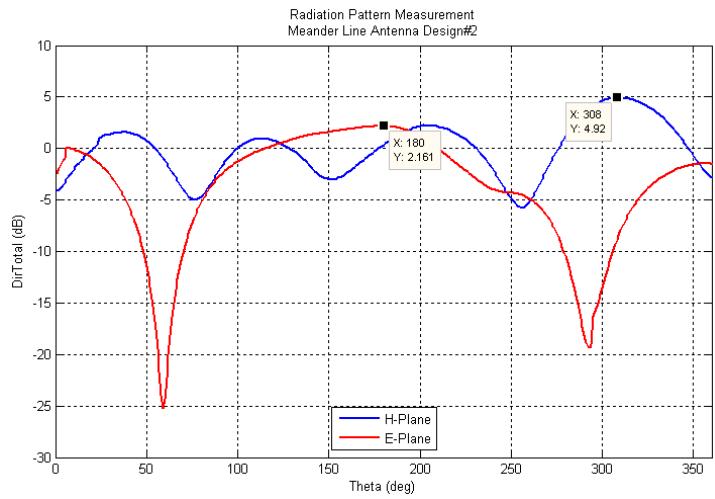
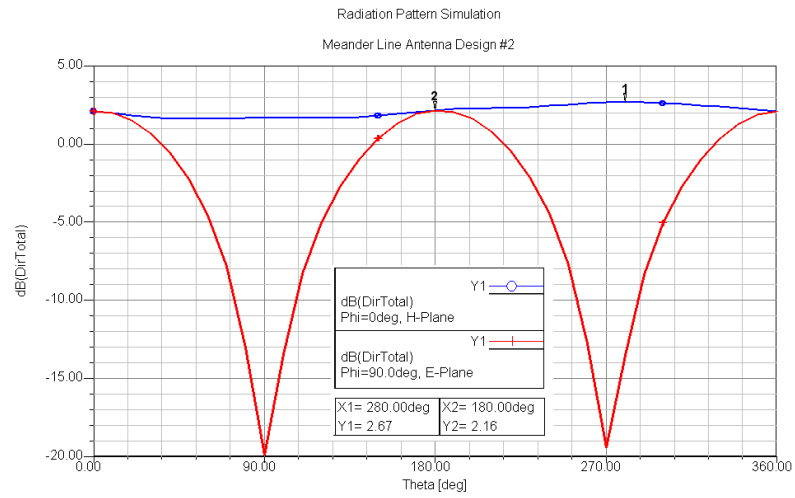


Figure 6.25 Simulated and measured 2-D radiation pattern (Directivity pattern for  $\phi=0$  (x-z) and  $\phi=90$  (y-z) planes) for the MLA 868 MHz UHF antenna design#2 and 3-D gain pattern. Antenna is located in the horizontal plane.

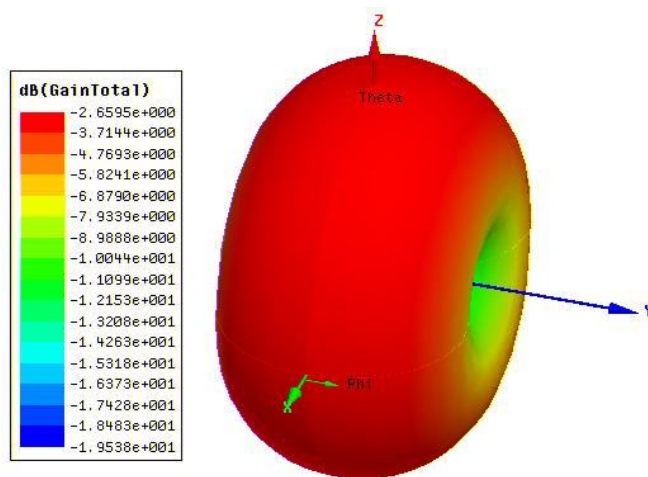
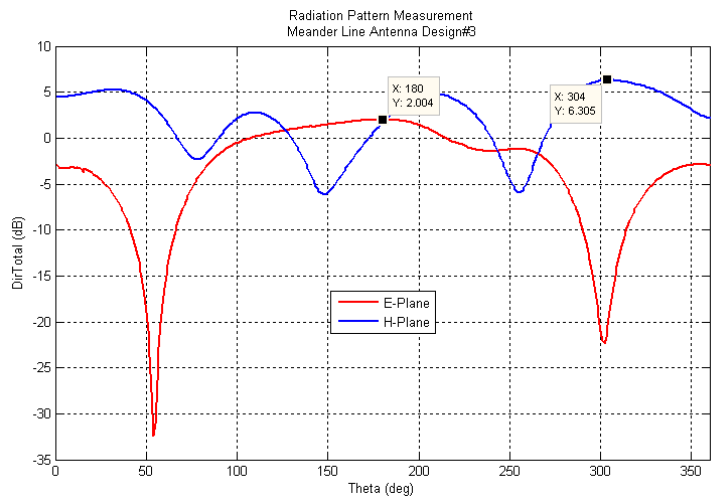
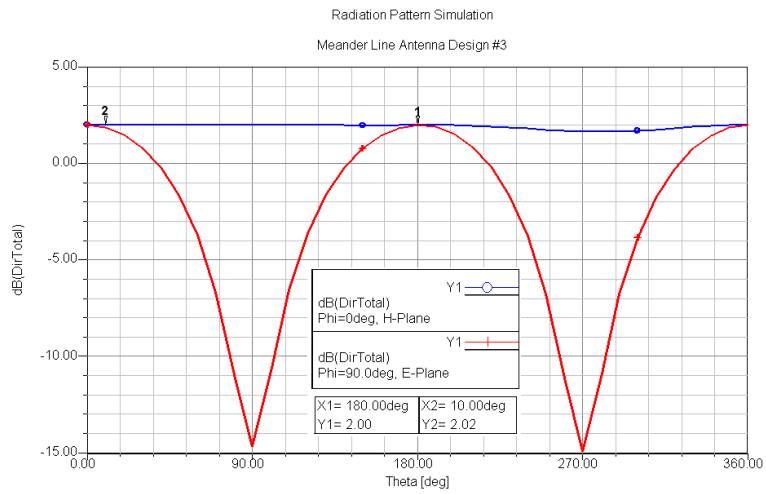


Figure 6.26 Simulated and measured 2-D radiation pattern (Directivity pattern for  $\phi=0$  (x-z) and  $\phi=90$  (y-z) planes) for the MLA 868 MHz UHF antenna design#3 and 3-D gain pattern. Antenna is located in the horizontal plane.

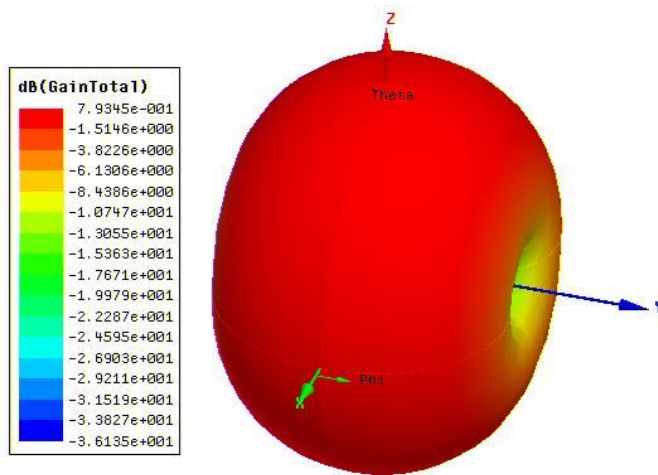
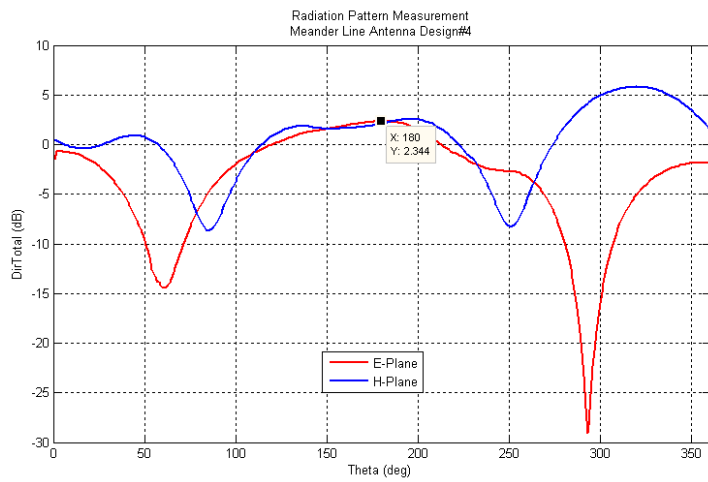
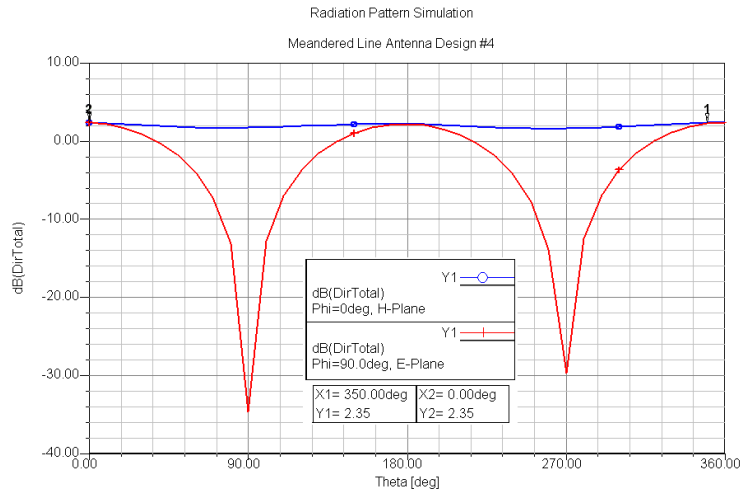
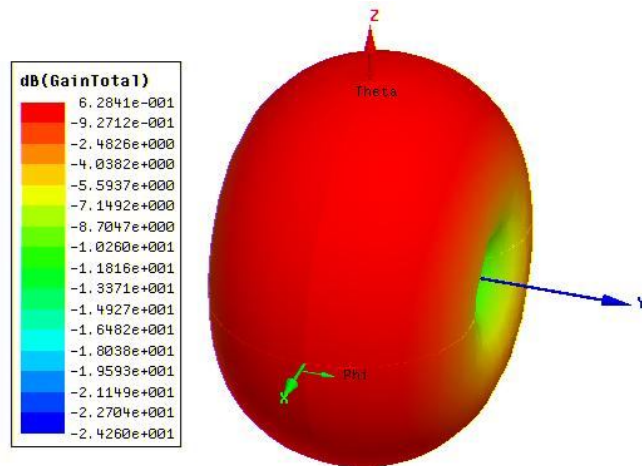
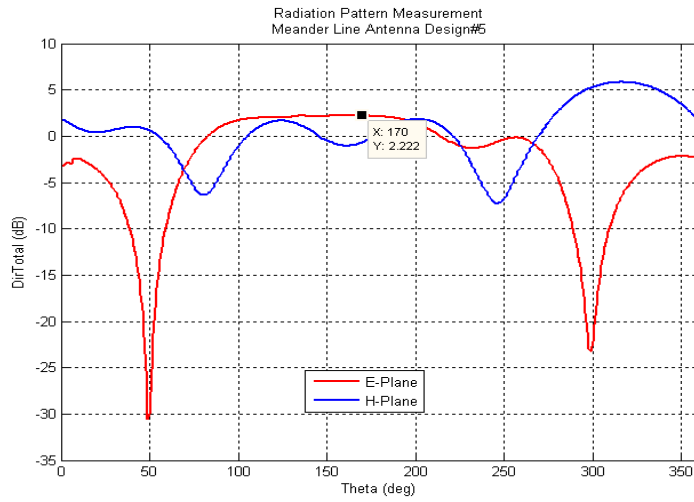
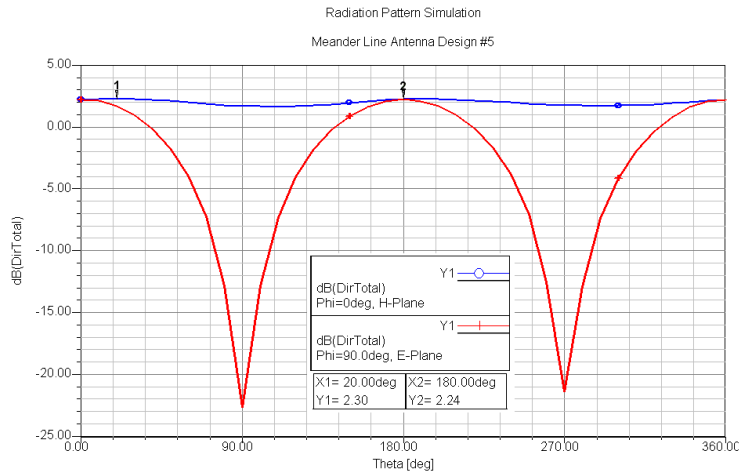
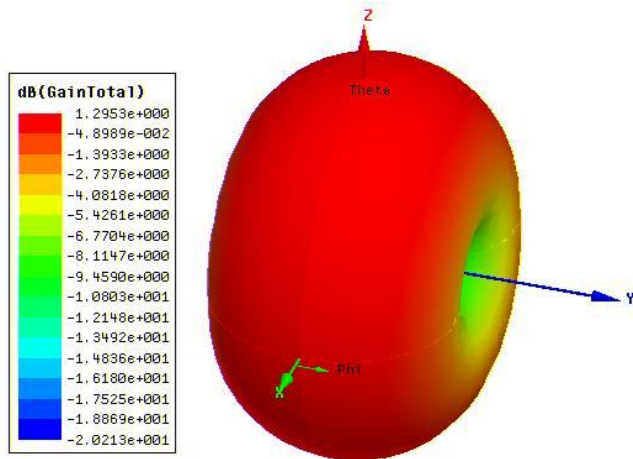
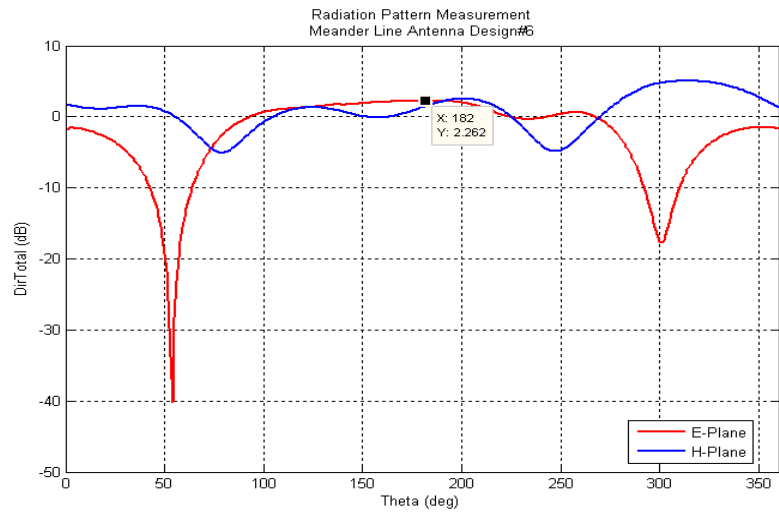
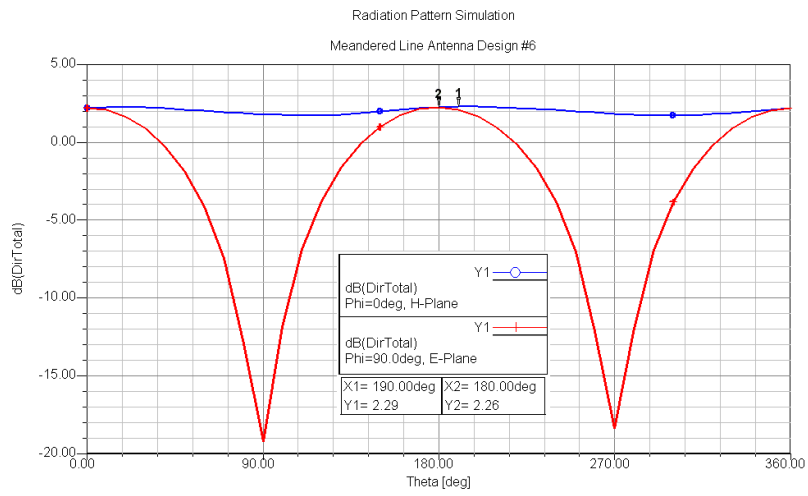


Figure 6.27 Simulated and measured 2-D radiation pattern (Directivity pattern for  $\phi=0$  (x-z) and  $\phi=90$  (y-z) planes) for the MLA 868 MHz UHF antenna design#4 and 3-D gain pattern. Antenna is located in the horizontal plane.



**Figure 6.28 Simulated and measured 2-D radiation pattern (Directivity pattern for  $\phi=0$  (x-z) and  $\phi=90$  (y-z) planes) for the MLA 868 MHz UHF antenna design#5 and 3-D gain pattern. Antenna is located in the horizontal plane**



**Figure 6.29 Simulated and measured 2-D radiation pattern (Directivity pattern for  $\phi=0$  (x-z) and  $\phi=90$  (y-z) planes) for the MLA 868 MHz UHF antenna design#6 and 3-D gain pattern. Antenna is located in the horizontal plane.**

The radiation patterns for the Meander-Line Antennas above are shown in Figure 6.24 to Figure 6.25. The measured E-Plane peak values are normalized to the simulated E-Plane peak values. As it can be seen from these 2D radiation patterns, the H-planes slightly differ at some degrees in all of the figures. These alterations are due to the SMA connectors which are not present in the simulated designs.

All of the antenna designs has doughnut-shaped radiation patterns in the  $\phi=0$  deg (x-z plane) and  $\phi=90$  deg (y-z plane) planes as expected since the antennas are dipole type. The creation of nulls in the horizontal plane (x-y plane) with dipole type of antennas is a restrictive factor. It is essentially desired to attain maximum radiation when the tag is read in the plane (x-z or y-z planes) that is perpendicular to the RFID antenna. The horizontal plane radiation is also important in relation to the orientation of the interrogator. The interrogator (reader) does not essentially have to be positioned on top or bottom with respect to the RFID transponder; however the RFID transponder should also have the functionality to be read from the sides as well. Making use of the two orthogonal transponders (x-y horizontal plane and x-z/y-z vertical planes) would overcome this obstacle in case the application requires effective radiation characteristics in the horizontal plane. The dual polarization (horizontal and vertical) capture will improve the detection in the direction vertical to the antenna (z-axis) where antenna is least likely to be read.

The load impedance values are displayed in Table 6.1 along with other radiation parameters namely return loss, gain, directivity, antenna efficiency, and theoretical & measured read range in free space.

Maximum read distance measurements were done with 13 dBi linearly polarized reader antenna with maximum power set to 1 Watts.

**Table 6.1 Simulated and measured antenna parameters.**

	Simulated Impedance (Ohm)	Simulated S11 (dB)	Measured S11 (dB)	Gain (dB)	Directivity (dBi)	Antenna Efficiency (%)	Theoretical read range (m)	Measured read range (m)
Ant#1	$14.5 + j151.2 \Omega$	-24.9	-18.9	-0.1	2.4	53.7	5.0	4.6
Ant#2	$20.5 + j220.8 \Omega$	-32.0	-35.5	0.6	2.7	62.4	5.6	5.9
Ant#3	$12.2 + j157.6 \Omega$	-39.5	-22.8	-2.6	2.0	34.0	3.6	2.8
Ant#4	$11.6 + j206.4 \Omega$	-27.3	-20.6	0.8	2.4	69.8	4.6	6.9
Ant#5	$15.4 + j142.2 \Omega$	-22.5	-16.6	0.6	2.3	68.0	6.0	5.5
Ant#6	$14.8 + j210 \Omega$	-23.4	-15.0	1.3	2.3	79.5	4.9	5.0

## 6.4 Chapter Summary

The shape of the meander line antennas can be periodic, as in the above designs ( designs 1 and 2), or even individually optimized to match a particular impedance (designs 3, 4, 5 and 6). For this purpose, the required inductive reactance may be achieved by allocating a wire (or strip) conductor longer than half a wavelength within a small space. Reduction of the antenna height down to fractions of a wavelength ( $\lambda/5 \times \lambda/5$ ) can be easily achieved in the antenna designs. Since the linear conductor's length for the optimized meander-line antenna is generally longer than half a wavelength, the tag's maximum gain may be nearly the same of a regular resonant dipole, in spite of the consistent size reduction. As expected, the total length of the meander-line antenna increases along with the reactance to be matched, while the antenna's height controls the resistance.

## CHAPTER 7

### CONCLUSIONS

The main objective of this thesis has been to design and implement RFID transponder antennas for passive (860-960 MHz) UHF tags as well as understanding the procedures and problems of the design process. The popularity of the UHF band have shown that optimization techniques will be of great interest in the various RFID applications from access control to supply chain.

Passive tags which operate in the passive UHF band generally suffer from poor impedance matching at the antenna-IC interface. The microchips come in with different impedance values. This is one of the main challenges when designing the antenna for such an IC. This thesis proved that the resistive stub, double inductive stub, T-match, proximity-coupled loop, nested-slot techniques can achieve conjugate matching to any IC input impedance. In addition, the meander-line antenna configurations reveals the largest number of degrees of freedom, which can be globally optimized to suit tag to a large diversity of microchips and sizes. Antenna's radiation properties are also important for the UHF band since this band is affected more than the HF or lower bands by environmental interference (i.e. metals, liquids, human body absorption). This necessitates the designer to improve antenna radiation characteristics such as radiation pattern, radiation efficiency and gain by improving the current flow on the antenna. The loss in the medium sometimes cannot be managed, so optimum performance must be achieved as discussed in previous chapters. Even the active tags undergo similar challenges from the environment surrounding the tag-reader system. One

must realize the obstacles from a higher system point of view not only at the lower tag design level.

In RFID technology each application comes with different and sometimes unique challenges. Transfer of information is increasing day by day in today's world. The same pattern is repeated with the RFID technology. The need to gather and store more information requires higher data rates and storage capacities. Integration of transponders with other active modules such as sensors (i.e. temperature, pressure) with batteries has caught a lot of attention recently. This means greater challenges are about to happen in terms of packaging constraints and frequency limitations.

Considering previous studies and the work in the thesis, there are possible future works on RFID antenna design. One area of future work will be to design of RFID antennas, the input and radiation properties of which remain nearly unchanged when the transponder is attached to different substrates, such as paper, wood, metal, or living tissues. The planar inverted F-antenna-like (IFA) structures will be a partial solution when the substrate is particularly metal.

Another area of future work will be to design of near field UHF RFID antennas for item level tagging. Some interesting research developments in this area include RFID transponders with dual HF/UHF functionality [40] and organic printed technology developed by several companies [41-43] which is currently making its way into HF RFID [44-50] and may one day reach the UHF band and be used in near field for item level tagging.

## REFERENCES

- [1] K. Finkenzeller, “RFID Handbook: Fundamentals and Applications in Contactless Smart Cards and Identification”, John Wiley and Sons Inc, New York, 2 edition, 2003.
- [2] The History of RFID Technology [Online], Available: <http://www.rfidjournal.com/article/articleview/1338/1/129>, 12 May 2009.
- [3] H. Stockman, “Communication by Means of Reflected Power”, *Proceedings of the IRE*, pp.1196-1204, October 1948.
- [4] J. Landt, “Shrouds of Time The History of RFID”, AIM Inc., ver. 1.0, October 2001.
- [5] EPC Global Home Page [Online], Available: <http://www.epcglobaleurope.org/>, 12 May 2009.
- [6] W. L. Stutzman and Gary A. Thiele, “Antenna Theory and Design”, John Wiley and Sons, Inc., Hoboken, NJ, 2nd edition, 1998.
- [7] C. A. Balanis, “Antenna Theory Analysis and Design”, John Wiley and Sons, Inc., Toronto, Canada, 2nd edition, 1997.
- [8] G. Swamy and S. Sarma, “Manufacturing Cost Simulations for Low Cost RFID systems”, Auto-ID Center, February 2003.
- [9] M. Keskilammi, L. Sydanheimo, and M. Kivikoski, “Radio Frequency Technology for Automated Manufacturing and Logistics Control. Part 1: Passive RFID Systems and the Effects of Antenna Parameters on Operational Distance”, *International Journal of Advanced Manufacturing Technology*, vol. 21, no. 10-11, pp. 769-774, 2003.
- [10] K. V. S. Rao, P. V Nikitin and S. F. Lam, “Antenna Design for UHF RFID Tags: A Review and a Practical Application”, *IEEE Transactions on Antennas and Propagation*, AP-53, pp. 3870-3876, 12 December 2005.

- [11] P.V. Nikitin, K.V.S. Rao, "Performance Limitations of Passive UHF RFID Systems", *IEEE Antennas and Propagation Society Symp.*, pp.1011-1014, July 2006.
- [12] G. De Vita, G. Iannaccone, "Design criteria for the RF section of UHF and microwave passive RFID transponders", *IEEE Transactions on Microwave Theory and Techniques*, vol. 53, no. 9, pp. 2978-2990, Sept. 2005.
- [13] V. Pillai, "Impedance Matching in RFID Tags: To Which Impedance to Match?", *IEEE Antennas and Propagation Society International Symp.*, pp.3505-3508, July 2006.
- [14] V. Pillai, J Peternel, H. Helnrich, R Martinez, K.V.S. Rao, "A Technique for Simultaneous Multiple Tag Identification", *IEEE Workshop on Automatic Identification Advanced Technologies*, pp. 35-38, October 2005.
- [15] K. S. Leong, M. L. Ng, P.H. Cole, "Positioning analysis of multiple antennas in a dense RFID reader environment", *International Symp. On Applications and the Internet Saint Workshops*, pp.4, January 2006.
- [16] D. Kim, M.A. Ingram, and W. W. Smith, "Measurement of small-scale fading and path loss for long range RF tags", *IEEE Transactions on Antennas and Propagation*, vol. 51, no. 8, pp. 1740-1749, November 2003.
- [17] P.R. Foster and R.A. Burberry, "Antenna Problems in RFID Systems", *Microwave and Antenna Systems IEEE*, pp.3/1-3/5, October 1999.
- [18] L.D. Griffin, G. D. Durgin, A. Haldi, B. Kippelen, "RF tag antenna performance on various materials using radio link budgets", *Antennas and Wireless Propagation Letters*, vol. 5, pp.247-250, 2006.
- [19] J. Siden, P. Jonsson, T. Olsson, and G. Wang, "Performance Degradation of RFID System Due to the Distortion in RFID Tag Antenna", *IEEE International Conference on Microwave and Telecommunication Technology*, pp. 371-373, June 2001.

- [20] S. Cichos, J. Haberland, H. Reichl, “Performance Analysis of Polymer Based Antenna-Coils for RFID”, *IEEE International Conference on Polymers and Adhesives in Microelectronics and Photonics*, pp.120-124, June 2002.
- [21] S. C. Q. Chen, V. Thomas, “Optimization of Inductive RFID Technology”, *Proceedings of the IEEE International on Electronics and the Environment*, pp. 82-87, May 2001.
- [22] G. Marrocco, “Gain-Optimized Self-Resonant Meander Line Antennas for RFID Applications”, *IEEE Antennas and Wireless Propagation Letters*, vol. 2, pp. 302-305, 2003.
- [23] G. Marrocco, A. Fonte, and F. Bardati, “Evolutionary design of Miniaturized Meander-line Antennas for RFID Applications”, *IEEE Antennas & Propagation Society International Symposium*, Vol. 2, pp.362-365, June 2002.
- [24] R. F. Harrington, “Effect of antenna size on gain, bandwidth, and efficiency”, *J. Res. Nat. Bureau Standards*, vol. 64D, pp. 1–12, Jan.-Feb. 1960.
- [25] H. A. Wheeler, “Small antennas”, *IEEE Trans. Antennas Propag.*, vol. AP-23, no. 4, pp. 462–469, Jul. 1975.
- [26] High-Frequency Structure Simulator, HFSS v9.2, trademark of Ansoft Corporation, Four Station Square, Pittsburgh, PA 15219-1119, USA.
- [27] X. Qing, N. Yang, “A folded dipole antenna for RFID”, in *Proceeding IEEE Antennas and Propagation Society International Symposium*, vol. 1, June 2004, pp. 97-100.
- [28] B. Yang, Q. Feng, “A Folded Dipole Antenna for RFID Tag”, *ICMMT2008 Proceedings*, 2008 IEEE.
- [29] S. Uda and Y. Mushiake, “Yagi-Uda Antenna”, Tokyo, Sasaki Printing and Publishing Co., 1954, pp. 119-131.
- [30] L. Ukkonen, M. Schaffrath, J. A. Kataja, L. Sydanheimo and M. Kivikoski, “Evolutionary RFID Tag Antenna Design for Paper Industry

- Applications”, *International Journal of Radio Frequency, Identification Technology and Applications*, 1, 1, January 2006, pp. 107-122.
- [31] C. Cho, H. Choo and I. Park, “Design of Novel RFID Tag Antennas for Metallic Objects”, *IEEE International Symposium on Antennas and Propagation Digest*, Albuquerque, NM, July 2006, pp. 3245-3248.
- [32] Y. Tikhov, Y. Kim and Y.-H. Min, “Compact Low Cost Antenna for Passive RFID Transponder”, *IEEE International Symposium on Antennas and Propagation Digest*, Albuquerque, NM, July 2006, pp. 10 15-1018.
- [33] H. W. Son and C. S. Tyo, “Design of RFID Tag Antennas Using an Inductively Coupled Feed”, *Electronics Letters*, 41, 18, September 2005, pp. 994-996.
- [34] W. Choi, H. W. Son, C. Shin, J.-H. Bae and G. Choi, “RFID Tag Antenna with a Meandered Dipole and Inductively Coupled Feed”, *IEEE International Symposium on Antennas and Propagation*, Albuquerque, NM, July 2006, pp. 6 19-622.
- [35] H. Kwon and B. Lee, “Meander-Line RFID Tag at UHF Band Evaluated with Radar Cross Sections”, in *Proceedings APCM 2005*.
- [36] G. Marrocco, "Body-Matched Antennas for Wireless Biometry", *European Conference on Antennas and Propagation*, Nice, France, November 2006, p. 795.
- [37] G. Marrocco, “RFID Antennas for the UHF Remote Monitoring of Human Subjects”, *IEEE Transactions on Antennas and Propagation*, AP-55, 6, June 2007, pp. 1862-1870.
- [38] G. Marrocco and C. Calabrese, "Automatic Design of Miniaturized Slot-Line RFID Antennas," *Second European Conference on Antennas and Propagation (EUCAP)*, Edinburgh, Scotland, November 2007.
- [39] N. Michishita and Y. Yamada, "A Novel Impedance Matching Structure for a Dielectric Loaded 0.05 Wavelength Small Meander Line Antenna," *IEEE International Symposium on Antennas and Propagation*, Albuquerque, NM, July 2006, pp. 1347-1350.

- [40] TwinLinux [Online], Available: <http://www.twinlinux.com>, 12 May 2009.
- [41] Organic ID [Online], Available: <http://www.organicid.com>, 12 May 2009.
- [42] PolyIC [Online], Available: <http://www.polyic.com>, 12 May 2009.
- [43] IMEC [Online], Available: <http://www.imec.be>, 12 May 2009.
- [44] V. Subramanian et al., “Progress toward development of all-printed RFID tags: materials, processes, and devices”, *Proceedings of the IEEE*, vol. 93, no. 7, Jul. 2005, pp. 1330 – 1338.
- [45] S. Steudel et al., “50 MHz rectifier based on an organic diode”, *Nature Materials*, no. 4, Aug. 2005, pp. 597 – 600.
- [46] A. Hellemans, “Could Belgian diode lead to printable RFIDs?”, *IEEE Spectrum*, vol. 42, no. 12, Dec. 2005, p. 14.
- [47] V. Subramanian, P. Chang, J. Lee, S. Molesa, S. Volkman, “Printed organic transistors for ultra-low-cost RFID applications”, *IEEE Transactions on Components and Packaging Technologies*, vol. 28, no. 4, Dec. 2005, pp. 742 – 747.
- [48] E. Cantatore et al., “A 13.56-MHz RFID System Based on Organic Transponders”, *IEEE Journal of Solid-State Circuits*, vol. 42, no. 1, Jan. 2007, pp. 84 – 92.
- [49] M. Berggren et al., “Organic materials for printed electronics”, *Nature Materials*, vol. 6, no. 1, Jan. 2007, pp. 3-5.
- [50] J.L. Botrel et al., “Polysilicon high frequency devices for large area electronics: characterization, simulation and modeling”, *Thin Solid Films (Elsevier Journal)*, article in press, available online at <http://www.sciencedirect.com>.
- [51] *Identification Cards - Contactless Integrated circuit(s) cards- Proximity cards-Part 2: Radio frequency power and signal interface*, ISO/IEC 14443-2, 2001.
- [52] *Identification Cards - Contactless Integrated circuit(s) cards- Vicinity cards-Part 3: Anti-collision and transmission protocol*, ISO/IEC 15963-3, 2009.

- [53] *Information technology – Radio frequency identification for item management – Part 4: Parameters for air interface communications at 2.45 GHz*, ISO/IEC 18000-4, 2008.
- [54] *Information technology – Radio frequency identification for item management – Part 6: Parameters for air interface communications at 860 MHz to 960 MHz*, ISO/IEC 18000-6, 2004.